A STRUCTURAL ANALYSIS of *Xenopus laevis* oocyte 5S rRNA

by

MARIA LUISA ISABEL LEAL CARRETERO
B.Sc., University of Victoria, 1984

A THESIS SUBMITTED IN PARTIAL FULFILLMENT

OF THE REQUIREMENTS FOR THE DEGREE OF

MASTER OF SCIENCE

in the Department

of

Biochemistry and Microbiology

ACCEPTED
FACULTY OF GRADUATE STUDIES

[redacted]
DEAN

DATE June 27, 1989

We accept this thesis as conforming
to the required standard

[redacted]

Dr. Paul. J. Romaniuk.

[redacted]

Dr. William W. Kay.

[redacted]

Dr. Thomas M. Fyles.

[redacted]

Dr. Michael J. Ashwood-Smith.

[redacted]

© M. L. ISABEL LEAL, 1989

University of Victoria

All rights reserved. This thesis may not be reproduced
in whole or in part, by mimeograph or other means,
without the permission of the author.

Supervisor: Dr. Paul J. Romaniuk

ABSTRACT

The purpose of this project was to investigate the secondary and tertiary structures of *Xenopus laevis* oocyte 5S rRNA using chemical and enzymatic probes.

Mutations were introduced into the *X. laevis* 5S rRNA gene in order to study the effect that these mutations would have on the structure of 5S rRNA transcribed from the gene. Four different mutants were constructed by introducing base substitutions in loops **D** and **E** of the 5S rRNA structure. Three of the mutants have sequence substitutions in loop **E** (Xlo73-76, Xlo99-101 and Xlo96-101), and mutant Xlo87-90 has sequence substitutions in loop **D.** The accessibility of all 5S rRNAs to single-strand specific nucleases (T_1,T_2,A, and S_1), and to a nuclease specific for double-stranded or structured regions (RNase V_1), was determined. The reactivity of nucleobases at N7, N3 and N1 positions to chemical probes (DMS, DEPC, and CMCT), was investigated under native (5mM $MgCl_2$, 100mM KCL, 20°C), and semi-denaturing (1mM EDTA, 20°C) conditions. N-ethylnitrosourea was used to identify phosphates not reactive to alkylation under native conditions.

The enzymatic accessibility and chemical reactivity results obtained from all four mutants, as well as from the wild-type 5S rRNA, confirm the presence of the five helical stems predicted by the consensus secondary structure model of 5S rRNA. A comparison of the data obtained from the four mutants with that obtained from wild-type 5S rRNA yielded the

following results: (i) The conformation of loops **A, B,** and **C** is virtually identical in wild-type 5S rRNA and in all four mutants. (ii) In mutants Xlo73-76 and Xlo99-101, region **E** is more reactive to chemical probes and more susceptible to enzymatic clevage, and helices **IV** and **V** are less stable than the corresponding regions in wild-type 5S rRNA. In Xlo96-101, region **E** is less reactive, and helices **IV** and **V** more stable than their corresponding wild-type regions. (iii) In mutant Xlo87-90, loop **D** is more susceptible to enzymatic cleavage and more reactive to chemical probes, and helix **IV** is less stable than the same regions in wild-type 5S rRNA. These results support the conformation of loops **C** and **D** as they appear in the computer graphic model proposed by Westhof *et al.* (in press) for the tertiary structure of *X. laevis* oocyte 5S rRNA. In particular, two important features of this model are supported by the structure probing of the four mutants studied here: (i) region **E** and loop **D** seem to contain unusual base pairing, consisting of non-canonical base-pairs; and (ii) no tertiary interactions appear to take place between loop **C** and either region **E** or loop **D**.

Dr. Paul J. Romaniuk

Dr. William W. Kay

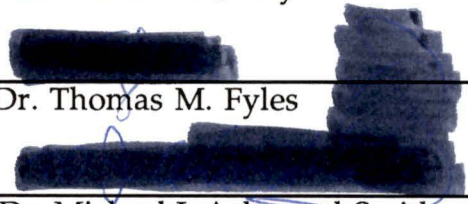

Dr. Thomas M. Fyles

Dr. Michael J. Ashwood-Smith

TABLE OF CONTENTS

LIST OF TABLES

LIST OF FIGURES

LIST OF ABBREVIATIONS

A: Adenine

ASIF: Accessible Surface Integrated Field

ATP: Adenosine triphosphate

BSA: Bovine serum albumin

BPB: Bromophenol blue

C: Cytosine

cDNA: Complementary deoxyribonucleic acid

CMCT: 1-Cyclohexyl-3-(2-morpholinoethyl) carbodiimide metho-p-toluene sulfonate

cpm: Counts per minute

CTP: Cytidine triphosphate

dATP: Deoxyadenosine triphosphate

dCTP: Deoxycytidine triphosphate

dGTP: Deoxyguanosine triphosphate

dTTP: Deoxythymidine triphosphate

ddATP: Dideoxyadenosine triphosphate

ddCTP: Dideoxycytidine triphosphate

ddGTP: Dideoxyguanosine triphosphate

ddTTP: Dideoxythymidine triphosphate

DEPC: Diethylpyrocarbonate

DMS: Dimethylsulphate

DNA: Deoxyribonucleic acid

DTT: Dithiothreitol

EDTA: Ethylenediamine-tetraacetic acid

ENU: N-ethylnitrosourea

G: Guanine

GTP: Guanosine triphosphate

HPLC: High performance liquid chromatography

mRNA: Messenger ribonucleic acid

N: Nucleotide

NMR: Nuclear magnetic resonance

PEG: Polyethylene glycol

RNA: Ribonucleic acid

rRNA: Ribosomal ribonucleic acid

RNase: Ribonuclease

RNasin: Ribonuclease inhibitor

S: Svedberg unit

SDS: Sodium dodecyl sulphate

TBE: Tris; Borate; EDTA

TF IIIA: Transcription Factor IIIA

tRNA: Transfer ribonucleic acid

Tris-HCl: Tris (hydroxymethyl) aminomethane-HCl

U: Uracil

UTP: Uridine triphosphate

w.t.: Wild-type

XC: Xylene cyanol

Xlo: *Xenopus laevis* oocyte

ACKNOWLEDGEMENTS

I would like to express my gratitude to Dr. P. J. Romaniuk for his assistance throughout this project as well as during preparation of this manuscript.

I would also like to express my appreciation to Florence Baudin, Pascale Romby, and Chantal and Bernard Ehresmann for their helpful advice during this research; and to Michael Chase for checking the correctness of my English.

My thanks also go to the University of Victoria for financial assistance in the form of scholarships.

A mi Madre que con su ejemplo
siempre me ha podido guiar.

A Miguel por su apoyo durante
el transcurso de este trabajo.

INTRODUCTION

RNA molecules perform a wide variety of functions within the cell, and for each function a specific type of RNA is required. RNAs are involved in all steps of protein synthesis, by storing genetic information (messenger RNA), by participating in the structure of the mRNA translating machinery (the ribosome), and by carrying amino-acids to the ribosome (transfer RNAs). In addition to these vitally important functions, recent findings point towards catalytic functions of certain RNA molecules (for a review see Cech and Bass, 1986). All of these mechanisms require specific and coordinated RNA-RNA and RNA-protein interactions, and point out the importance of studies leading to a better understanding of the structural dynamics of RNA molecules, since the three-dimensional structure of RNAs determine many of their biological activities.

Structure of 5S rRNA

This project is concerned with the study of the effect of specific mutations on the structure of the African toad *Xenopus laevis* oocyte 5S rRNA. The following brief description of 5S rRNA is provided in order to orient the reader with regards to what is known about the secondary and tertiary structure of 5S rRNA.

Location of 5S rRNA

Ribosomes are made up of proteins and RNA, and the ribosomal RNA (rRNA) itself consists of several different molecules that differ in chain length, as well as in secondary and tertiary structures. Prokaryotic ribosomes

consist of two subunits of unequal size, the larger having a sedimentation coefficient of 50S and the smaller of 30S. The 50S subunit contains one molecule of 23S rRNA, one molecule of 5S rRNA and 34 proteins. The 30S subunit contains one molecule of 16S rRNA and 21 proteins. The cytoplasmic ribosomes of eukaryotic cells are larger than prokaryotic ribosomes, and also consist of two subunits: 60S and 40S. The small subunit contains an 18S rRNA, and the large subunit contains 5S, 5.8S and 28S rRNA. Altogether, eukaryotic ribosomes contain over 70 different proteins.

The 5S ribosomal RNA is the smallest ribosomal RNA, and it is not only a universal component of the large subunit of prokaryotic ribosomes and cytoplasmic ribosomes of eukaryotic cells, but it is also present in chloroplastid ribosomes and in plant mitochondria. Since the discovery of 5S rRNA in 1963 by Rosset *et al*, this molecule has, because of its small size, ubiquity and relative structural simplicity, been the subject of numerous investigations concerning its structure, function, evolution and protein interactions. We know from sequence analysis that this small rRNA is usually 120 nucleotides long and, in general, does not contain modified nucleotides (Erdmann, 1981). Immune electron microscopy experiments have shown that in *Escherichia coli*, 5S rRNA is located in the central protuberance of the large ribosomal subunit (Shatsky *et al*, 1980; Clarck and Lake, 1983).

5S rRNA Interactions with Proteins

Eukaryotic and eubacterial 5S rRNAs interact with a number of different types of proteins. In the *E coli* ribosome, 5S rRNA associates *in vitro* with three ribosomal proteins designated L5, L18 and L25 (Garrett *et al*, 1981; Stahl

et al, 1984). In eukaryotic ribosomes, the 5S rRNA associates with a large protein designated L3 in *Xenopus* and *Sacharomyces*, and L5 in rat liver (Picard and Wegnez, 1979; Nazar *et al*, 1979; Huber and Wool, 1986).

There are two types of 5S rRNA in *Xenopus:* oocyte 5SrRNA, which is found only in oocytes, and somatic 5S rRNA, which is found exclusively in somatic tissues. Proteins other than ribosomal proteins also recognize and associate with 5S rRNA. In *Xenopus laevis* the oocyte 5S rRNA is found associated with the protein transcription factor III A (TFIIIA); together they form 7S ribonucleoprotein storage particles in the cytoplasm of immature oocytes. The function of these storage particles is to stabilize the 5S rRNA until is required for ribosome assembly later in oocyte development (Picard and Wegnez, 1979; Pelham and Brown, 1980). In eukaryotes, it is known that the 5S rRNA genes form an independent transcriptional unit and are transcribed by RNA polymerase III (Birkenmeier *et al*, 1978). TFIIIA is required for the transcription of the 5S rRNA gene and by binding to the internal control region of the 5S gene, it initiates a process in which two other proteins (TFIIIB and TFIIIC) form a stable ternary complex that directs the initiation of transcription by RNA polymerase III (Segall *et al*, 1980; Shastry *et al*, 1982). TFIIIA is unusual in that it interacts specifically with both 5S DNA and its gene product, 5S RNA. *Xenopus laevis* oocyte 5S rRNA is also found complexed with two nonribosomal proteins and tRNA in a 42S storage particle (Pelham and Brown, 1980).

Function of 5S rRNA

The presence of 5S rRNA is strictly required for the structure and function of the ribosome. It has been observed that particles lacking 5S

rRNAs show greatly reduced biological activity (Erdmann *et al*, 1971; Nomura, 1973).

Several functional roles have been postulated for 5S rRNA. One possible function is ribosomal subunit association (Azad and Lane, 1973; Azad, 1979). These authors proposed that intermolecular base-paired interactions between complementary sequences near the 3' end of 5S rRNA in the large ribosomal subunit, and eukaryotic 18S rRNA (or prokaryotic 16S rRNA) in the small ribosomal subunit may be involved in the reversible association of ribosomal subunits.

5S rRNA is also believed to be involved in the functioning of the peptidyl transferase center of the ribosome (Raacke 1971). It has been suggested, based on space filling models, that peptidyl-5S rRNA may be the donor for the peptide elongation reaction. These models show that when the peptide is on the tRNA, at the end of the previous elongation step, the 3'-OH of 5S rRNA is in a stereochemically perfect position for executing a nucleophilic attack on the carbonyl of the peptide, thereby effecting its transfer to 5S rRNA. On the other hand, when the peptide is on the 5S rRNA, the amino group of the acceptor aminoacyl-tRNA, in turn, is in a stereochemically perfect position for a nucleophilic attack on the carbonyl of the peptide, causing its transfer to the aminoacyl-tRNA, and synthesis of a new peptide bond.

Another functional role that has been postulated for 5S rRNA is tRNA binding. In ribosomal particles that lacked 5S rRNA, the enzymatic binding of aminoacyl-tRNA to the ribosomal A-site was reduced significantly (Erdmann *et al*, 1971; Nierhaus and Dohme, 1974). This observation is in accordance with a previous hypothesis, which suggested that the T-Ψ-C-G

sequence, strongly conserved in loop IV of tRNAs, interacts with the constant G44-A-A-C47 sequence of 5S rRNAs to help anchor tRNA to the 5S rRNA site on the ribosome during protein synthesis (Brownlee *et al*, 1968; Ofengand and Henes, 1969). Several experiments have, however, raised doubts concerning this putative function. In one experiment, carried out in solution, direct pairing between the sequences G -A -A-C of free *E. coli* 5S rRNA and T-Ψ-C-G could not be demonstrated (Erdmann *et al.*, 1973). Moreover, excision of the G-A-A-C segment followed by reconstitution of the excised 5S rRNA into ribosomes, produces a functional ribosome (Pace *et al.*, 1982). More recently, Lorenz *et al.* (1987) investigated the hybridization of d(GTTCGG) to eubacterial 5S rRNAs, 5S rRNA-protein complexes, 70S ribosomes, and 50S and 30S ribosomal subunits, using RNase H hydrolysis. As these authors considered this oligonucleotide to be an analogue of the TΨCG loop of tRNAs, they selected it for use in the investigation of a possible interaction between tRNAs and ribosomal components during protein synthesis Their results showed that nucleotides in loop C (positions 42-47), are available for interaction with the oligonucleotide in free *E. coli* and *Bacillus stearothermophilus* 5S rRNAs, and not available in the corresponding 5S rRNA-protein complexes. The 70S and ribosomal subunits did not interact with the oligonucleotide. Assuming that the d(GTTCGG) is an acceptable analogue to the corresponding tRNA sequence GTΨCGR, Lorenz *et al.* (1987) concluded from their results that in non-synthesising ribosomes, the TΨCG loop of tRNAs does not interact via standard Watson-Crick base pairs with the ribosomal 5S, 16S or 23S rRNAs. It has been observed that 5S rRNA undergoes a structural alteration when tRNA is bound to the ribosome (Göringer *et al.*, 1984). This is an interesting result because the notion that 5S

rRNA exists in a number of different conformations, which are believed to be related to different functional states (see page 29), shows the intrinsic relation between the structure and function of this molecule.

Finally, Gaunt-Klöpfer and Erdmann (1975) have proposed that 5S rRNA has GTPase activity. Specific 5S rRNA-protein complexes were reconstituted from *E. coli* 5S rRNA and 50S ribosomal proteins. These complexes consisted of 5S rRNA, L18 and L25. Enzymatic activity analysis showed that ATP and GTP were hydrolyzed and that this hydrolysis was independent of elongation factors.

However, despite all this extensive research the true functional role of 5S rRNA in the structure of the ribosome and in protein biosynthesis still remains unknown. The question whether 5S rRNA is merely a static structural component of the ribosome, or whether it takes part in the dynamic process of protein biosynthesis, can not yet be answered satisfactorily. The universal or nearly universal presence of this molecule in ribosomes does, however, make an important role appear likely. A thorough knowledge of 5S rRNA structure will enhance our understanding of its biological significance. Further research into the tertiary structure of 5S rRNA will no doubt contribute to an understanding of how this molecule interacts with specific proteins, and help to elucidate its functional role.

Generalized Structure of the 5S rRNAs

Two approaches can be used to derive secondary structure models: (i) by means of sequence comparison of homologous RNAs from different organisms covering a large evolutionary range; (ii) by means of searching for the most favorable structure by using thermodynamic parameters, for which

computer programs have been elaborated (Nussinov *et al.*, 1982). It is known that while RNA molecules do not possess the regular interstrand hydrogen-bonded structure characteristic of DNA, they do have the capacity to form double-helical regions, which are formed between two segments of the same chain folded back on itself. The RNA folds into a secondary structure which is similar to the A form of DNA. However, the helical regions formed in this manner are seldom regular, as the segments of the chain brought into opposition do not have entirely complementary sequences, so non-bonded residues "loop out" of the structure.

The sequences of 5S rRNAs have been determined from a wide range of eukaryotic organisms, representative of the metazoa (vertebrates and arthropods), protozoa, plants, algae and fungi (Erdmann, 1982). It has become apparent that eukaryotic 5S rRNAs have common nucleotide sequences in particular positions of the molecule. Furthermore, it has been shown that the eubacterial, archaebacterial, and organelle 5S rRNAs share many of these positions; indeed they have been termed universal positions since they contain sequences which have been conserved throughout evolution (Delihas, 1982). These universal positions are distributed throughout the 5S molecule and reveal a remarkable constancy in all the compared 5S rRNA sequences. As of December 31, 1987, the Berlin RNA Data Bank contains a total of 509 sequences of 5S rRNAs or their genes. It covers sequences from 38 archaebacteria, 184 eubacteria, 14 plastids, 4 mitochondria, 258 eukaryotes and 11 eukaryotic pseudogenes (Wolters and Erdmann, 1988). Indeed, the comparison of nucleotide sequences from this wide range of organisms has led to the elaboration of a universal secondary structure for all 5S rRNAs (Delihas and Andersen, 1982; De Wachter, 1982; and Erdmann and Wolters,

1986) (Figure 1), based upon the minimal secondary structure model originally proposed by Woese and Fox (1975). The fact that all 5S rRNA sequences can be folded into a common structure implies that the conserved sequences could be important in maintaining the structure of this RNA molecule or as recognition sites for binding to other macromolecules. In fact, several of these conserved residues especially the ones found in internal loop regions, are implicated in protein binding (Pieler and Erdmann, 1983; Christiansen *et al.*, 1987).

The number of nucleotides separating several of the universal nucleotides appears to be specific to either eubacterial, archaebacterial or eukaryotic 5S rRNA. This is due to the presence of a small number of insertions or deletions of sequences that are scattered throughout the molecule, and it is the major distinguishing feature between these 5S rRNAs (Delihas and Andersen, 1982; Wolters and Erdmann,1988). Generalized structures for the eubacterial, archaebacterial and eukaryotic 5S rRNAs, showing conserved positions, insertions and deletions, can be seen in Figure 2. In contrast to the relatively homogeneous structures of eukaryotes and eubacteria 5S rRNAs, there are many differences in the structure of this molecule within the different groups of the archaebacteria. In the interest of brevity, therefore, the model of the Halophilic-methanogenic 5S rRNA secondary structure has beem chosen as representative for the archaebacterial kingdom.

Conformation of 5S rRNA Derived from Enzymatic and Chemical Studies

Although the comparative analysis of nucleotide sequences has proven to be a very important approach for deriving secondary structure models for 5S rRNA, it has limitations in regards to the dynamic aspects of RNA

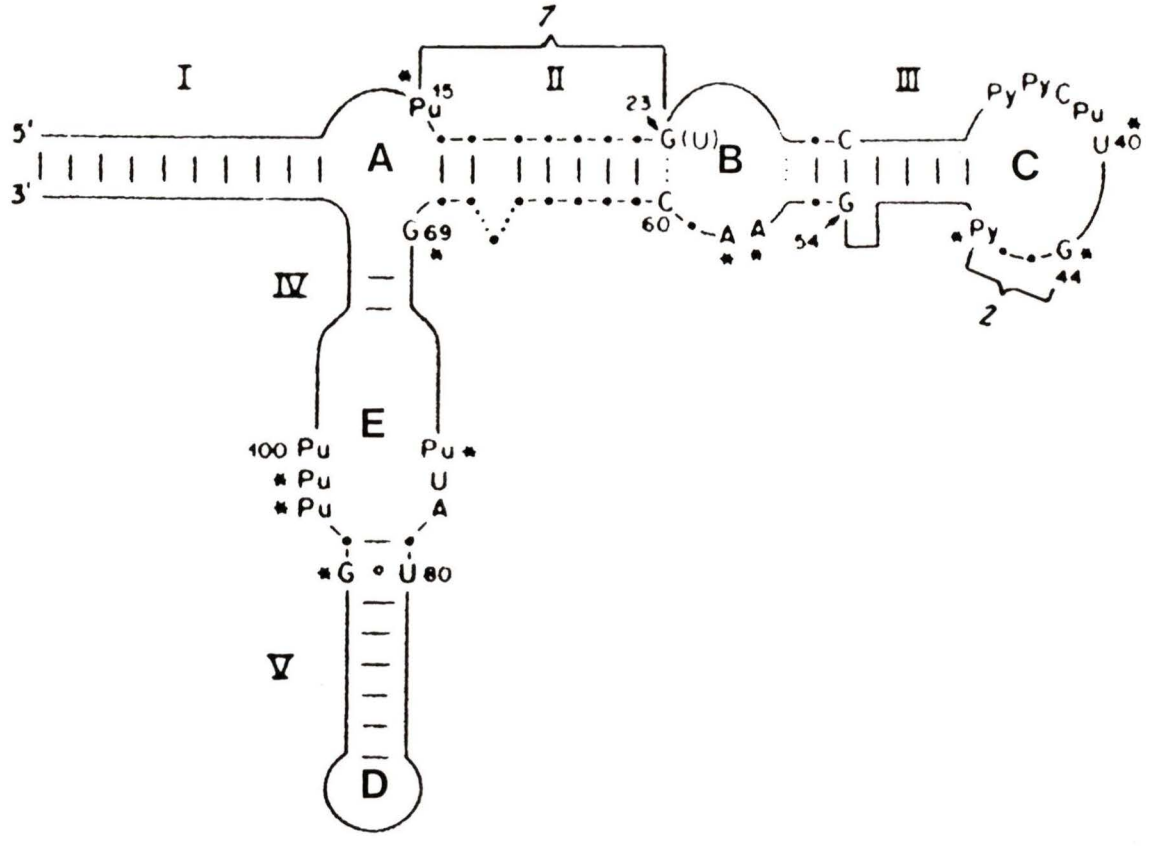

Figure 1: Generalized structure for the 5S ribosomal RNA. The numbering system corresponds to that of the *E. coli* 5S RNA. The five helices of the secondary structure model are labeled I-V, the loops A-E. Nucleotide positions shown are universal positions. Positions marked with asterisks designate total invariance. Dots represent constant chain lengths between universal positions found in most compared 5S RNAs; the chain lengths between Pu15 and G23 and G44 and Py47 are always 7 and 2 nucleotides, respectively. Pu represents purine; Py pyrimidine (after Delihas and Andersen, 1982).

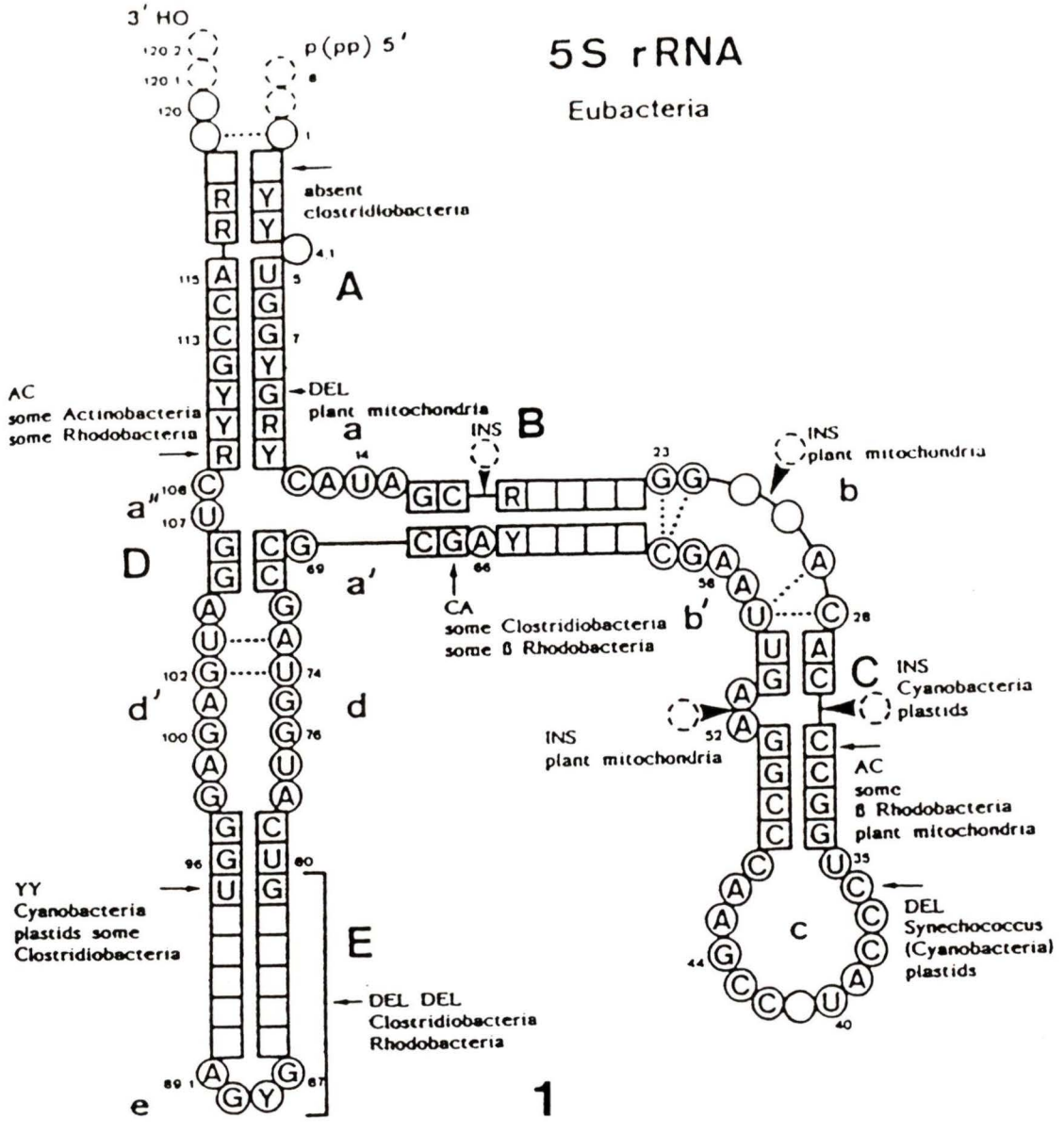

Figure 2: Minimal models of 5S rRNA secondary structure. (1) Eubacteria; (2) Eukaryotes; (3) Archaebacteria. Squares indicate conserved base-pairing; circles unpaired nucleotides; tiny circles between bases A:C or pyrimidine: pyrimidine; diamond purine:purine odd base-pairs; dotted lines possible helix extension. Bases indicated in these models are supposedly conserved (ancestral) in the respective group; hypervariable positions remain blank. Insertions/ deletions and odd base-pairs are marked if they occur in a specific monophyletic group represented by at least 2 species. The numeration of bases is according to the *E. coli* sequence (after Wolters and Erdmann, 1988).

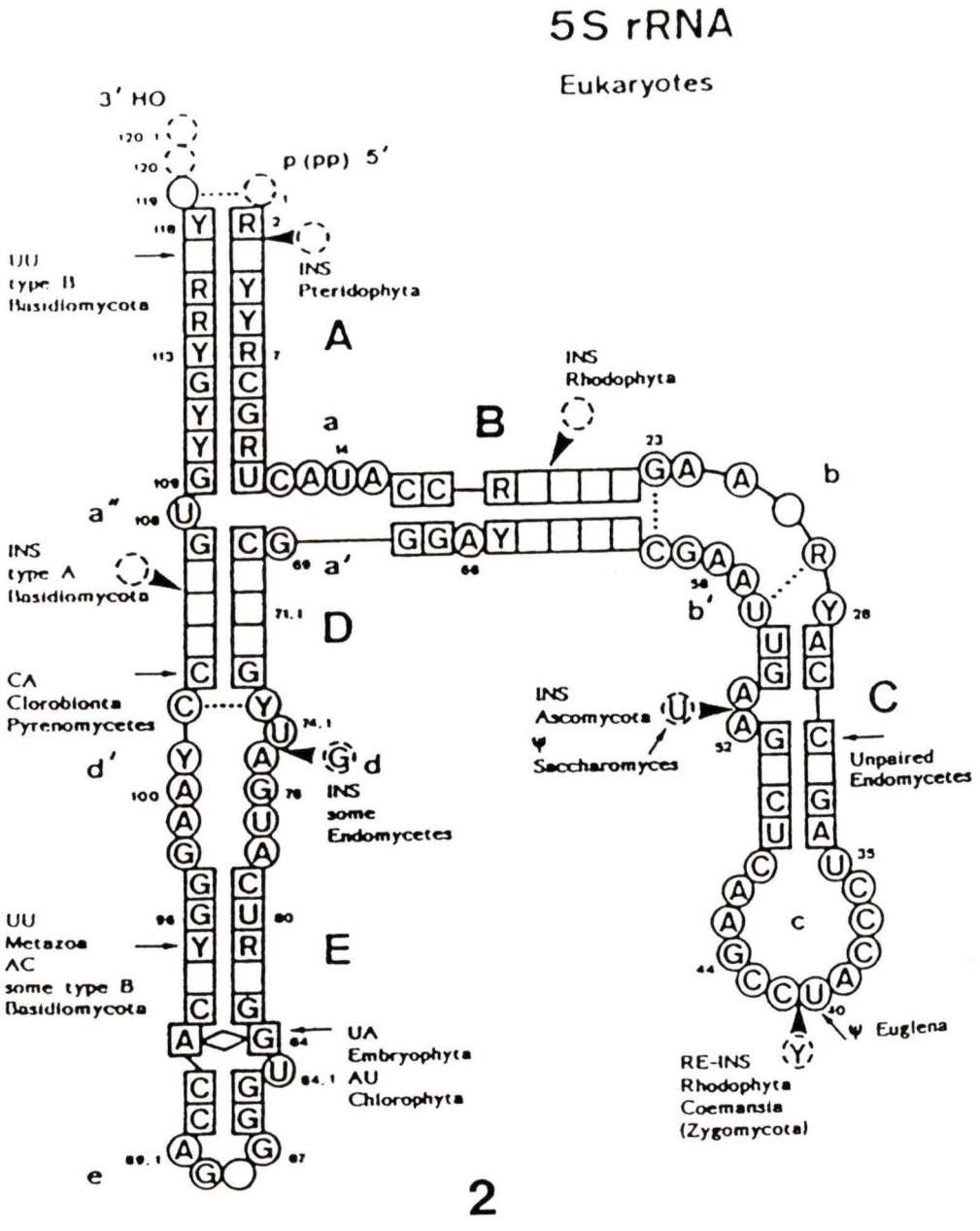

Figure 2 (continued)

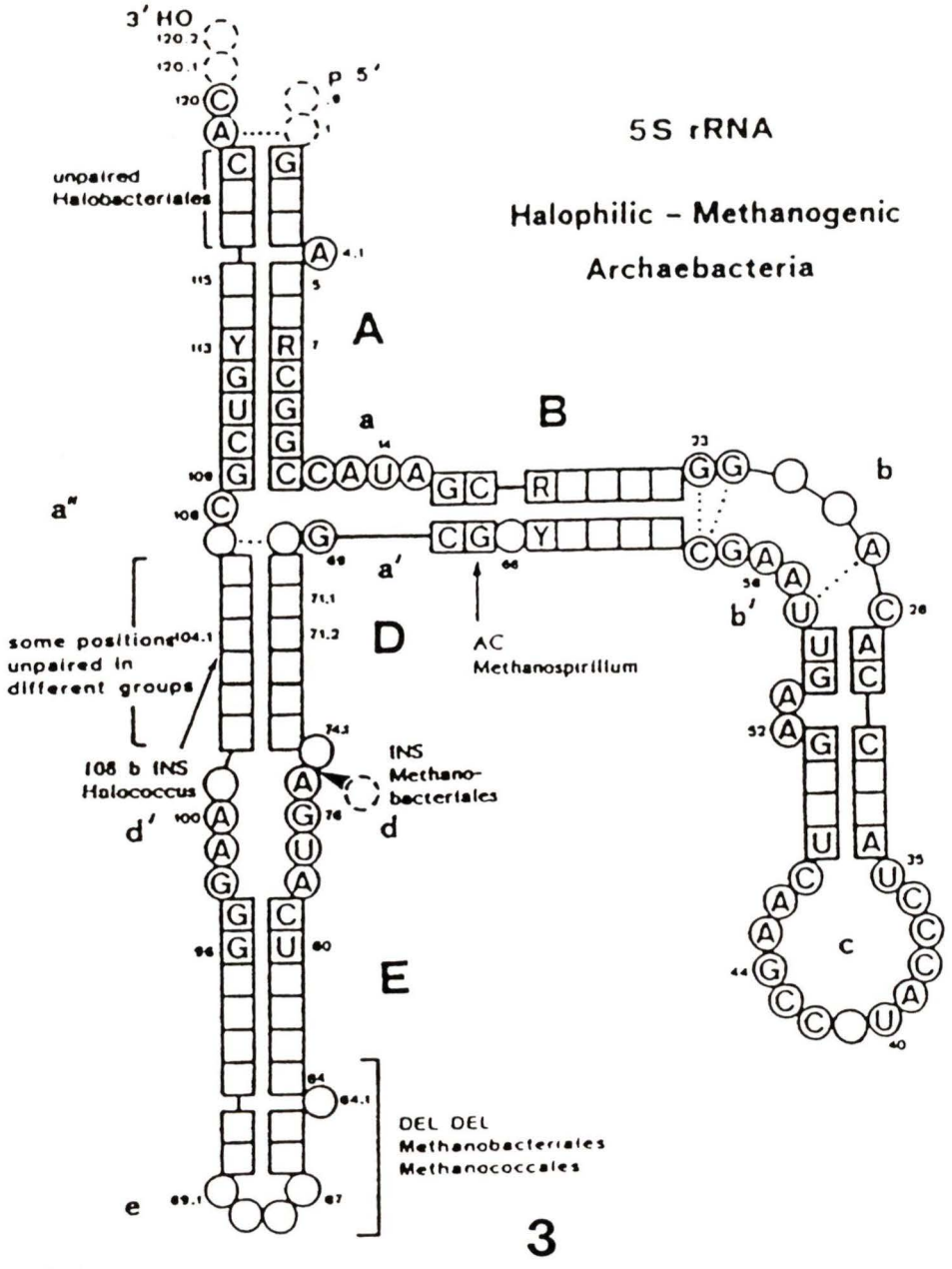

Figure 2 (continued)

conformation. For this reason, several independent groups have obtained direct experimental information on the structure of 5S rRNA, using a variety of nucleases and chemicals as effective probes of RNA structure. The reactivity of these probes is highly dependent upon secondary and/or tertiary structural features. There is now general agreement that the common secondary structure of all 5S rRNAs is composed of five helices, **I** to **V**, connected by loops **A** to **E**. Although no crystallographic data support the proposed structure, its strength is derived from experimental data in which the major features of this model have been confirmed by the study of solution structures of prokaryotic and eukaryotic 5S rRNAs using enzymatic and chemical probes (Noller and Garret, 1979; Toots *et al.*, 1981; Troutt *et al.*, 1982; Silberklang *et al.*, 1983; Kjems *et al.*, 1985; Digweed *et al.*, 1986; Sneath *et al.*, 1986; and Romaniuk *et al.*, 1988). Although data from these experiments are mainly in agreement with the accepted general secondary structure model, several regions of the molecule have not been completely explained by these methods.

Helix **V** constitutes one of the most pronounced differences in the structural organization of eubacterial, archaebacterial and eukaryotic 5S rRNA. The presence of a helix **V** in eubacteria of at least 2bp was detected biochemically by MacDowell and Colwell (1985) and Wolters *et al.* (1986), and is now undisputed. Nevertheless, the chain length and base-pairing scheme of this region as a whole still remains the major difference between eubacteria and eukaryotes as well as between various archaebacterial groups.

The extended base-pairing scheme, as well as A-G bonding in the region between helices **IV** and **V** were first formulated by Stahl *et al* (1981). There is both phylogenetic and experimental evidence for the presence of

non-Watson Crick A-G base-pairing in the stem of 5S rRNA that contains helices **IV** and **V**. For example, gram-positive bacteria and most other eubacterial 5S rRNA have the conserved pair A_{104}-G_{72}. However, in *Streptococcus cremoris* 5S rRNA, helix **V** appears to be "rearranged" with an insertion of one base pair , but the A-G pairing is maintained at positions 103 and 73 (Neimark *et al.*, 1983). According to these authors, the significance of this transposition lies in the apparent conservation of the A-G pair as opposed to the conservation of nucleotides A and G at positions 104 and 72, respectively. As pointed out by Stahl *et al* (1981), helix **V** can be extended in most 5S rRNAs by the inclusion of conserved A-G pairing. The exceptions are the cyanobacterial and chloroplast 5S rRNAs, but these RNAs have the following Watson-Crick or non-Watson-Crick pairing at the same positions: A-U (*Anacystis nidulans*), A-C (*Synechococcus lividus*), and A-A (chloroplast). It is interesting to note that the 5S rRNA from the thermoacidophile archaebacterium *Sulfolobus acidocaldarius* contains Watson-Crick base pairs along the whole arm that contains helices **IV** and **V.** According to Stahl *et al.*, (1981) the presence of Watson-Crick base pairs in this region of the *Sulfolobus* 5S rRNA provided phylogenetic evidence for the extension of base pairing between helices **IV** and **V** in all 5S rRNAs which contained phylogenetically conserved A-G base pairs.

In subsequent studies on the structure of *Xenopus* oocyte 5S rRNA, Andersen *et al.* (1984) proposed a base-paired conformation in the region between helices **IV** and **V**, consisting of A_{74}-U_{102}, G_{75}-A_{101}, U_{76}-A_{100}, and A_{77}-G_{99}, leaving U_{73} unpaired (Figure 3). Experimental evidence for this continued base-pairing came from cleavages caused by cobra venom ribonuclease V_1 (which is specific for double-stranded or structured regions)

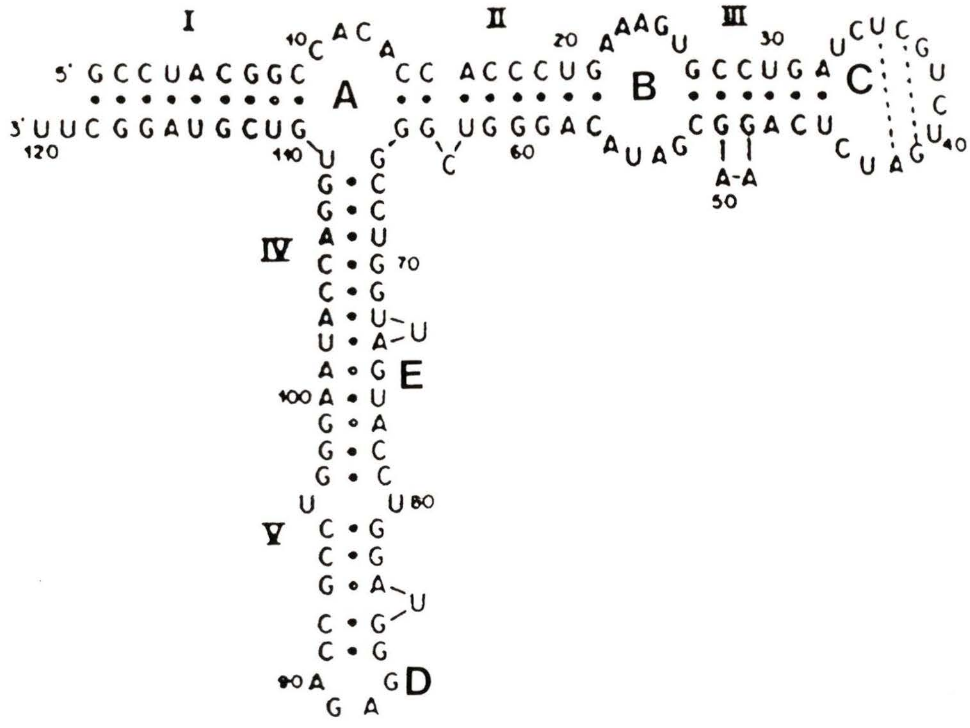

Figure 3: Proposed *X. laevis* oocyte 5S RNA secondary structural model. On the basis of RNase V1 cleavage data, the Xlo 5S RNA sequence is shown with extended base pairing between helices IV and V. Potential phylogenetically conserved base pairing between C36 and G41 and between U35 and A42 is represented by dotted lines (after Andersen *et al.*, 1984).

at putative single-stranded loop **E** located between helices **IV** and **V**. More recently, based upon chemical reactivity data, a model of the structure of loop **E** in *Xenopus laevis* oocyte 5S rRNA was also proposed by Romaniuk *et al.*, (1988). However, in this model the structure of loop **E** consists of an extended conformation of non-canonical base-pairing between U_{73}-U_{102}, A_{74}-A_{101}, G_{75}-A_{100}, and U_{76}-G_{99}, leaving A_{77} unpaired (Figure 4). In addition, recent enzymatic and chemical reactivity studies on spinach chloroplast 5S rRNA, have shown that this region contains an extended and unwound conformation based on several A-A and A-G base-pairs (Romby *et al*, 1988). In summary, these observations suggest that in the cases mentioned above the nucleotides of loop **E** are involved in base-pairing not previously shown in the secondary structure model of 5S rRNA.

Besides the five double-helical segments, the secondary structure of 5S rRNA has several features such as internal loops and bulged residues in helical regions that are not found in tRNA. Internal loops have been postulated to be directly involved in the orientation of the helical regions, and bulged nucleotides have been proposed to have a role in protein binding (Peattie *et al.*, 1981; Christiansen *et al.*, 1985).

Tertiary Interactions

Little is known of the tertiary structure of RNA; only in the case of tRNA do we have exact knowledge of a tertiary structure from the data provided by X-ray crystallography studies of $tRNA^{Phe}$ (Jack *et al.*, 1976; Quigley *et al.*, 1975;) and $tRNA^{Asp}$ (Westhof *et al.*, 1984). By means of X-ray crystallography, it has been shown that extensive folding of the duplex arms of tRNA molecules occurs through hydrogen bonds between certain bases. This hydrogen-bonding is believed to be important in stabilizing the tertiary

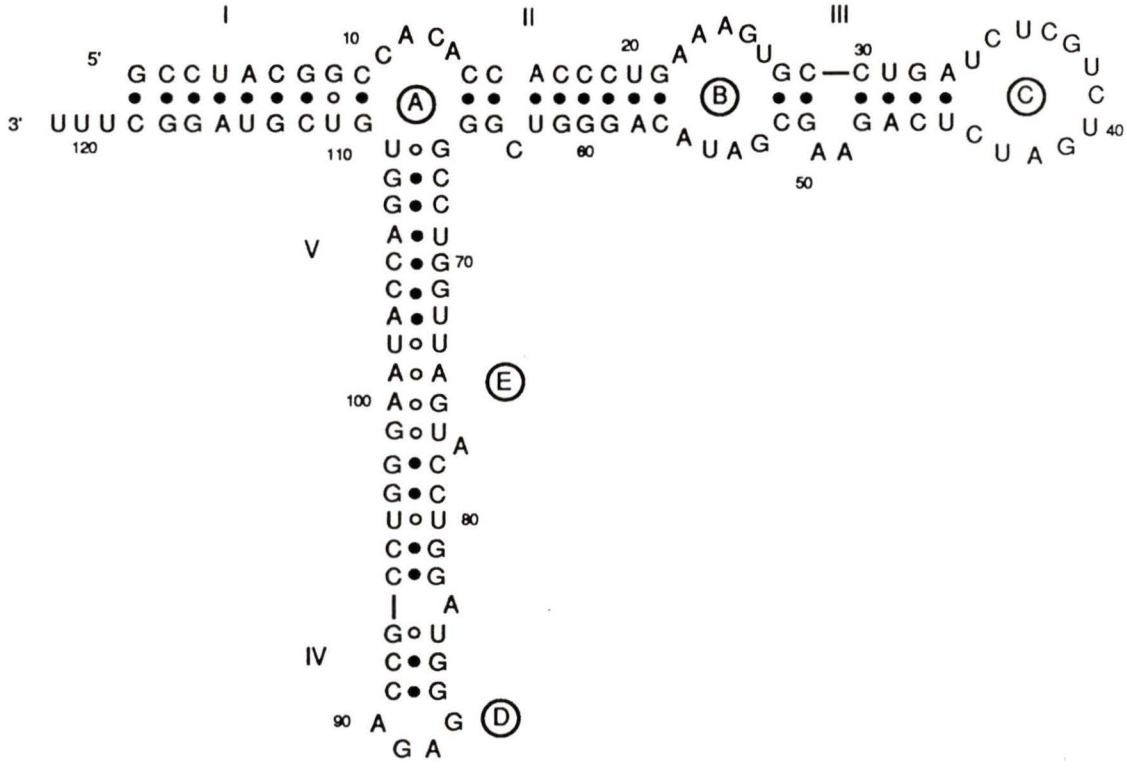

Figure 4: *X. laevis* oocyte 5S rRNA secondary structural model. On the basis of enzymatic cleavage and chemical modification data, the Xlo 5SrRNA secondary structural model has been modified by extended base pairing in the region between helices IV and V (Romaniuk *et al.*, 1988).

folding of RNA. These studies have provided evidence that RNA has the capacity to form a variety of tertiary interactions different from the classical Watson-Crick base-pairing types, such as base stacking-interactions, triple base interactions and non-canonical base pair interactions. Some observed non-canonical interactions are listed in Table 1. This list is not exhaustive, and it is probable that other hydrogen bonding combinations, not yet observed, exist.

As yet, relatively little is known about the tertiary structure of 5S rRNA, although a number of different studies, utilizing a variety of physical and chemical probes, suggest that 5S rRNA has a more complex structure than that postulated by current estimates of the secondary structure. Several tentative tertiary structure models have been proposed, essentially for *E. coli* 5S rRNA, which would bring loops **C** and **E** into close proximity.

In one study, Hancock and Wagner (1982) showed that in *E. coli* 5S rRNA G_{41} could be cross-linked to G_{72}, using the bifunctional reagent phenyldiglyoxal, and suggested that the G_{72}-G_{76} sequence interacts with C_{37}-G_{41} to fold the molecule into a three-dimensional structure (Figure 5).

In another study, based on enzymatic accessibility, a tertiary structure model for *E. coli* 5S rRNA was proposed by Pieler and Erdmann (1982). In this model, the arm of helix **III** folds to form base-pair contact points with a region of the arm encompassing helices **IV** and **V**, and tertiary base-pairing between $GCCG_{44}$ and $UGGU_{77}$ is formed (Figure 6). For many (but not all) eubacterial 5S rRNAs, at least three base-pairs from these two regions can be formed with Watson-Crick and G-U pairing. In addition, Böhm *et al* (1981), on the basis of infrared spectroscopy, have proposed that in *E. coli* 5S rRNA, loop **C** is organized in a highly ordered structure and is involved in tertiary interactions which consist of parallel base pairing between $C_{37}CAU_{40}$ and

Table 1. Non-canonical interactions in nucleic acids.*

Interaction	Hydrogen Bond	Observed in
A-U	(N7,N6)-(N3,O2)	$tRNA^{Phe}$, $tRNA^{Asp}$: A_{14}-U_8, A_{58}-T_{54}[1,2,3]
A-U	(N1,N6)-(N3,O2)	$tRNA^{Asp}$: A_{15}-U_{48}[3]
A-G	(N1,N6)-(N1,O6)	$tRNA^{Phe}$, $tRNA^{Asp}$: A_{44}-G_{26}[1,2,3]
A-G	(N6)-(N7)	$tRNA^{Asp}$: A_{46}-G_{22}-U_{13}[3]
A-A	(N6,N7)-(N7,N6)	$tRNA^{Phe}$, $tRNA^{Asp}$: A_9-A_{23}-U_{12}[1,2,3]
G-G	(N3,N2)-(N2,N3)	β-dodecamer[4]
G-G	(N6)-(N7,O6)	$tRNA^{Asp}$: G_{45}-G_{10}-U_{25}[3]
G-G	(N6)-(O6)	$tRNA^{Phe}$: G_{45}-G_{10}-C_{25}[1,2]
G-G	(N1,N2)-(N7,O6)	$tRNA^{Phe}$: m^7G_{46}-G_{22}-C_{13}[1,2]
U-U	(N3,O4)-(O2,N3)	$tRNA^{Asp}$: U_{35}-U_{35}[3] (anticodon-anticodon interaction)
C-C	(N4,N3)-(N3,O2)	$tRNA^{Gly}$: C_{35}-C_{35}[5] (anticodon-anticodon interaction)
C-C	(N4,N3,O2)-(O3,N3,N4)	poly C[6]

[1] Quigley *et al.* (1975)
[2] Jack *et al.* (1976)
[3] Westhof *et al.* (1985)
[4] Wing *et al.* (1980)
[5] Romby *et al.* (1986)
[6] Cantor and Schimmel (1980)
*(after Ehresmann *et al.*, 1987)

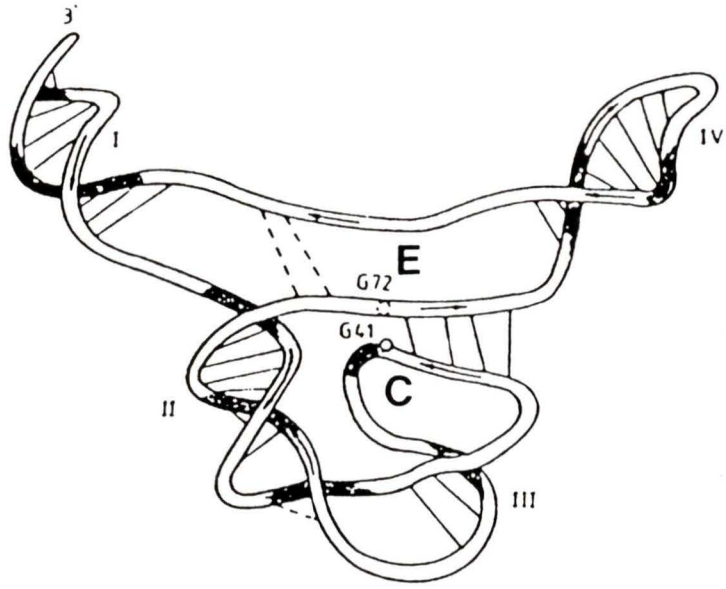

Figure 5: Schematic representation of the three-dimensional arrangement of *E. coli* 5S RNA. The 5'- to 3'-direction is indicated by arrow. Crosslinked guanosines are numbered. Dark areas are behind the plane of the figure whereas white areas are in front (after Hancock and Wagner, 1982).

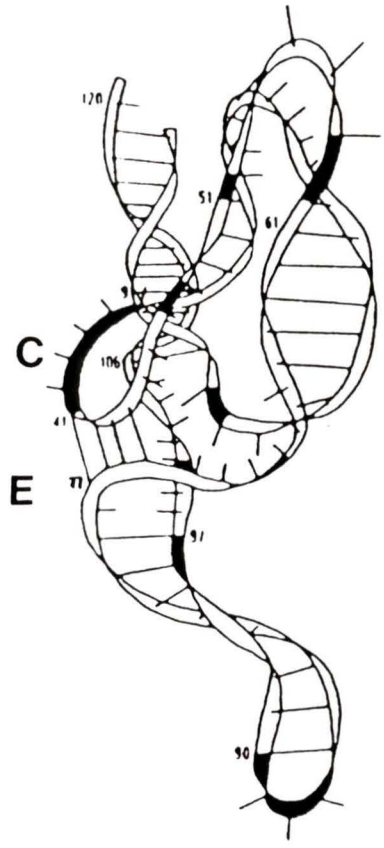

Figure 6: Schematic representation of a molecular tertiary structure model of *E. coli* 5S RNA based on single-strand nuclease S1 digestion studies. Shaded areas indicate sites of nuclease S1 cleavage (after Pieler and Erdmann, 1982).

$G_{75}GUA_{78}$ (Figure 7). Furthermore, in *E. coli* 5S rRNA, a model with a pseudoknotted structure between helix **IV** and loop **C** has been proposed by Göringer and Wagner (1986). A pseudoknotted structure is a specific folding of RNA, experimentally proven for a number of RNA molecules and found to occur when bases within a loop interact with single-stranded bases outside the stem region of this loop (Pleij *et al.*. 1985). In their model, Göringer and Wagner (1986) propose that a helical segment can be formed by parallel tertiary base pair interaction between nucleotides C_{35} to C_{37} and G_{105} to G_{107}. Helix **III** is then extended by coaxial stacking, thereby forming a quasi-continuous helix (Figure 8).

In eukaryotes, McDougall and Nazar (1983) have examined the tertiary structure of 5S rRNA by using N-ethylnitrosourea (ENU) reactivity as a probe for phosphodiester bonds. In these experiments, three different 5S rRNAs of diverse origin (rat liver, *Saccharomyces cerevisiae*, *Thermomyces lanuginosus*) were found to contain phosphates protected from reaction with ENU in the same three regions of the sequence, corresponding to residues G_{99}-A_{101}, A_{88}-G_{89}, and G_{75} in the rat 5S rRNA molecule. The ENU reactivity results, together with the observation that four of these residues (G_{75}, G_{89}, G_{99}, A_{100}) are universally present in all 5S rRNAs, suggested to these authors that these regions could participate in tertiary structure formation. Based on these data, a model was postulated in which the two arms that constitute regions **C** and **D** of the secondary structure overlap to form a tertiary structure in the shape of a loop or " lollipop "-like structure. As shown in Figure 9, in such a structure the phosphodiester bonds of the five residues which are less reactive to ENU would be free to interact with the opposite arm or at least could be screened by this interaction.

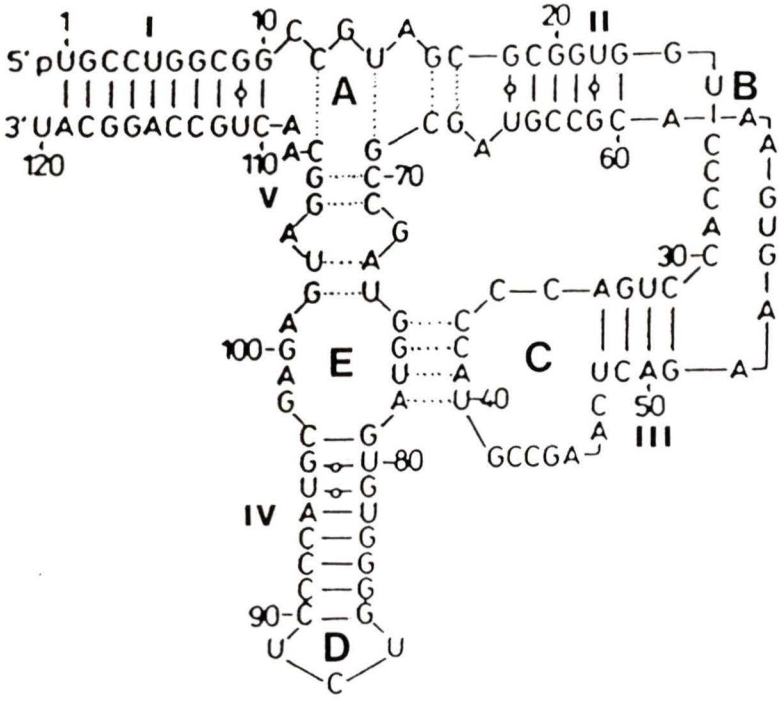

Figure 7: Proposed base-pairing scheme of *E. coli* 5S RNA adapted to the proposed generalized base-pairing scheme of prokaryotic 5S RNAs: ___ more stable base pairs; ..... less stable base pairs; . . . weak secondary / tertiary structure base pairs; (I-V) helices; (A-E) loop regions (after Böhm *et al.*, 1981).

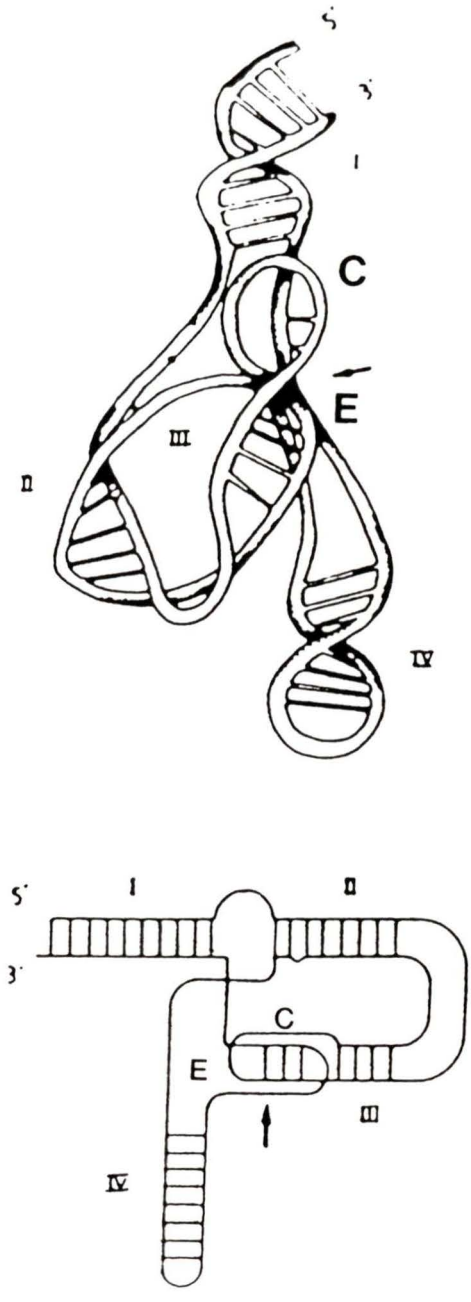

Figure 8: Schematic illustrations of the *E.coli* pseudoknotted 5S rRNA structure. Spatial illustration of the 5S rRNA structure (top); schematic arrangement of the 5S rRNA structure (bottom). Helices I to IV are indicated by roman numerals. Arrows point to the regions where pseudoknots are formed (after Göringer and Wagner, 1986).

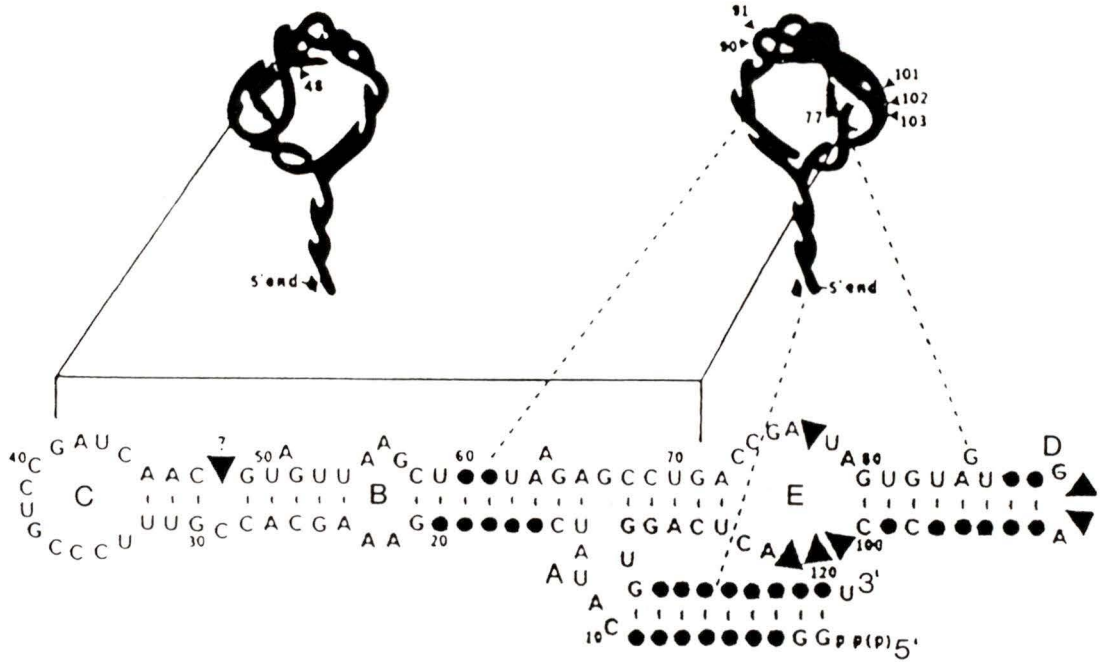

Figure 9: Topography of ethylnitrosourea-resistant phosphates in estimates of the secondary and tertiary structures of the yeast ribosomal 5S RNA. Solid triangles indicate residues partially resistant to ethylnitrosourea modification; solid circles and broken lines indicate modified residues or helical regions in which base modifications were previously shown to be partially excluded from the 5S RNA-protein complex (Pieler and Erdmann, 1983); solid line joins nucleotides which have been chemically cross-linked in the *E. coli* 5S RNA (Hancock and Wagner, 1982) (after McDougall and Nazar (1983).

Furthermore, two distinct conformers of rat liver 5S rRNA were investigated by Toots *et al.* (1982) using enzymatic cleavage techniques. The cleavage pattern results showed differences in secondary structure and possibly different tertiary base-pairing interactions between the two 5S rRNA conformers. As a result, these authors proposed a structure where the $UCUC_{36}$ sequence in rat liver 5S rRNA has the potential to form a Watson-Crick base paired interaction with the $GAGA_{90}$ sequence of loop D.

More recently, Westhof *et al.* (in press) have constructed a detailed atomic model of a eubacterial 5S rRNA (spinach chloroplast 5S rRNA) and of a eukaryotic 5S rRNA (somatic and oocyte 5S rRNA from *Xenopus laevis*) by computer graphic modelling. These models combine stereochemical constraints and experimental data on the accessibility of bases and phosphates towards structure-specific probes (Figure 10). According to these authors, by combining experimental data resulting from structure probing of RNA in solution and specific information collected from the known crystallographic structures of tRNAs, it is possible to construct three-dimensional models of RNA. The validity of their procedure is supported by the fact that in tRNA there is a good correlation between the results obtained from structure probing experiments and those obtained from X-ray crystallographic studies (Peattie and Gilbert, 1980; Romby et al., 1985; 1987). The following conclusions were reached by generalizing the features of the above mentioned models: (i) both models adopt a distorted Y-shape structure with helices **II** and **V** not far from coaxiality; (ii) no tertiary interactions exist between loop **C** and region **E** or loop **D**; (iii) internal loop **E** contains several non-canonical base pairs of A-A, U-U, and A-G types; (iv) invariant residues appear to be more important for protein or RNA binding than for maintaining the tertiary structure. It is

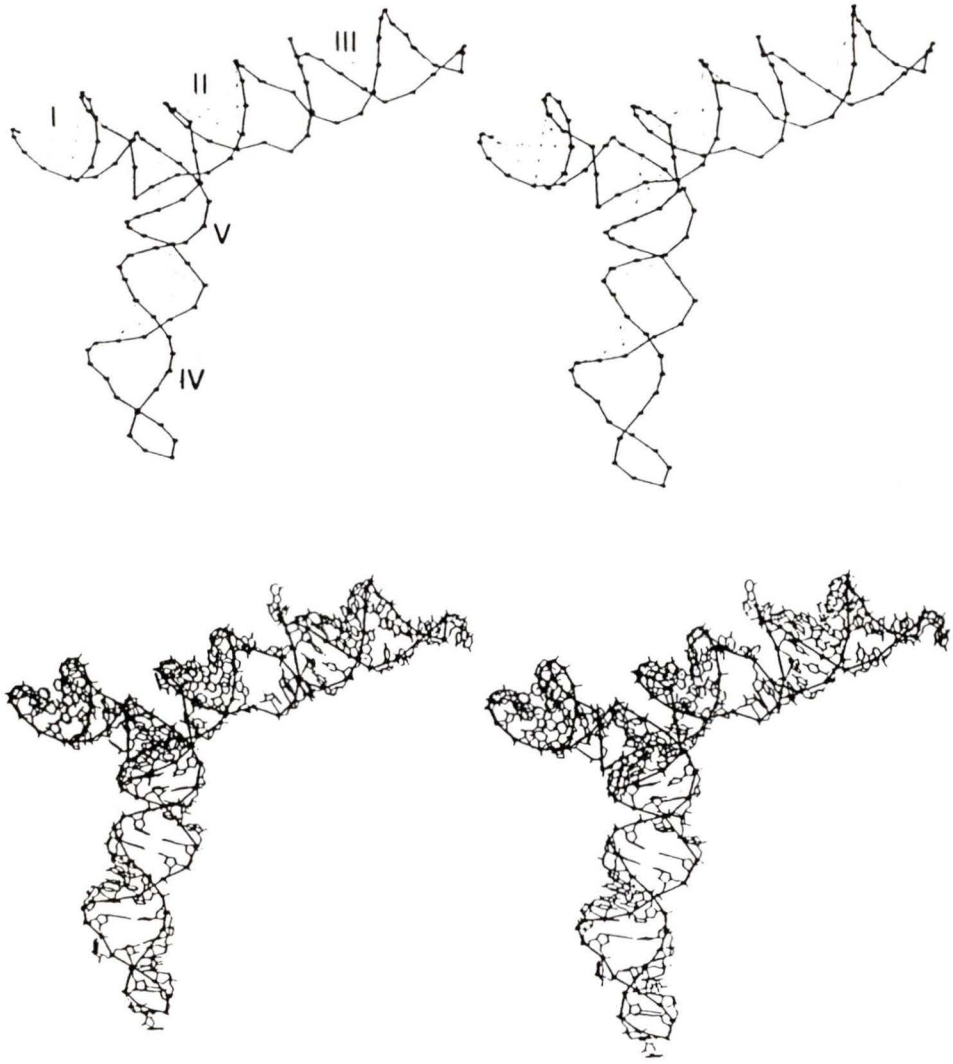

Figure 10: Three-dimensional models of *X. laevis* oocyte 5S rRNA. (Top) Phosphate backbone with the Watson-Crick base pairs joined by lines and the non-canonical or tertiary base pairs joined by dotted lines. (Bottom) Atomic view in the same orientation with the phosphate backbone shown in heavy lines. All stereo views were drawn with the program PLUTO (after Westhof *et al.*, in press).

interesting to note that this model follows closely the secondary structure of 5S rRNA, and does not resemble any of the previously discussed models. Most of the differences between this model and the previously published models occur at the fork of the Y-structure. However, the Y-shaped structure proposed in this model is similar to models previously proposed for *E. coli* 5S rRNA by Osterberg *et al.*, (1976) on the basis of small angle X-ray scattering, and by Fox and Wong (1979) on the basis of hydrodynamic measurements. This model is, moreover, supported by additional observations: (i) the coaxiality between helices **II** and **V** had previously been suggested for *X. laevis* oocyte 5S rRNA to explain the binding site of TF IIIA (Christiansen *et al.*, 1987); (ii) the chloroplast 5S rRNA binding sites of two ribosomal proteins are well explained by this model (Toukifimpa *et al.*, 1988). The *E. coli* ribosomal protein binding site for L18 and L25 also agree with this model (Christiansen *et al.*, 1985; Kime and Moore, 1983).

However, no tertiary structure model has been shown to be universally applicable by phylogenetic sequence comparisons. More data on the tertiary structure of 5S rRNA is no doubt required before we can ascertain whether any of the models so far proposed accurately represents the structure of this molecule. For now, the models presented here indicate important regions which should be considered in any future model of the overall structure of 5S rRNA.

It should be pointed out that crystallographic studies have been carried out on a fragment of *E. coli* 5S rRNA, on a complex of this fragment with ribosomal protein L25 (Abdel-Meguid *et al*, 1983), on *Thermus thermophilus* 5S rRNA (Morikawa *et al*, 1982), and, more recently, on a complex of *X. laevis* oocyte 5S rRNA and transcription factor IIIA (Brown, 1985). To date, the

quality of these crystals has not been sufficient to obtain an X-ray structure at high resolution; nevertheless, the molecular structure of some of these crystals has been studied using electron microscopy (Morikawa *et al*, 1986; Brown *et al*, 1988).

Alternate 5S rRNA Structures

Part of the difficulty in determining 5S rRNA structure derives from the multiplicity of forms the molecule can assume, depending on treatment and buffer conditions. The best known transformation is the transition between the A and B forms of the *E. coli* 5S rRNA, in which heat or urea treatment converts the 5S rRNA from the native or A form to the denatured or B form (Aubert *et al*, 1968). These two conformations remain in chemical equilibrium over a wide range of temperature and ionic strength and were discovered because of their difference in electrophoretic and chromatographic mobility. The transition requires an activation energy of 65 kCal/mol and involves the disruption and re-forming of an estimated nine base pairs (Lecanidou and Richards, 1975). However, this transition from native to denatured form is not believed to be important in ribosomal function because of the harsh conditions necessary for interconversion, and the fact that only one of these forms, the A form, complexes specifically with ribosomal proteins in ribosomal subunit reconstitution experiments (Bellemare *et al*, 1972). Furthermore, Christensen *et al* (1985) have recently examined the stucture of the B form by employing single- and double-strand-specific nucleases and nucleotide-specific reagents. In this study they show that the B form exhibits a secondary structure only a part of which is both universal and conformationally homogeneous, and have concluded that the B form cannot participate in protein biosynthesis.

Besides the conformers A and B, there is evidence that 5S rRNAs have additional conformational switches. In several studies, a less dramatic change has been recorded within the tertiary structure of the A form. In one of these studies, two structural forms of the *E. coli* 5S rRNA were detected by nuclear magnetic resonance (Kime and Moore, 1982). NMR spectral changes indicated the existence of two distinct conformers of the molecule which meet the operational definition of the A form or native 5S rRNA. Both are easily distinguished spectroscopically from the denatured, B form 5S rRNA, and the interconversion of the two forms is dependent upon the addition of monovalent or divalent cations and salt, for which reason they were termed high- and low-salt forms. The NMR data indicated that a substantial difference in the arrangement of bases must exist between these two forms. It has been suggested that these two forms correspond to the high- and low-temperature states of the *E. coli* 5S rRNA which had previously been identified optically, using laser light scattering studies, by Kao and Crothers (1980). The transition between these two states, which occur at near physiological temperatures and pH, is characterized by overall compaction of the molecule and by the production of a detectable hyperchromic effect in 5S rRNA preparations. In subseqent studies, Rabin *et al.* (1983) investigated *E. coli* 5S rRNA in the low and high salt forms by partial digestion with single-strand specific ribonuclease T_1. These authors observed differential changes of accessibility when magnesium and salt concentrations were increased to bring about the low to high transition.

It has been shown that the high-salt or high-temperature form (A_H) binds ribosomal proteins and assembles into the 50S subunit, and the low-salt or low-temperature form (A_L), of uncertain biological relevance, binds at

least one ribosomal protein and appears to differ in tertiary structure from the A_H form (Rabin *et al*, 1983). In addition, Christensen *et al* (1985) have studied the progressive structural changes that occur during the transition from A_H to A_L by using chemical and enzymatic reactivity studies, and have provided evidence that a functionally important structural change occurs in loop **B** during this transition.

In eukaryotes, three different conformers of rat liver 5S rRNA were investigated by Toots *et al.* (1982) on the basis of enzymatic accessibility. These authors found that urea-treated and renatured 5S rRNA co-migrate on non-denaturing gels, but exhibit distinct differences in their nuclease cleavage patterns. The third conformer of 5S rRNA with higher electrophoretic mobility was generated by EDTA treatment, and its cleavage pattern was found similar to that of the renatured 5S rRNA. The results of this study demonstrate differences in secondary structure and possibly different tertiary base-pairing interactions in these 5S rRNA conformers.

Moreover, De Wachter *et al* (1984) have studied equilibria in eukaryotic 5S rRNA secondary structure. These authors propose that 5S rRNA can form a series of slightly different structures of nearly equal stability. These different structures arise from the existence of sets of alternative base-pairing schemes in bulged helices and the adjacent interior loops. These alternative schemes are not just a subset of the huge number of base-pairing possibilities that could occur in any sequence having the same length as that of 5S rRNA, because exactly the same sets, in exactly the same sequence areas, are encountered in a wide variety of 5S rRNAs (De Wachter *et al.*, 1984). Therefore, these authors postulate that these base pairing schemes correspond to actually existing alternative secondary structures,

which are in dynamic equilibrium with each other. Some of these equilibria are believed to be completely universal, such as forms C1 and C2, others are confined to eukaryotic 5S rRNAs, such as the potential for the equilibria in helix **IV** of forms E1 to E5 (Figure 11). In summary, these different forms are believed to correspond to actual structures assumed at different moments by the 5S rRNA molecule, and the significance of these secondary structure equilibria may lie in the fact that they provide the otherwise rigid helices with the flexibility required to participate in the movement of a dynamic 5S rRNA molecule. A change in secondary structure in specific areas may influence the relative orientation of the surrounding helices, while the bulges and interior loops may serve as articulations to give rise to a flexible tertiary structure (De Wachter *et al.*, 1984).

So far, there is no strong indication of whether the different conformational states of 5S rRNA are functionally relevant, but their occurrence is no doubt significant, and their detailed characterization is very important for the study of 5S rRNA structure. In summary, some of these conformational switches, which might have a functional role, are also reponsible for some of the discrepancies found in the proposed models, since they complicate studies on the structure of 5S rRNA. Despite multiple approaches to the study of the structure of this molecule, its three-dimensional arrangement still remains unsolved, and additional precise information of the structure is still needed.

Structural Elements Involved in the 5S rRNA-TFIIIA Interaction

Recently, several groups have investigated the structural requirements for the interaction of *Xenopus laevis* oocyte 5S rRNA with the eukaryotic transcription factor IIIA. It is known that the binding of TFIIIA to 5S rRNA is

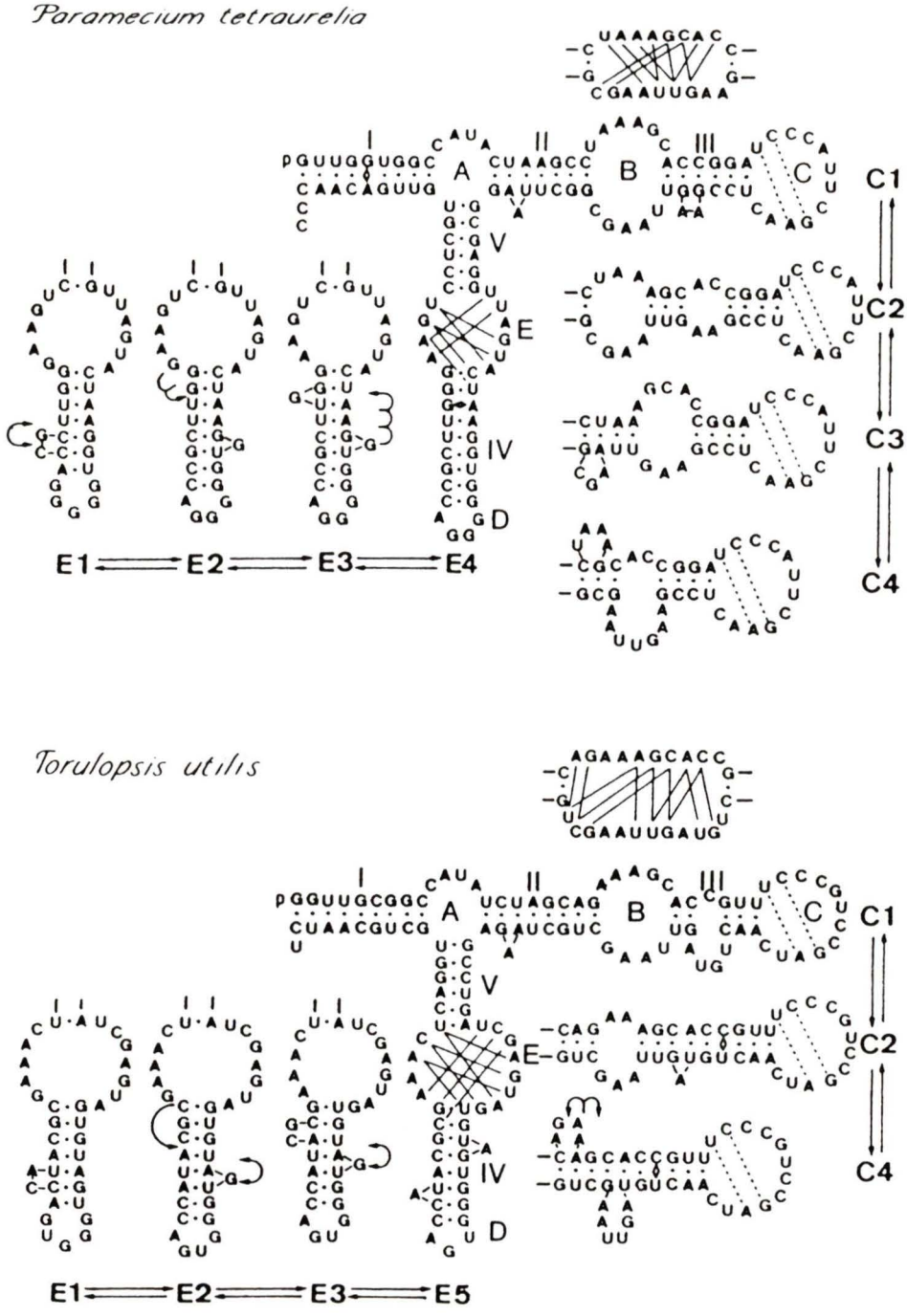

Figure 11: Equilibrium forms in 5S RNA secondary structure.The base-pairs G-C and A-U are indicated by a dot; non-standard base-pairs by a losenge. Lines connecting nucleotides above area B and in area E indicate ambiguous base-pairing opportunities. Alternative secondary structures in loop B and helix III are numbered C1 to C4, and in helix IV, E1 to E5. Alternative positons of bulges are indicated by arrows. Broken lines in loop C indicate potential (U-A) and (G-C) pairing (after De Wachter et al., 1985).

highly specific. For example, the affinity of TFIIIA for tRNA is over 100 times lower than it is for *Xenopus* 5S rRNA. Footprinting experiments, using a variety of structural probes, have shown that TFIIIA interacts primarily with the helix **II**/loop **B** and helix **IV**/loop **E**/helix **V** structural domains of the 5S rRNA (Romaniuk, 1985; Pieler and Erdman, 1983; Andersen *et al*, 1984; Huber and Wool, 1986; Christensen *et al*, 1987) (Figure 12). Further, several independent studies have shown that only a small amount of conserved RNA sequences are essential for the binding of TFIIIA with the 5S rRNA molecule, whereas universal 5S rRNA secondary structure features seem to be required. For example, in one study using *in vitro* transcription competition assays, a variety of eukaryotic, eubacterial and archaebacterial 5S rRNAs inhibited the transcription of *X. laevis* 5S rRNA genes (Pieler *et al*, 1984). In another study, several eukaryotic and eubacterial 5S rRNAs have been shown to interact specifically with TFIIIA in an RNA exchange assay (Romaniuk, 1985; Andersen and Delihas, 1986). What all these 5S rRNAs have in common is the generalized secondary structure for 5S rRNA, and from these results it becomes apparent that universal secondary structure elements, rather than conserved sequences, appear to be required for the interaction of TFIIIA with 5S rRNA. Furthermore, experimental evidence reveals that maintenance of the higher order structure of *Xenopus laevis* oocyte 5S rRNA is essential for the RNA to complex with the protein (Pieler *et al*, 1986; Romaniuk *et al*, 1989). According to Romaniuk *et al.* (1989) TFIIIA may bind to 5S rRNA by recognizing its unique tertiary structure and forming a number of relatively weak sequence-specific contacts with the nucleotides in single stranded loops.

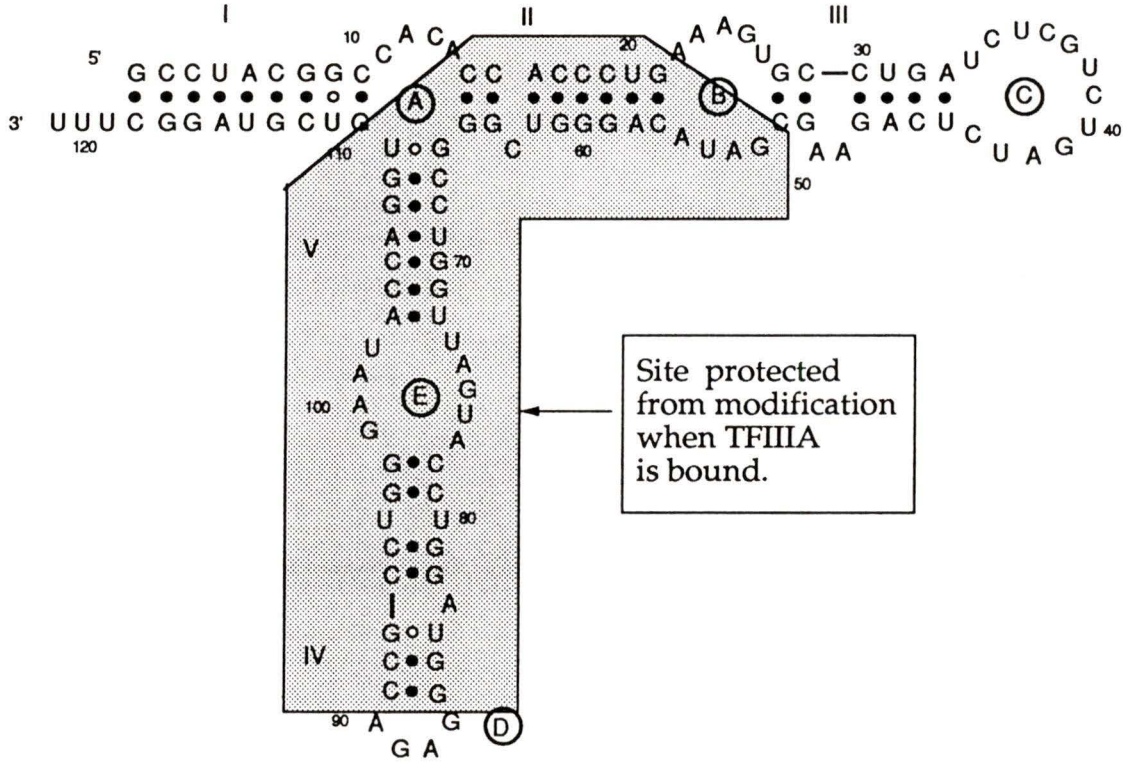

Figure 12: Secondary structure of *X. laevis* 5S rRNA showing the TFIIIA footprint area (Romaniuk, 1985; Pieler and Erdmann, 1983; Christiansen *et al.*, 1987).

Description of Project

Recent advances in the synthesis of oligonucleotides have provided a powerful technique that can be used to introduce specific mutations into DNA, RNA or protein in order to probe its structure. For this project, it was decided to introduce several mutations into the *Xenopus laevis* oocyte 5S rRNA gene in order to study the effect that these mutations would have on the structure of the 5S rRNA transcribed from the gene. Four different mutants (Xlo 73-76, Xlo 87-90, Xlo 99-101 and Xlo 96-101) were constructed by means of introducing base substitutions in loops **D** and **E** of the 5S rRNA structure (Figure 13). Three of the mutants shown in Figure 13 have sequence substitutions in loop **E** (Xlo 73-76, Xlo 99-101 and Xlo 96-101). Mutant Xlo 96-101 contains three nucleotide substitutions, in order to convert the unusual loop **E** conformation into a Watson-Crick base paired A-type RNA double helix, and mutant Xlo 87-90 has sequence substitutions in loop **D**. The mutations were chosen in these particular regions because these single-stranded regions have been phylogenetically conserved throughout the eukaryotic kingdom (Figure 14). In the construction of these mutants the following considerations were taken into account: if the nucleotide to be substituted was highly conserved, then the substitution was chosen to be semi-conservative (e.g. a purine exchanged by a purine), in order to create a small conformational change. On the other hand, if the nucleotide to be substituted was not conserved, then a purine was exchanged for a pyrimidine, or viceversa. As shown in Figure 14, loop **E** has the following highly conserved residues: A_{74}, G_{75}, U_{76}, A_{77} and G_{99}, while A_{100} and A_{101} are semi-conserved residues. In loop D, residues G_{87}, G_{89} and A_{90} are all known to be highly conserved. The fact that these sequences have been conserved implies

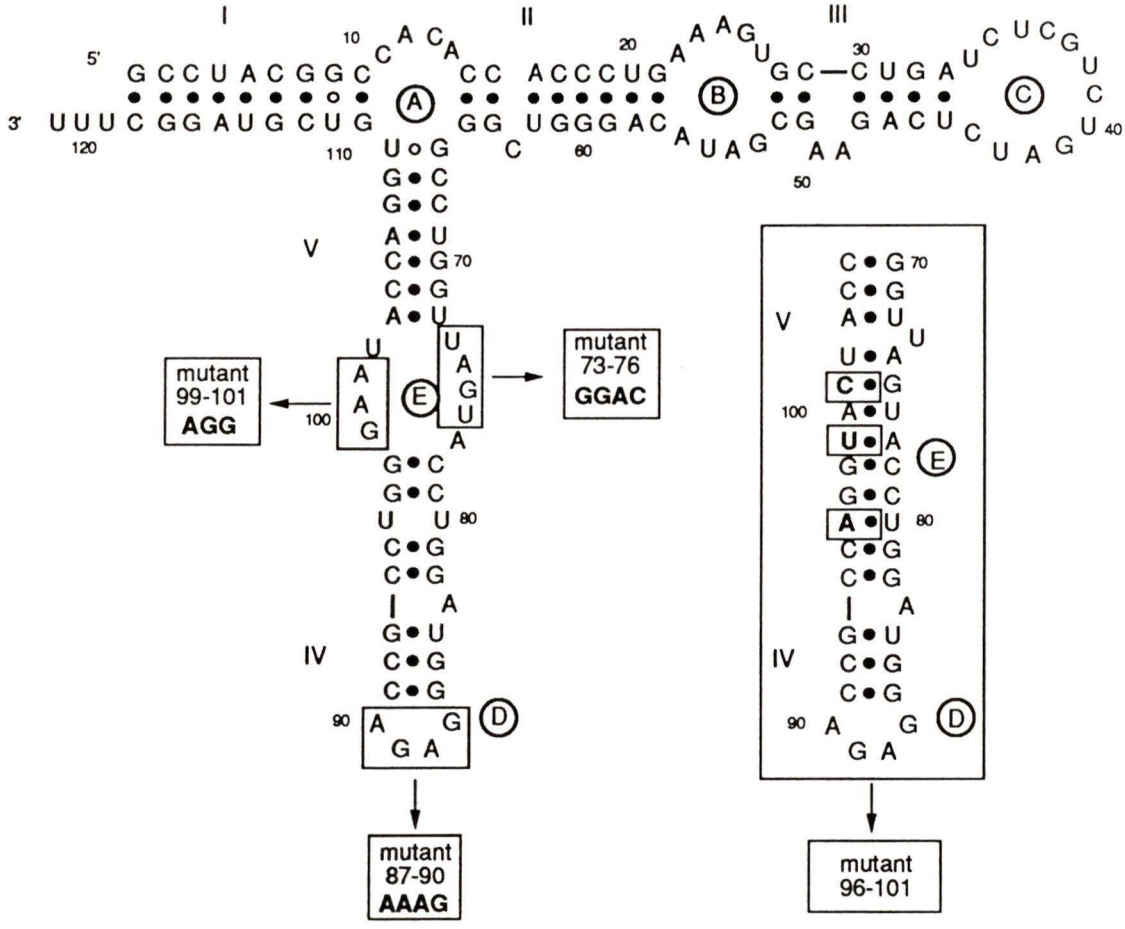

Figure 13: Four mutant 5S rRNA molecules. Secondary structure model of *X. laevis* oocyte 5S rRNA, showing the base substitutions introduced to create the four mutants used in this study.

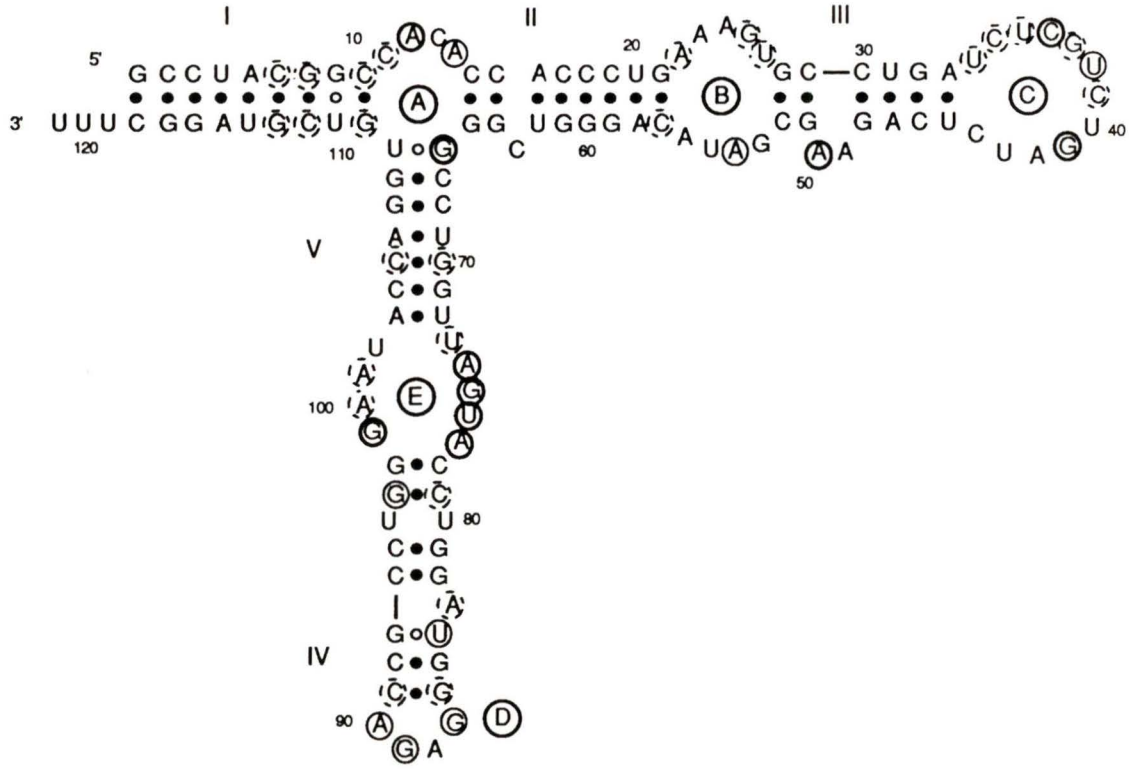

Figure 14: Conserved residues of eukaryotic 5S rRNA shown on the secondary structure of *X. laevis* oocyte 5S rRNA. The strictly conserved residues (in 258 sequences of eukaryotic 5S rRNAs) are circled with bold lines, the residues conserved above 95% are circled with thin lines and the semi-conserved residues are circled with broken lines (adapted from Westhof *et al.*, in press).

that they could play a role in the function of 5S rRNA, or may contribute to its tertiary structure. Therefore, the study of the effect of these substitutions on the structure of 5S rRNA might offer some information that can be used to refine the structure models for loops **D** and **E** of *Xenopus laevis* 5S rRNA.

In the present work, the effect of these mutations on the 5S rRNA structure was investigated by testing the reactivity of nucleotides to structural probes in the form of enzymatic and chemical reagents. These studies were conducted using the single-strand specific nucleases T_1, T_2, A and S_1, and the double-strand- or structure-specific ribonuclease V_1. The accessibility of purine N7 positions was determined using the chemical probes dimethyl sulfate (DMS) for guanines, and diethylpyrocarbonate (DEPC) for adenines, under native and semi-denaturing (absence of magnesium) conditions. The accessibility of Watson-Crick positions in both native and semi-denatured 5S rRNAs was determined at A-N1 and C-N3 positions using DMS, and at G-N1 and U-N3 positions using N-cyclohexyl-N'-(2-morpholinoethyl) carbodiimide metho-p-toluene sulfonate (CMCT). The reactivity of phosphate residues to alkylation under native conditions was determined using ethylnitrosourea (ENU).

The procedures just enumerated will become more clear in the following section, where an attempt is made to familiarize the reader with the methods used to probe the structure of 5S rRNA.

Overall Probing Strategy of 5S rRNA

The precise mapping of the secondary and tertiary structure of 5S rRNA may contribute towards an improved understanding of the function of this molecule in the ribosome. The study of RNA structure can be carried out

in solution or by X-ray crystallography. The latter is the most powerful method currently available for the detailed description of the tertiary structure of RNA, but, so far, only tRNAs have yielded crystals which diffract at high resolution (Quigley *et al.*, 1975; Jack *et al.*, 1976; Sussman *et al.*,1985; Westhof *et al.*, 1985). X-ray crystallographic studies have, however, a disadvantage in that they provide information only about the static form of RNA molecules, since all molecules in a crystal tend to adopt the same conformation. Information on the structure of RNA in solution can be obtained by physical methods such as X-ray and neutron scattering or NMR studies. However, all of the above-mentioned techniques have a disadvantage in that they require large amounts of highly purified material (Ehresmann, *et al.*, 1987).

The method used in this project is that of probing the structure of RNA in solution; it consists in testing the reactivity of each nucleotide to chemical and enzymatic probes, with a view to obtaining an accurate picture of RNA folding. This method requires only a small amount of RNA and, like all methods which study RNA in solution, it allows us more closely to approximate natural conditions in that, unlike X-ray crystallograpy, it investigates the different conformations that RNA molecules can adopt. The secondary and tertiary structures of RNA molecules, whether free or engaged in a protein complex, have recently been studied by means of this methodology (Dumas et al., 1987; Mougel et al., 1987; Baudin et al., 1987; Romby et al., 1987).

This method is applied as follows: first, the 5S rRNA is subjected to limited ribonuclease (RNase) hydrolysis or chemical modifications using specific structure probes. It is very important that the enzymatic cleavages or

chemical modifications not be carried out to such an extent as to give a ratio of more than one cut or modification per RNA molecule. Any additional cuts or modifications could not be expected to be representative of the native structure, because of potential conformational changes following the first cleavage or modification (Ehresmann *et al.*, 1987). Control experiments are incubated simultaneously under the same conditions, but in the absence of the probe, in order to detect nicks in the RNA template, or stops in reverse transcription linked to prominent secondary structure features. Modified nucleotides and RNase cleavages can be detected by two different methods: the direct method (using end-labeled RNA) and the indirect method (using primer-extension) (Ehresmann *et al.*, 1987). The results from both methods are interpreted by using nucleic acid sequencing methodology.

The Direct Method

In this method the RNA molecule is radioactively labeled with ^{32}P at its 5' or 3' end, prior to RNase hydrolysis or chemical modification. The labeled RNA is then subjected to attack by the probes, in the presence of carrier tRNA, which is added in order to control the probe:RNA ratio (Ehresmann *et al*, 1987). Chemical modification experiments must be followed by further chemical treatment, leading to strand scission at modified nucleotides. This technique allows the detection only of scissions of the RNA chain that arise from RNase hydrolysis or chemical treatment. Control experiments are incubated at the same time in order to detect spontaneous nicks in the RNA molecule. The generated RNA fragments are then separated according to size using electrophoresis on denaturing polyacrylamide gels. To determine the size of the fragments, sequencing

reactions and an alkaline hydrolysis ladder are run on the same gel (for example, RNase T_1 gives the position of G residues). This method is used to detect the possible involvement of the N7 position of purines in hydrogen bonding or base stacking: for example N7-G is determined by means of DMS; N7-A by means of DEPC. The accessibility of nucleotides at the surface of molecules is determined by means of enzymes, and the involvement of phosphates in hydrogen bonding by means of ENU.

The Indirect Method

This method uses primer extension to detect transcription stops at modified or cleaved nucleotides. The unlabeled RNA is first subjected to chemical modification. Then, the 5S rRNA is hybridized with an oligodeoxyribonucleotide complementary to a sequence in the 5S rRNA. This oligomer is then used as a primer for the enzyme reverse transcriptase. Elongation proceeds from the 3' end of the primer towards the 5'-end of the RNA (in the presence of the four dNTPs). The result is that prematurely terminated cDNAs are obtained, instead of fully elongated chains which are normally synthesized on an unreacted or unmodified RNA template. These chain terminations are the result of chemical modifications. Indeed, modifications at Watson-Crick positions block the progress of reverse transcription at the nucleotide preceding the modified residue. This is the method used to detect Watson-Crick base-pairing (N1-A and N3-C by means of DMS; and N1-G and N3-U by means of CMCT). Detection of the synthesized cDNA chains is achieved by radioactively labeling the primer at its 5'-end with ^{32}P prior to hybridization. To determine the size of the cDNA chains, dideoxy sequencing reactions, carried out on unmodified RNA, are

run on the same gel. One limitation of the primer extension method is that because it is difficult for reverse transcriptase to melt some regions of the 5S rRNA structure, reverse transcription cannot proceed beyond these regions. For this reason, elongation controls on unreacted 5S rRNA have to be run simultaneously in order to detect these natural stops which are linked to certain stable regions of the secondary structure.

Enzymatic and Chemical Probes

The reaction of an enzyme or a chemical depends on several factors: (i) reactivity of the probe; (ii) reaction conditions, and (iii) accessibility of the residues to the probing reagent. For example, while certain sites (residues or sequences) may be exposed, and thus readily accessible to the probe, other sites may be totally inaccessible owing to tertiary structure folding.

I. Enzymatic Probes

The accessibility of 5S rRNA molecules to enzymatic cleavage was determined by ribonucleases specific to single-stranded or double-stranded regions of RNA. The various RNases used in this work are presented in Table 2 with their molecular weight, origin and specificity.

II. Chemical Probes

The different chemical probes that were used, their respective targets, and the mode of detection for each chemical modification are shown in Table 3. Also, the target positions for these chemicals are shown on a Watson-Crick base-pairing scheme in Figure 15. As mentioned above, in addition to these classical Watson-Crick interactions, other non-canonical interactions may occur, which participate in the tertiary folding of the RNA molecule. Some

Table 2. Enzymatic probes: Molecular weight, specificity and origin of ribonucleases.

Enzymatic Probes	Molecular Weight	Specificity	Origin
RNase A	13,700	Unpaired C, U	Bovine pancreas
RNase T_1	11,000	Unpaired G	*Aspergillus orizae*
RNase T_2	36,000	Unpaired A>C>U	*Aspergillus orizae*
Nuclease S_1	32,000	Unpaired N	*Aspergillus orizae*
RNase V_1	15,900	Paired or stacked N	cobra *Naja naja oxiana* venom

Table 3. Chemical probes: Molecular weight, specificity and mode of detection.

Chemical Probes	Molecular Weight	Specificity	Mode of detection used	
			End-labeled RNA	Primer Extension
DMS	126	N1-A[1]	-	+
		N3-C[1]	+*	+
		N7-G[2]	+*	-
CMCT	424	N1-G[1]	-	+
		N3-U[1]	-	+
DEPC	174	N7-A[2]	+*	-
ENU	117	Phosphates[3]	+*	-

* Indicates that an additional chemical treatment was necessary to split the ribose-phosphate chain.

The presence of reactivity indicates that the position is:

[1] not involved in Watson-Crick base pair interactions

[2] not involved either in tertiary interactions or in base stacking interactions

[3] not involved either in tertiary interactions or in cation coordination

(Tables 2 and 3 adapted from Ehresmann *et al.*, 1987).

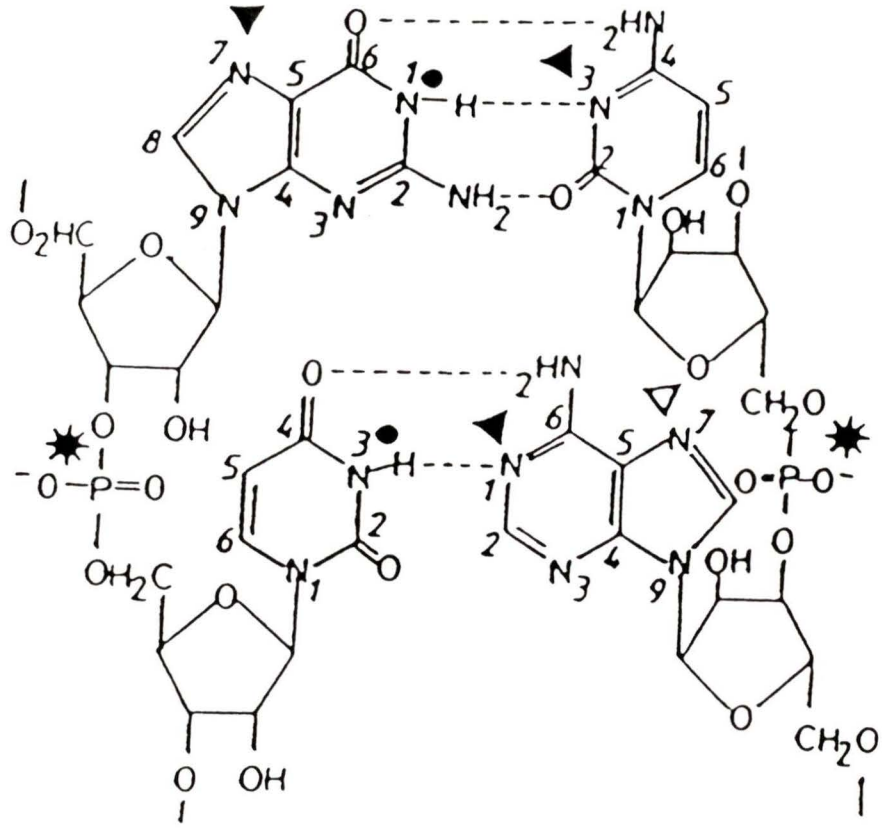

Figure 15: Canonical Watson-Crick interactions and target positions of the chemical probes: (▼) DMS; (▽) DEPC; (●) CMCT; (✷) ENU (adapted from Ehresmann *et al.*, 1987).

of these interactions have already been observed in nucleic acids (Westhof *et al.*, 1985; Jack *et al.*, 1976; Quigley *et al.*, 1975; Wing *et al.*, 1980; Romby *et al*, 1986; Cantor *et al*, 1980), and are listed in Table 1. The reaction mechanisms of each of the chemical probes used in this work is shown in Figure 16.

Dimethylsulfate (DMS). DMS reacts primarily with N7-G, N1-A and N3-C at neutral pH (Brookes and Lawley, 1961; Lawley and Brookes, 1963). The use of this reagent for probing the conformation of RNAs was first described by Peattie and Gilbert (1980).

1) Guanine Reaction. The addition of a methyl group on the N7 position leads to the presence of a positive charge which perturbs the electron resonance of the purine ring (Kochetov and Budowski, 1972). The perturbed 7,8-double bond of the alkylated ring can be reduced in a dilute sodium borohydride solution at pH 8.3 (Figure16a) (Wintermeyer and Zachau, 1975).The resulting m^7-dihydroguanosine provides a site for aniline induced strand scission (Figure 16c) (Wintermeyer and Zachau, 1975). This reaction locates free N7-G in RNA. The absence of reactivity indicates that this position is involved in non-canonical base pairs or is in coordination with ions such as magnesium (Ehresmann *et al.*, 1987).

2) Cytosine reaction.Unpaired cytosines are methylated at their N3 position . The resulting methyl-3-cytosine can be detected directly by primer extension. However, a further chemical treatment is required when end-labeled 5S rRNA is used. Methyl-3-cytosine is sensitive to hydrazinolysis, (Figure 16a)

Figure 16: Mechanism of the chemical reactions. (A) DMS alkylation of N1-A, DMS alkylation of N3-C followed by hydrazine treatment, and alkylation of N7-G followed by sodium borohydride reduction; (B) Carbethoxylation of N7-A by means of DEPC; (C) aniline strand scission: after the hydrolysis of the glycosidic bond between the modified base and the ribose, the exposed ribose forms an open-ring tautomer. The free aldehyde group of this tautomer reacts with aniline to form an aldimine, and the 3'-phosphoester bond is cleaved via a β-elimination mechanism; (D) CMCT modification at N3-U and N1-G; (E) Alkylation of phosphate by means of ENU followed by alkaline treatment (adapted from Ehresmann *et al.*, 1987).

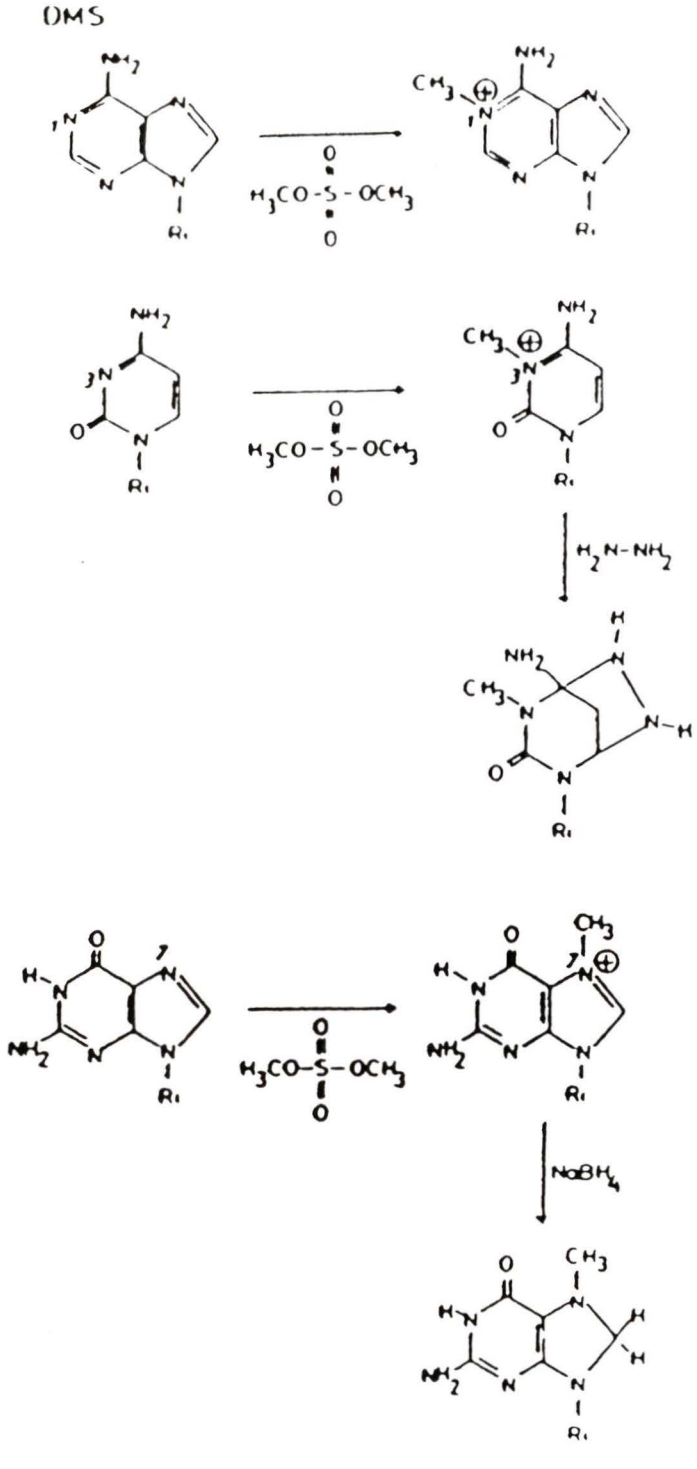

A

Figure 16 (continued)

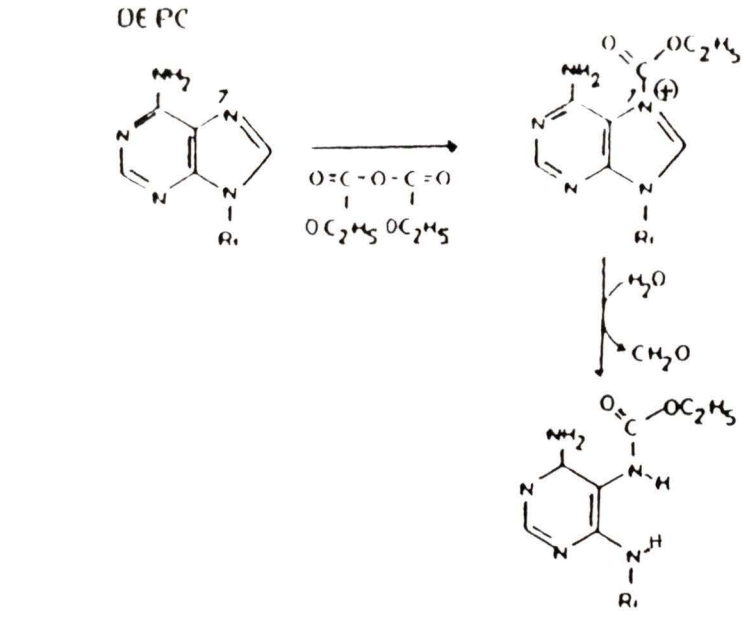

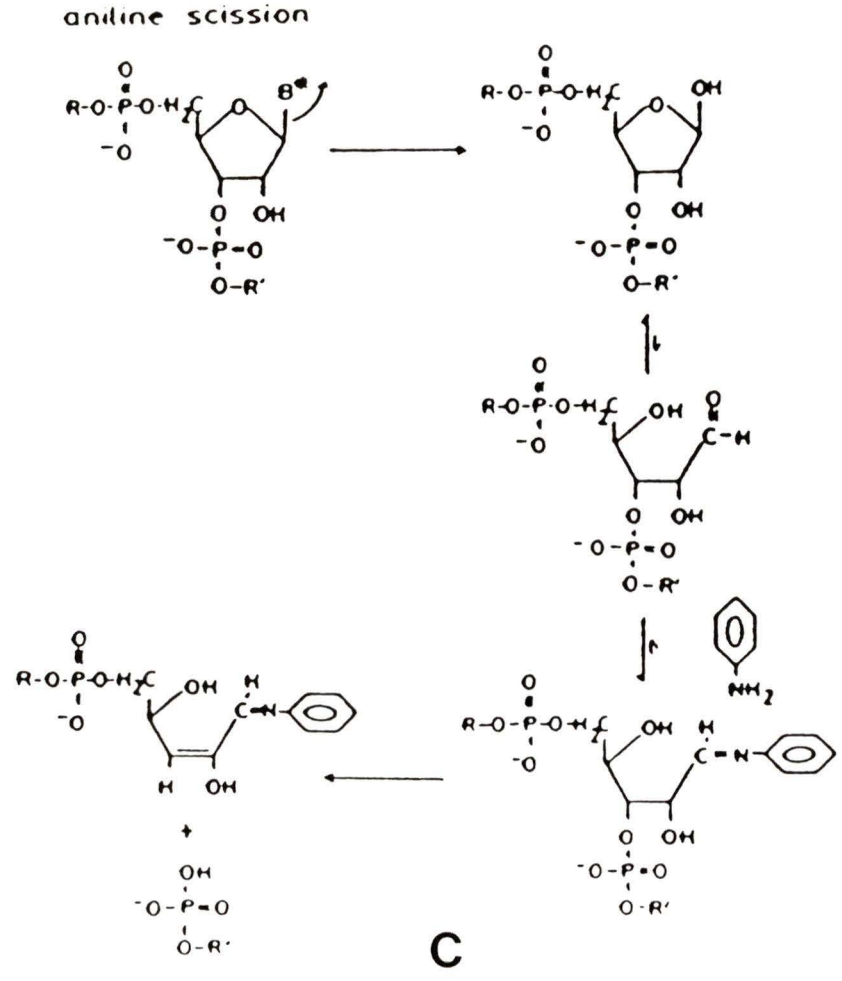

Figure 16 (continued)

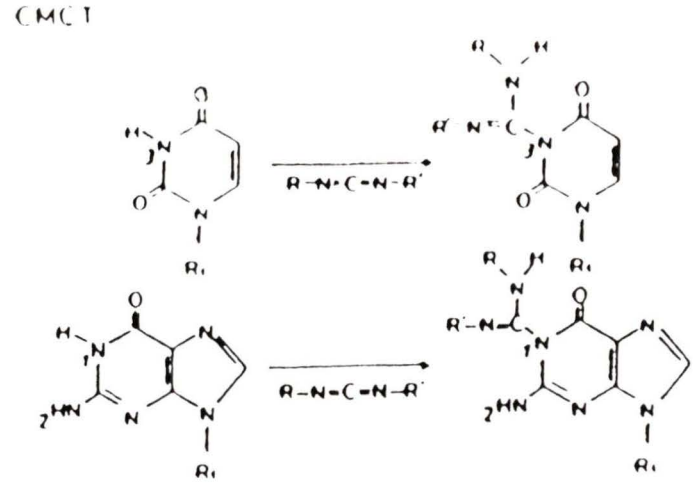

D

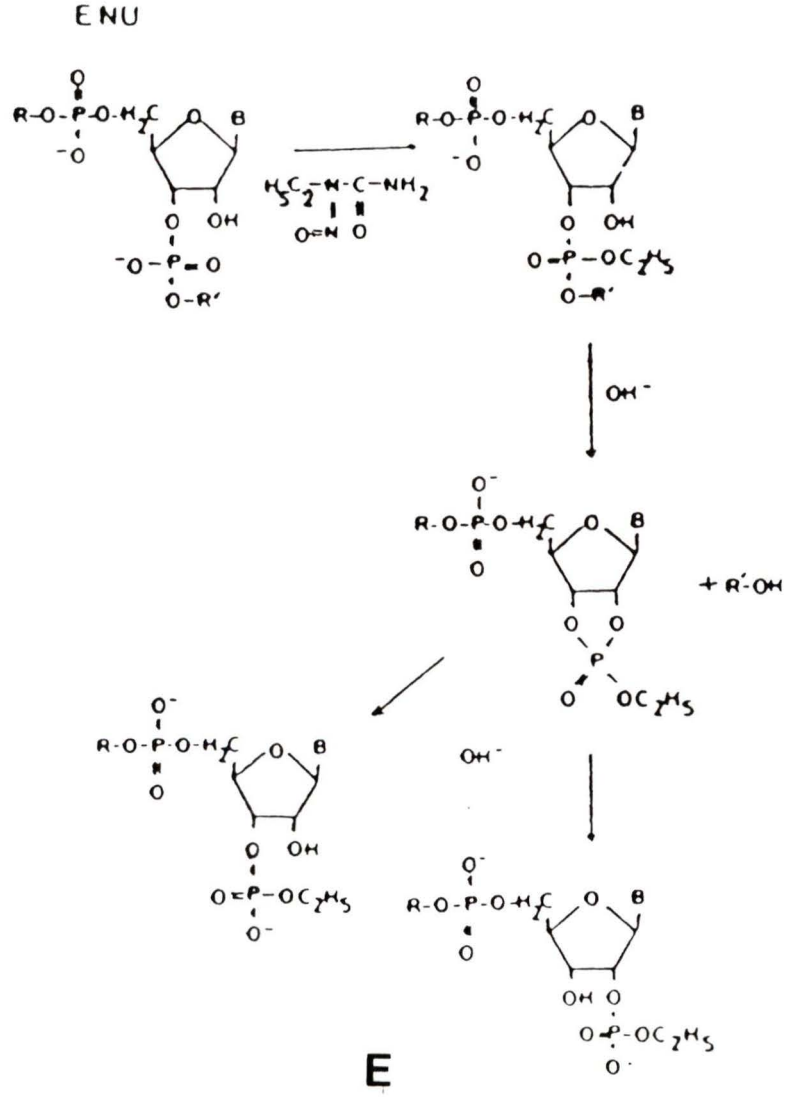

E

Figure 16 (continued)

and this then provides a site for aniline scission (Figure 16c) (Ehresmann *et al*, 1987).

3) Adenine Reaction. Since no chemical splitting of the RNA chain at methyl-1-adenine exists, this modification can only be detected when the primer extension method is used. This reaction identifies single-stranded adenines (Figure 16a) (Ehresmann *et al*, 1987).

Diethylpyrocarbonate (DEPC).; The N7 atom of adenosine is particularly susceptible to carbethoxylation (Leonard *et al*, 1971; Vincze *et al*, 1973; Ehrenberg *et al*, 1976) at neutral pH. This modification destroys the resonance of the heterocyclic ring, and the imidazole ring opens between atoms N7 and C8 (Figure 16b) (Leonard *et al*, 1971), thereby creating a site for aniline strand scission (Peattie, 1979). This chemical reaction monitors the involvement of N7-A in tertiary interactions (as described for N7-G alkylation to DMS). Owing to a higher molecular weight of the adduct, DEPC is more sensitive to base stacking than DMS, and all adenines in helices are unreactive (Ehresmann *et al*, 1987).

1-cyclohexyl-3-(2-morpholinoethyl) carbodiimide metho-p-toluene sulfonate (CMCT). CMCT reacts primarily with N3-U and N1-G at pH 8 in the order N3-U > N1-G (Figure 16d) (Van Stolk and Noller, 1984; Gihlam, 1962; Naylor *et al*, 1966). CMCT is used to locate unpaired uridines and guanosines.

Ethylnitrosourea (ENU). ENU is a N-nitroso-alkylating reagent which has a high affinity for the oxygens of the phosphate groups of nucleic acids, in

contrast to other alkylating reagents, such as DMS, which primarily alkylates ring nitrogens (Figure 16e) (Singer, 1976; Jensen and Reed, 1978; Singer and Fraenkel-Conrat, 1976). In the case of RNA, the resulting phosphotriesters are unstable and are easily split by mild alkaline treatment (Kusmierek and Singer, 1976). This alkylation is used to locate phosphates engaged through hydrogen bonds in tertiary interactions, or likewise phosphates that are involved in cation coordination (Vlassov *et al.*, 1981; Romby *et al.*, 1985). Compared to other chemical probes, ENU has the advantage of not being selective, since its reactivity is sequence- and secondary structure-independent (Ehresmann *et al.*, 1987).

III Experimental Conditions

Since the optimal conditions vary with the different probes, there is a possibility that subtle conformational changes may occur under different incubation conditions. Therefore, it is very important to probe the conformation of RNA under strictly defined buffer conditions (pH, ionic strenth, magnesium concentration and temperature).

The degree of stability of the structure is estimated by modifying the 5S rRNA under two kinds of conditions: (i) native conditions (at low temperature, in the presence of magnesium), and (ii) semi-denaturing conditions (at low temperature, in the absence of magnesium). Enzymatic hydrolysis or chemical modifications are carried out under native conditions so that the conformation of the molecule is conserved. Semi-denaturing conditions are important because they allow us to estimate the degree of stability in helices during the partial denaturation of 5S rRNA caused by these conditions. For instance, it is well known that tertiary interactions are less

stable than Watson-Crick interactions. Tertiary interactions are therefore expected to melt under semi-denaturing conditions (Ehresmann *et al*, 1987).

IV Advantages and Limitations of the Probes

Enzymes. The hydrolysis of a region of RNA is influenced by the following factors: (i) the position of this region in relation to the surface of the molecule, (ii) size of the enzyme, and (iii) enzyme specificity. Owing to their bulky size, nucleases are susceptible to steric hindrance, especially in the case of extensive folding of RNA. For example, some sites on the RNA molecule may be inaccessible to the enzymes because of the enormous size of the nuclease itself. In addition, special care must be taken in the choice of hydrolytic conditions, since enzymatic cleavages at a particular position may alter the structure of the RNA, thereby introducing additional cuts on the same RNA chain. These cuts appear most often during prolonged periods of incubation. Such cleavages, designated as secondary cuts, can be easily differentiated from primary cuts on end-labeled RNA by comparing hydrolysis patterns of 5'- and 3'-end-labeled molecules. Secondary cuts, which are weaker than primary ones, are only observed in one of the two end-labeled molecules. However, despite these limitations, enzymes can yield useful information on the accessibility of the RNA regions under study (Ehresmann *et al*, 1987).

Chemicals. Chemical probes have the advantage of being small, and therefore are not very susceptible to steric hindrance. This allows us to obtain accurate information by probing the minute characteristics of RNA structure at the atomic level. However, the various nucleotide positions do not react identically to all probes. For example, N3-C reacts slower than N1-A with DMS, and N1-G slower than N3-U with CMCT. In addition, the reactivity of

N7-A to DEPC is more sensitive to stacking than N7-G to DMS (Ehresmann *et al.*, 1987).

It would be incorrect to assume that chemical probes necessarily determine the accessibility of nucleotide positions, since the probes may not react identically with every position. A given nucleotide position may be accessible without being reactive. Reactivity is largely influenced by the electrostatic environment of the molecule, which can inhibit the chemical reaction of the probe. This problem has been discussed by Lavery and Pullman (1984), who have introduced a new theoretical index, which combines steric and electrostatic factors (ASIF, "Accessible Surface Integrated Field" index). In general, the more negative the ASIFs, the more likely are the chemical modifications to occur. Romby *et al* (1985) have already observed that a good correspondance is found between theoretical calculation of ASIF indexes, based on X-ray structure, of $tRNA^{Asp}$ and $tRNA^{Phe}$, and the observed reactivities to ENU.

The utilization of structure-specific probes, together with the determination of accessible sites by rRNA end-labeling and primer extension represents a powerful approach for probing secondary and tertiary structure models (Inoue and Cech, 1985; Lempereur *et al*, 1985; Moazed *et al*, 1986; Mougel *et al*, 1987; Baudin *et al*, 1987). This approach allows us to determine which nucleotides are possibly involved in tertiary interactions. However, like all experimental approaches, this technique has intrinsic limits. One of the most obvious of which is its inability, in the absence of other independent information such as that provided by X-ray crystallography or RNA-intramolecular cross-linking, to identify without ambiguity which nucleotides are participating together in tertiary long-range interactions.

MATERIALS AND METHODS

Materials

Chemicals and Enzymes

Commonly used chemicals were purchased from BDH, Fisher or Sigma. Yeast extract and tryptone were purchased from DIFCO Laboratories. Agar was purchased from GIBCO. Acrylamide, bis-acrylamide and urea were purchased from SERVA. DMS, DEPC and sodium borohydride were purchased from BDH; CMCT, ENU and aniline were purchased from Sigma; Hydrazine from Kodak; Calf intestinal phosphatase was purchased from Boehringer; RNases T_1, U_2, S_1, and V_1 were purchased from Pharmacia; T_4 RNA ligase and T_4 polynucleotide kinase were purchased from New England Biolabs; avian myeloblastosis reverse transcriptase was purchased from Life Sciences; RNasin was purchased from Promega Biotec; T_7 RNA polymerase was purified from *E. coli* strain BL21/pAR1219 by a published procedure (Davanloo *et al*, 1984); [γ-^{32}P]ATP (3200 Ci/mmol) and [5'-^{32}P]pCp (3000 Ci/mmol) were purchased from New England Nuclear.

Methods

I. Construction of Cloned Mutant 5S rRNA Genes

Mutant 5S rRNA genes were constructed using a modification of the method of oligonucleotide-directed mutagenesis by micro-scale ligation developed by Gründstrom and co-workers (1985). The cloned genes were synthesized as a series of oligonucleotides. For each mutant the appropriate

oligonucleotides for both strands were synthesized and substituted for the corresponding wild-type oligonucleotides in a shotgun ligation reaction. These oligonucleotides were subsequently annealed and ligated into vector pUC18. The mutant 5S rRNA genes were placed under the control of the T7 promoter (see section II below). An Eco RI linker at the 5'-end of the T7 promoter and a Bam HI linker at the 3'-end of the gene were introduced After ligation, the reaction mixture was digested with Kpn I to linearize any re-sealed pUC 18 vector before transformation (Figure 17).

The oligonucleotides were synthesized by Dr. P. Romaniuk in a Biosearch 8600 DNA synthesizer using the phosphite method (Sinha *et al*, 1984). After the synthesis was completed, the oligonucleotides were deprotected by incubating them in 1 ml of concentrated ammonium hydroxide solution, first at room temperature for one hour and then at 50°C overnight (Biosearch Model 8600 Instruction Manual, 1985). After this incubation, the ammonium hydroxide solution was evaporated on a RH40-11 Speed Vac concentrator. The dry oligonucleotides were dissolved in 100 µl sterile distilled water and their concentration determined by absorbance at 260 nm. Ten O.D. units of each oligonucleotide were purified by polyacrylamide gel electrophoresis and reverse phase chromatography using a C18 Sep-Pak column (Water Associates) as described by Atkinson and Smith (1984). Prior to the annealing and ligation of oligonucleotides, 5 µg of each oligonucleotide was phosphorylated by incubating at 37°C for 60 minutes in 60 µl of a buffer containing 50 mM HEPES pH 7.5, 10 mM $MgCl_2$, 10 mM DTT, 50 µg/ml BSA, 0.1 mM ATP and 3 units of T_4 polynucleotide kinase. The reaction was then diluted with 1 ml TE (10 mM Tris-HCl pH 8, 1 mM EDTA) buffer, the oligonucleotides were purified by reverse phase chromatography (Atkinson

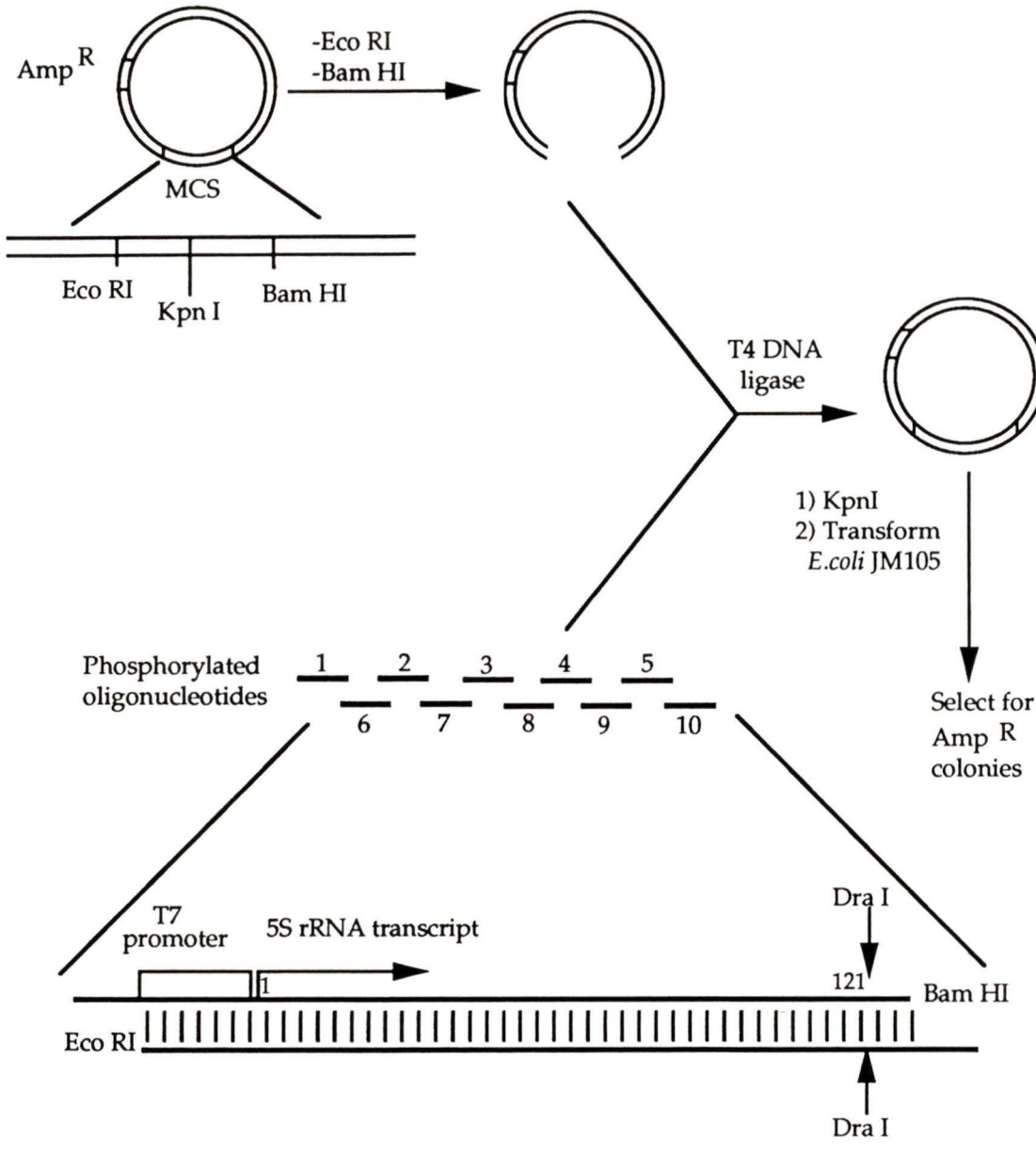

Figure 17: *Xenopus laevis* 5S rRNA mutant genes constructed from oligonucleotides 1-10 using the microscale shotgun ligation method. The oligonucleotides also contain sequences that generated both EcoRI and BamHI restriction sites as well as the T7 promoter. MCS= Multiple Cloning Site; Restriction sites: Eco RI, Kpn I, Bam HI, and Dra I; Amp R= Ampicillin Resistance (adapted from Romaniuk *et al.*, 1987).

and Smith, 1984), and stored as 10 μM solutions at -20°C. The oligonucleotides (0.5 pmol) were annealed by incubating for 1 hour at 37°C in 8 μl of 50 mM Tris-HCl pH 7.5, 10 mM $MgCl_2$, 20 mM DTT, 0.1 mM spermidine and 1 mM ATP. The vector pUC18 (0.1 pmol) that had previously been digested with EcoR I and BamH I was added together with 200 units of T_4 DNA ligase, and incubation was continued overnight at 20°C. The reaction was then heated to 70°C for 10 min. to inactivate T_4 ligase, and then 20 μl of Kpn buffer (10 mM Tris-HCl pH 7.5, 10 mM $MgCl_2$, 1 mM DTT, 0.01% Triton X-100) was added together with 10 units of the restriction nuclease Kpn I.

After incubation at 37°C for 60 minutes, 3-6 μl of the reaction (containing 20-40 ng of DNA) was used to transform *E. coli* strain JM105, made competent by $CaCl_2$ treatment (Maniatis *et al*, 1982). Bacteria that contained the plasmid DNA were selected on the basis of ampicillin resistance. For screening purposes, mini-preparations of plasmid DNA were made from 10 isolates according to Maniatis *et al* (1982). The DNA from these preparations was analyzed both for the presence of a new Dra I restriction site, and the ability to produce 5S rRNA transcripts. After this analysis, the correct sequence of each clone was verified by dideoxynucleotide sequencing of plasmid DNA using the M13 reverse sequencing primer and reverse transcriptase (Zaug *et al*, 1984). In general, it was found that 40-70% of plasmids from mini-preparations contained the correct sequence.

II. Synthesis of Mutant 5S rRNA From Cloned Genes

Linearization of plasmid DNA. Before *in vitro* transcription, each plasmid containing the mutant 5S rRNA gene was linearized by digestion with the

restriction enzyme Dra I, which defines the 3' terminus of the transcripts as nucleotide +121 of the gene. The Dra I recognition site was introduced at the 3'-end of the gene in order to generate run-off transcripts that have the same length as the natural 5S rRNA (Figure 17).

For all mutants, 50 μg of plasmid DNA was dissolved in 100 μl of 10 mM Tris-HCl pH 7.5, 10 mM $MgCl_2$, 1 mM DTT and 100 μg/ml BSA and digested with 100 units of the restriction endonuclease Dra I for 60 min. at 37°C. The extent of digestion was analyzed by electrophoresis of an aliquot of the reaction mixture in a 1% agarose gel (run for 1 hour at 50 V) (Figure 18). The reaction was then extracted with 100 μl of phenol:chloroform (1:1 v/v), followed by two extractions with 100 μl of chloroform. The DNA was then recovered by precipitation with 95% ethanol, washed with 70% ethanol, and redissolved in TE buffer to give a solution of 1 μg/μl.

Synthesis of Mutant 5S rRNA. In order to obtain 5S RNA transcripts from the cloned genes, the mutant 5S rRNA genes were placed under the control of a promoter for T7 RNA polymerase (Figure 17). T7 RNA polymerase is a protein derived from the T7 bacteriophage which shows a very high specificity for its promoter, since only the genes under its control are transcribed, producing a high yield of specific transcripts. The 5S rRNA genes were constructed in such a fashion that the T7 transcripts have 5' and 3' termini identical to those found in natural 5S rRNA molecules (Romaniuk *et al*, 1987).

In vitro transcription was carried out using T7 RNA polymerase purified by a published procedure (Davanloo *et al*, 1984) from *E. coli* strain BL21/pAR1219 provided by Dr. F.W. Studier. In the reaction mixture a final volume of 200 μl contained: 40 mM Tris-HCl pH 8, 30mM $MgCl_2$, 5 mM DTT,

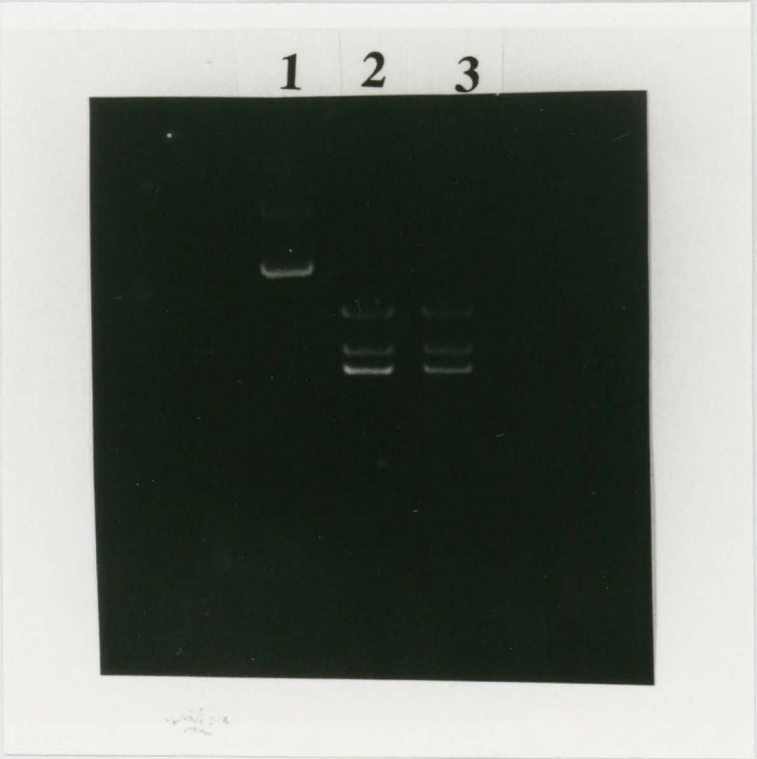

Figure 18: Analysis of plasmid DNA restriction digest with Dra I. Lane 1: undigested control of Xlo w.t.; lane 2: restricted Xlo 73-76; lane 3: restricted Xlo 87-90 (direction of electrophoresis from top to bottom).

1 mM spermidine, 0.1 mg/ml BSA, 1.25 mM each ATP, UTP, CTP, GTP, 8% PEG(8000), 0.01% Triton X-100, 200 U RNasin, 25 μg linearized template DNA, and 15 μg T7 RNA polymerase. After incubation for 4 hours at 37°C, the reaction was extracted with 200 μl of phenol:chloroform (1:1 v/v), followed by two extractions with 200 μl of chloroform. The crude RNA was then ethanol precipitated, and then redissolved in 50 μl of TE buffer. *In vitro* transcription was analyzed by electrophoresis of an aliquot (1 μl) of the reaction mixture on a 8% polyacrylamide 8.3 M urea mini-gel (run for 20 min. at 300 V) (Figure19). 5S rRNA transcripts from each mutant were separated from DNA template and unincorporated nucleotides by gel permeation HPLC using a BioRad TSK-125 column (7.5 mm x 30 cm) and an elution buffer of 0.2 M sodium acetate, 1% methanol pH 6.0 (Figure 20). Fractions containing 5S rRNA were concentrated by evaporation on a RH40-11 Speed Vac concentrator, and the RNA was recovered by ethanol precipitation. Yields of pure 5S rRNA were 30-50 μg. 5S rRNA was stored at -20°C as an aqueous 1 mg/ml solution.

III. End Labeling of 5S rRNA

Before labeling 5S rRNA at the 5' terminus, 25 μg of 5S rRNA were dephosphorylated with 24 units of calf intestinal phosphatase using a published procedure (D'Alessio, 1982). The dephosphorylated 5S rRNA was then purified by electrophoresis on a 8M urea-12% polyacrylamide gel for 1.5 hours at 700 V. The recovered 5S rRNA was 5' end labeled using [γ-^{32}P]ATP and polynucleotide kinase. 5S rRNA was labeled at the 3' terminus with [5'-^{32}P]pCp using T_4 RNA ligase (England and Uhlenbeck, 1978). 3' end labeled 5S rRNA was purified by electrophoresis on a 6% polyacrylamide: 8 M urea gel for 4 hours at 30 mA. Before each chemical and enzymatic modification

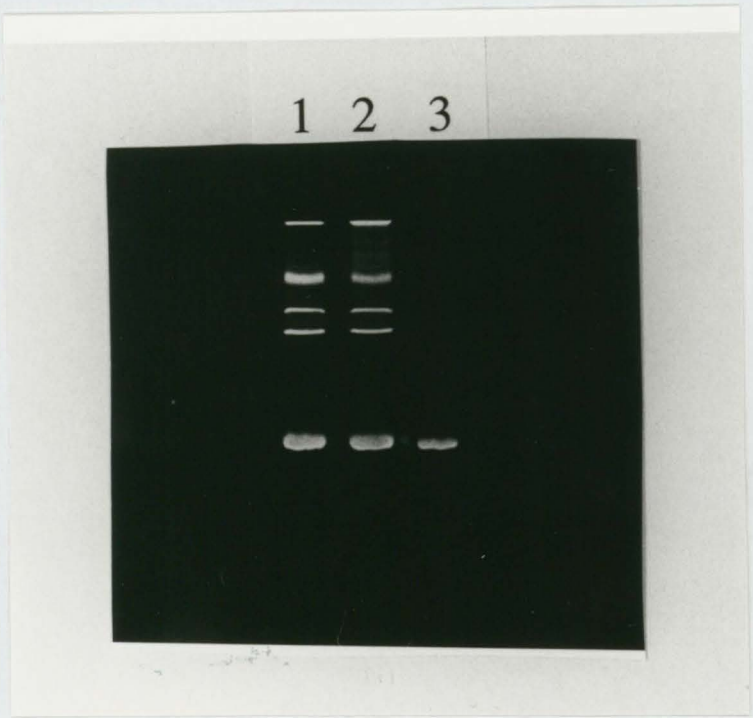

Figure 19: Analysis of *in vitro* transcription from the linearized plasmid containing the 5S rRNA gene: (1), Xlo 99-101 5S rRNA; (2), Xlo 96-101 5S rRNA; (3), *E. coli* 5S rRNA (direction of electrophoresis from top to bottom).

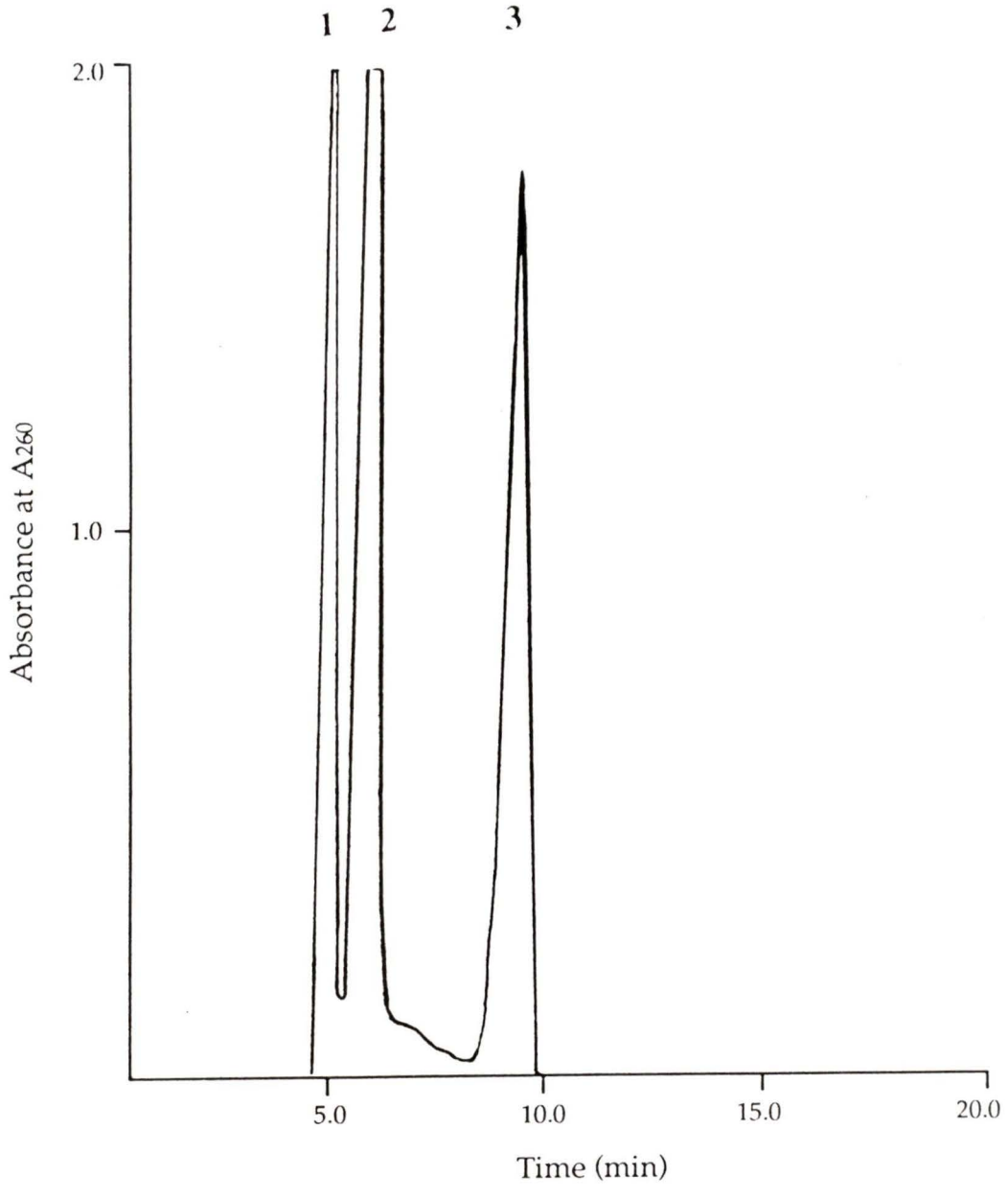

Figure 20: Elution profile of mutant Xlo 73-76 by gel permeation HPLC. Legend: (1) plasmid DNA; (2) Xlo 73-76 5S rRNA; (3) unincorporated nucleotide triphosphates.

experiment, the 5S rRNA was eluted overnight in 0.6 M ammonium acetate, 0.1% SDS and 1 mM EDTA. Then the 5S rRNA was precipitated twice with 95% ethanol, washed with 70% ethanol and resuspended in water.

IV. Limited Enzymatic Hydrolysis of Labeled 5S rRNA

Before enzymatic digestion, an aliquot of end-labeled 5S rRNA (40,000 cpm Cerenkov) was renatured by incubating at 55°C for 10 min. in 100 µl of TMK buffer (20 mM Tris-HCl pH 7.5, 5 mM $MgCl_2$, 100 mM KCl) followed by slow (60 min.) cooling to 20°C. In each experiment, labeled 5S rRNA was supplemented with 10 µg of total tRNA as carrier. The 5S rRNA was then digested for 20 min. at 20°C using the following nucleases: T_1 (0.1-3 units), T_2 (0.01-0.3 units), A (0.1-10 ng), S_1 (22-110 units), and V_1 (0.22-0.7 units). The reaction mixtures were then extracted with 100 µl of phenol:chloroform, and the 5S rRNA was recovered from the aqueous phase by precipitation using 95% ethanol, washed with 70% ethanol and vacuum dried. Then the 5S rRNA samples were redissolved in 5 µl of urea-dye buffer (8.5 M urea, 0.05 M boric acid, 0.05 M Tris, 0.001 M EDTA, 0.025% BPB and xylene cyanol), and heat-denatured for 2 min. at 90°C prior to gel electrophoresis. Each reaction mixture (20,000 cpm Cerenkov) was subjected to electrophoresis on a 8M urea-12% polyacrylamide sequencing gel (40x20x0.04 cm) and run in TBE buffer (0.05 M Tris-borate, 0.001 M EDTA) at 1500 V for 2 hours for the short migration gel, and 4 hours for the long migration gel. The positions of nuclease cuts were identified by running in parallel RNases T_1, U_2 and alkaline hydrolysis ladders. Control samples were treated identically throughout except for omission of enzyme. At the end of electrophoresis, the

gel was dried at 80°C for 30 min. and exposed to an X-ray film overnight at -70°C.

V. Alkylation of 5S rRNA by Ethylnitrosourea

Phosphate alkylation was carried out essentially as described by Vlassov *et al* (1981). Labeled 5S rRNA (40,000 cpm Cerenkov) was supplemented with 2 µg of tRNA as carrier. In the native reaction: the 5S rRNA was renatured by incubating at 50°C for 5 min. and cooled slowly (30 min.) at 20°C in 20 µl of buffer N-1 (300 mM sodium cacodylate pH 8, 5 mM $MgCl_2$, 100 mM KCl). A saturated solution of ethylnitrosourea in ethanol (5 µl) was added, and then the 5S rRNA was incubated for 3 hours at 20°C. In the denaturing reaction: buffer D-1 (300 mM sodium cacodylate pH 8, 1 mM EDTA) was used instead, and incubation was for 2 min. at 80°C with the same amount of ethylnitrosourea. After alkylation, 2 µl of 3 M sodium acetate pH 6 was added, and the 5S RNA was precipitated with 3 volumes of 95% ethanol. After reprecipitation of the RNA from 0.3 M sodium acetate containing 1 mM EDTA, the RNA was washed twice with 70% ethanol. The alkylated 5S rRNA was cleaved at phosphotriester positions in 0.1 M Tris-HCl pH 9.0, and the liberated oligonucleotides were analyzed on a 8 M urea-12% polyacrylamide sequencing gel, as indicated above. The position of the phosphates was determined by running in parallel RNases T_1, U_2, and alkaline hydrolysis ladders. The extent of phosphate alkylation at each position was measured by densitometry scanning of the autoradiogram with a Beckman DU-65 Spectrophotometer using a gel scan program.

VI Chemical Modification of the Bases

In each experiment, 5S rRNA (labeled or unlabeled) was supplemented with 10 μg of tRNA as carrier. End-labeled 5S rRNA (3' and 5' end-labeled) was used to detect methylation of N7-G with DMS and carbethoxylation of N7-A with DEPC.

Dimethylsulfate modification. Native reaction: 5S rRNA was renatured as described above in 200 μl of buffer N-2 (50 mM sodium cacodylate pH 7.5, 5 mM $MgCl_2$, 100 mM KCl). DMS (0.5 μl) was added, and the reaction was incubated for 5-20 min. at 20°C with occassional stirring. Semi-denaturing reaction: the same procedure as above was used, except that renaturation of 5S rRNA was carried out in buffer D-2 (50 mM sodium cacodylate pH 7.5, 1 mM EDTA). After incubation, 100 μl of 0.3 M sodium acetate pH 6 was added, and the modified 5S rRNA was precipitated with 2.5 volumes of 95% ethanol. Then the RNA pellets were resuspended in 100 μl of 0.3 sodium acetate pH 6, reprecipitated with ethanol, washed with 70% ethanol, and vacuum dried.

Diethylpyrocarbonate Modification. Buffers and renaturation conditions were the same as those used for DMS modification. Modification was carried out by adding 20 μl of DEPC to each sample, and incubation for 15-30 min. at 20°C, with occasional mixing. After incubation, the RNA was recovered as outlined above.

Carbodiimide Modification. Native reaction: 5S rRNA was renatured in 150 μl of buffer N-3 (50 mM sodium borate pH 8, 5 mM $MgCl_2$, 100 mM KCl). The reaction was started by incubating 5S rRNA at 20°C for 15, 30, and 60 min. in

the presence of 50 µl of CMCT (42 mg/ml aqueous solution). Semi-denaturing reaction: The procedure was the same as for native conditions but in buffer D-3 (50mM sodium borate pH 8, 1 mM EDTA), and incubation was at 20°C for 5 and 15 min. 5S rRNA was then recovered as outlined above.

VII Detection and Analysis of Modified Bases

Cleavage of labeled 5S rRNA at modified positions. End-labeled 5S rRNAs containing guanosines methylated by DMS at position G-N7 were cleaved by incubating for 5 min. at 0°C in 1 M Tris -HCl pH 8.2 containing 0.2 M sodium borohydride. To detect cytidines methylated at C-N3 position by DMS, 5S rRNA was incubated in 10% hydrazine at 0°C for 5 minutes. In both cases the 5S rRNA was ethanol precipitated twice from 0.3 M sodium acetate pH 6, washed with 70% ethanol and vacuum dried. 5S rRNA modified at G-N7, C-N3, and A-N7 was then cleaved with aniline buffer pH 4.5 at 60°C in the dark for 10 min. The liberated oligonucleotides were analyzed by electrophoresis on 8 M urea-12% acrylamide sequencing gels as described above.

Primer Extension with Reverse Transcriptase. The primer extension method was used to detect the bases modified by DMS [A(N1) and C(N3)] and CMCT [G(N1) and U(N3)]. The oligonucleotide primer AAGCCTACG, complementary to nucleotides 112-120 of the 5S rRNA, was synthesized by the phosphoramidite method using a Biosearch instrument. The primer was labeled with ^{32}P at the 5' end according to the method of Silberklang *et al* (1977). The hybridization mixture, containing modified or unmodified 5S rRNA (1 µg) and the primer (80,000 cpm) was incubated at 65°C for 5 min. in 8 µl of water. Then 2 µl of annealing buffer (250 mM Tris-HCl pH 8.3, 30 mM

$MgCl_2$, 200 mM KCl) were added and incubation continued for a further 5 min. at 65°C. The annealing mixture was then slowly cooled to room temperature (10 min.). Primer extension was performed in 15 µl of annealing buffer at 37°C for 35 min. in the presence of 5 units of reverse transcriptase and 0.25 mM each of dATP, dGTP, dCTP, and dTTP. Dideoxy-sequencing reactions were made in parallel on unmodified 5S rRNA in the additional presence of 5 µM of the appropriate ddNTP as described by Sanger *et al* (1977). The elongation reaction was stopped by adding 200 µl of 0.3 M sodium acetate pH 6 and 3 volumes of 95% ethanol. Pellets were redissolved in 100 µl of 0.3 M sodium acetate pH 6, reprecipitated with ethanol, washed with 70% ethanol and vacuum dried. Pellets were then resuspended in 6 µl of loading buffer (deionized formamide, 0.03% bromophenol blue and xylene cyanol), and heated for 2 min. at 90°C prior to gel electrophoresis. Electrophoresis was carried out on 8 M urea:10% polyacrylamide sequencing gels for 2 or 4 hours at 1500 Volts as outlined above.

RESULTS and DISCUSSION

Reactivity of 5S rRNAs to enzymes

The 5S rRNA molecules from mutants: Xlo73-76, Xlo87-90, Xlo99-101 and Xlo96-101 were carefully renatured in the presence of magnesium ions prior to modification, in order to study the native conformation of these RNA molecules. The conformation of all 5S rRNAs was tested using uniform conditions of pH, salt concentration and temperature for all enzymes. These conditions are the same as those used previously to study the solution structure of *Xenopus* oocyte 5S rRNA (Romaniuk *et al.*, 1988).

The solution structures of 5S rRNAs from all four mutants Xlo73-76, Xlo87-90, Xlo99-101 and Xlo96-101 were probed with single-strand specific nucleases: T_1, T_2, A and S_1, and with RNase V_1 specific for structured regions, using a range of enzymatic concentrations. All enzymes were used on both 5'- and 3'-end labeled 5S rRNA molecules, in order to differentiate between primary and secondary cuts, which do not reflect the native conformation of the 5S rRNAs. The primary cleavage sites caused by nucleases under native conditions have been summarized on the secondary structure models of the 5S rRNAs from the four mutants (Figures 21 to 24). These results can be compared to the results obtained for the *Xenopus* oocyte wild type 5S rRNA (Figure 25). For convenience, enzymatic cuts were designated by the position in the sequence of the nucleotide located directly at the 5'-side of the scission. A typical experiment is shown in Figure 26.

The enzymatic digestion pattern to single-strand specific nucleases in both wild-type 5S rRNA and its four mutants appears to be basically the same for loops **A**, **B** and **C**. There are differences, however, in the nuclease

Xlo 73-76

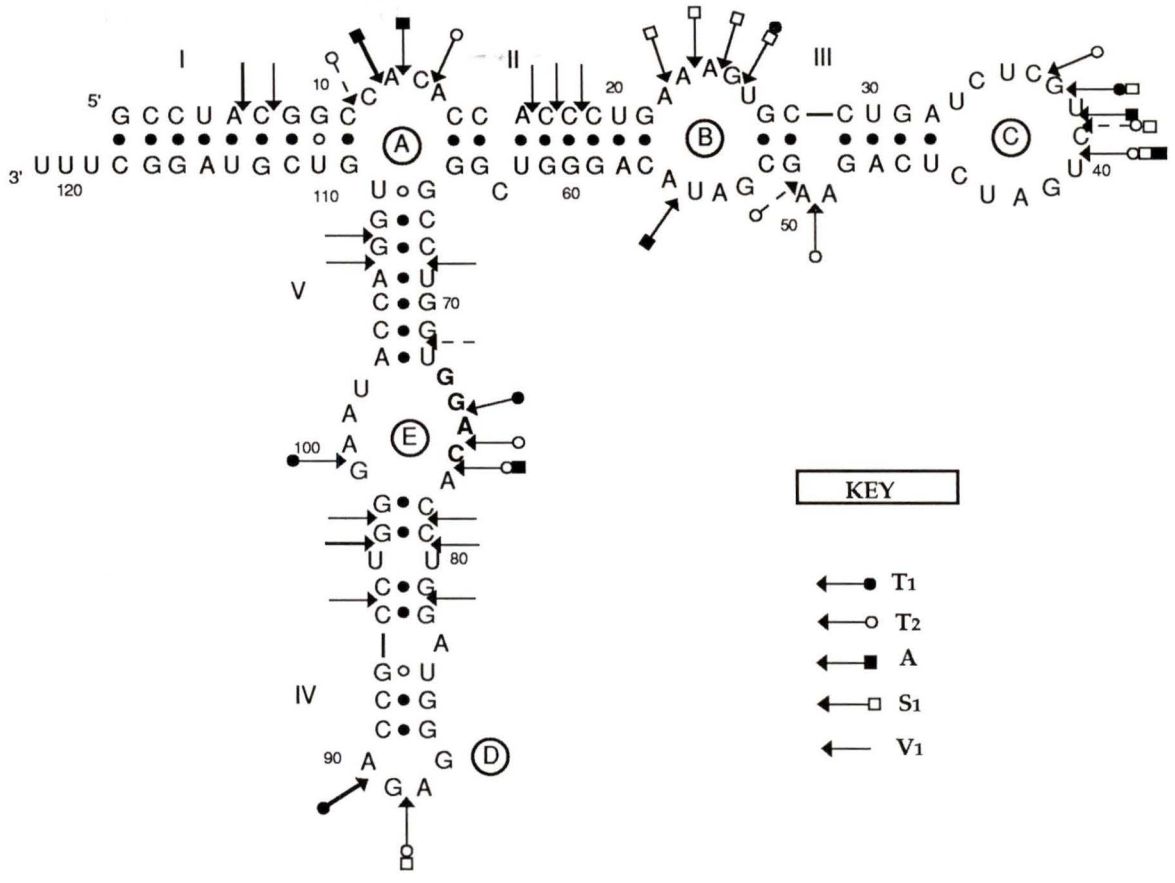

Figure 21: Summary of nuclease cleavages of Xlo 73-76 5S rRNA. The extent of cleavage is indicated by: thick line, strong; thin line, moderate; broken line, weak.

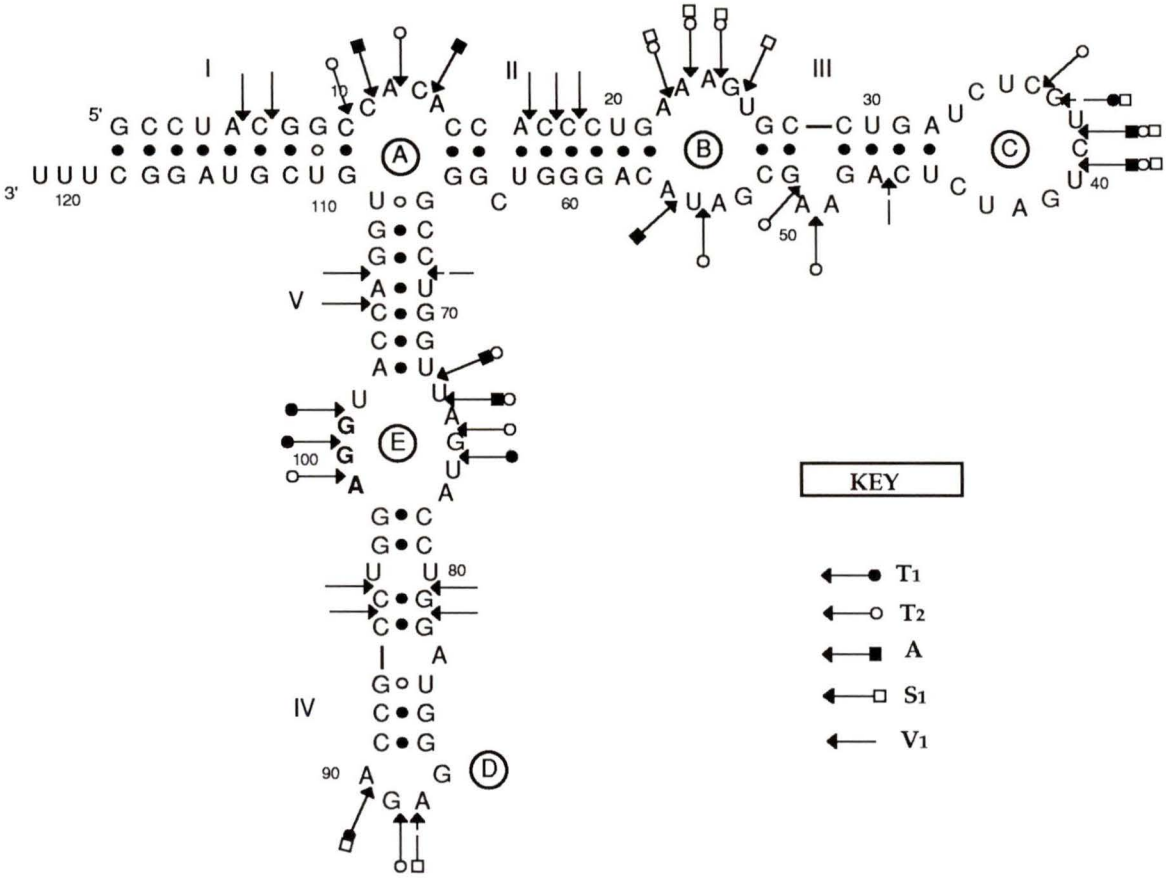

Figure 22: Summary of nuclease cleavages of Xlo 99-101 5S rRNA. The extent of cleavage is indicated by: thick line, strong; thin line, moderate; broken line, weak.

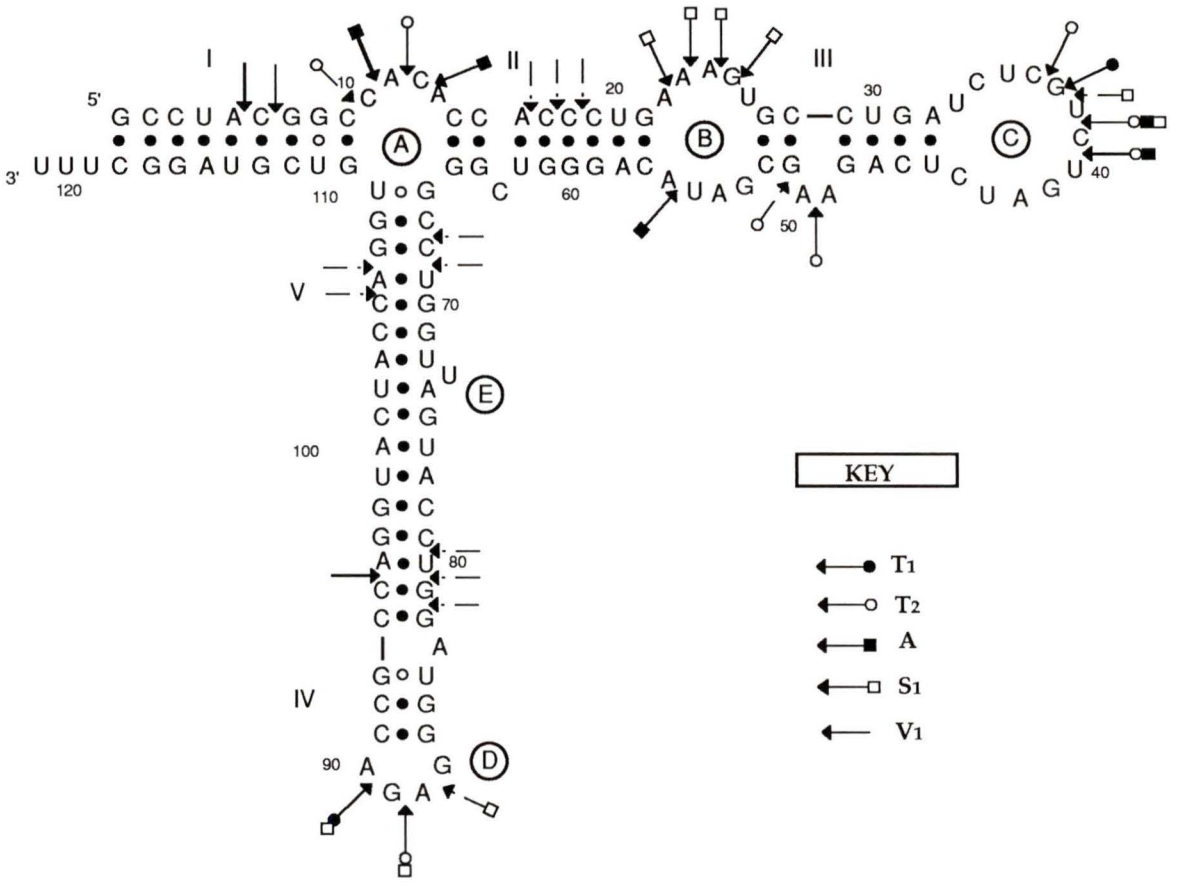

Figure 23: Summary of nuclease cleavages of Xlo 96-101 5S rRNA. The extent of cleavage is indicated by: thick line, strong; thin line, moderate; broken line, weak.

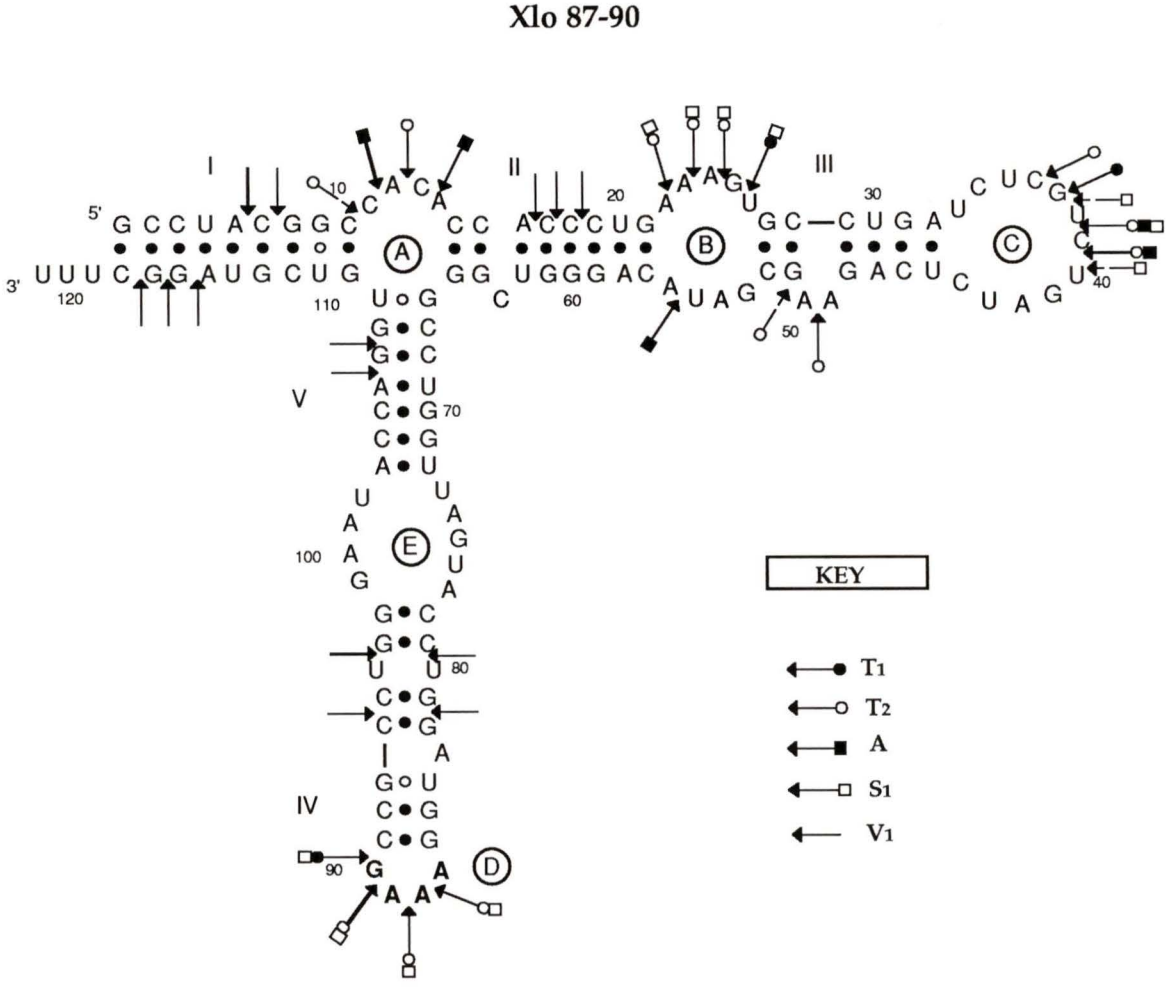

Figure 24: Summary of nuclease cleavages of Xlo 87-90 5S rRNA. The extent of cleavage is indicated by: thick line, strong; thin line, moderate; broken line, weak.

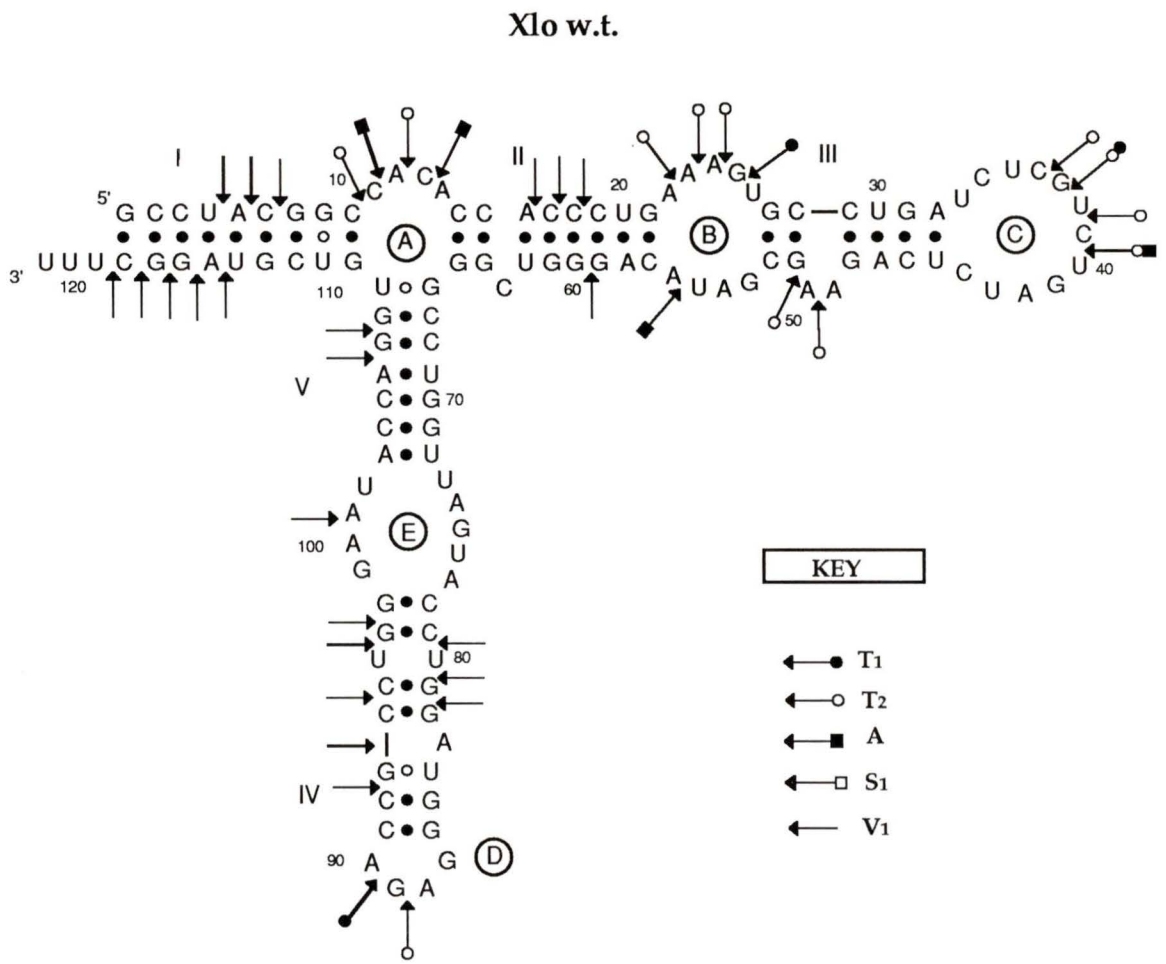

Figure 25: Summary of the nuclease digestion experiments of Xlo w.t. 5S rRNA, showing moderate and strong cleavages on the secondary structure model of 5S rRNA (adapted from Romaniuk *et al.*, 1988).

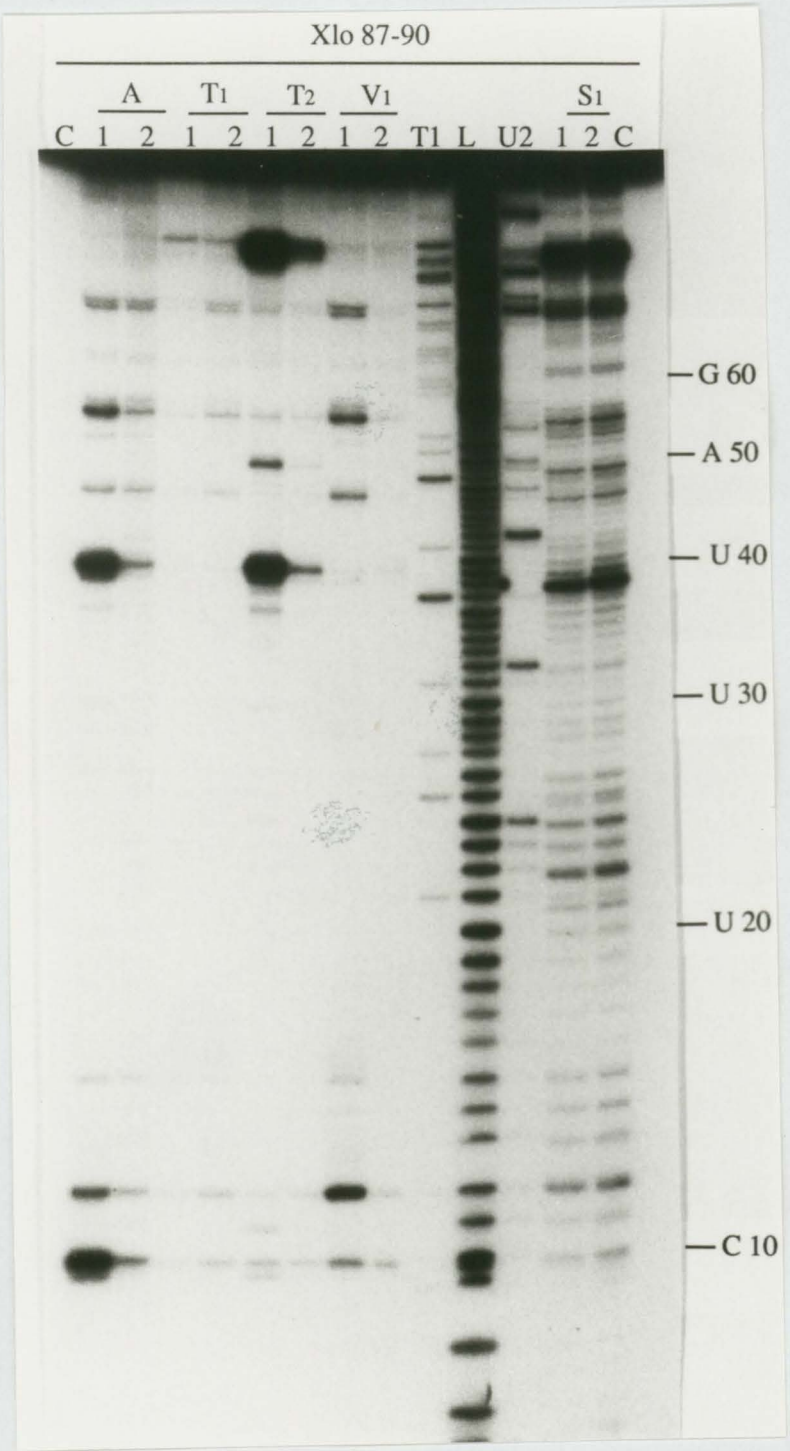

Figure 26: Gel electrophoresis fractionation showing enzymatic digests of 5'-end labeled Xlo 87-90 5S rRNA. Legend: C, control (no nuclease); Nuclease A: 1, 0.1 ng; 2, 10ng; T_1: 1, 0.1U; 2, 3U; T_2: 1, 0.01U; 2, 0.3U; V_1: 1, 0.22U; 2, 0.7U; S_1: 1, 22U; 2, 110U; L, base hydrolysis ladder; T_1, T_1 sequencing reaction; U_2, U_2 sequencing reaction.

digestion patterns of loops **E** and **D**. One can see that in wild-type 5S rRNA, the most accessible regions to single-strand specific nucleases are loop **A** as well as some regions in loops **B**, **C** and **D**, whereas no cleavages were observed in loop **E** (Figure 25). It is in loop **E** that nucleotide sequences were changed in order to produce three different 5S rRNA mutants. 1) In the 5' side of loop **E**, mutant Xlo73-76 5S rRNA has the nucleotide sequence $UAGU_{76}$ changed to $GGAC_{76}$ 2) In the 3' of this loop, in mutant Xlo99-101, the nucleotides at positions GAA_{101} were changed to AGG_{101} 3) In mutant Xlo96-101, U_{96} was changed to A_{96}, G_{99} to U_{99}, and A_{101} to C_{101} in order to create an extended base pairing between helices **IV** and **V** with Watson-Crick base pairs. From the nuclease digestion pattern obtained for the mutant 5S rRNAs, one can observe that in the 5S rRNA from Xlo73-76, loop **E** has become more accessible to single-strand specific nucleases such as T_1, T_2, and A (Figure 21). Similarly, in Xlo99-101 5S rRNA loop **E** appears to be more susceptible to cleavage, especially the 3' side of the loop, where one can see strong T_1 and T_2 cleavages (Figure 22). However, in Xlo96-101 5S rRNA, there is resistance towards single-strand specific nucleases between helices **IV** and **V** (Figure 23). In addition, the enzymatic cleavage pattern of loop **D** produced by single-strand specific nucleases differs between the wild type and Xlo87-90 5S rRNAs. The nucleotide changes for mutant Xlo87-90 5S rRNA: $GAGA_{90}$ to $AAAG_{90}$ are located in the tetranucleotide loop **D**. In Xlo87-90 5S rRNA, loop **D** appears much more accessible to single-strand specific nucleases than in the wild-type 5S rRNA. In this mutant one can observe S_1 cleavages at every single position of this loop, together with some T_1 and T_2 cleavages (figure 24). However, the wild-type and Xlo87-90 5S rRNA do not differ in the nuclease digestion pattern of loop **E** (Figures 24 and 25).

Strong RNase V_1 cuts are observed in each of the five helical stems of 5S rRNA from the wild-type and all four mutants. However, in Xlo96-101 and Xlo99-101 5S rRNAs it was difficult to assess the reactivity of helix I to RNase V_1 cleavages. In Xlo96-101 5S rRNA, a strong cleavage with RNase V_1 was observed at position A_{96}-U_{80}, and in Xlo99-101 5S rRNA, additional V_1 cleavages were observed at positions C_{46} and C_{68}, thus suggesting the existence of base pairing in these regions (Figures 22 and 23). In general, cleavage by single-strand specific nucleases did not occur in the helical regions of either the wild-type 5S rRNA, or of the 5S rRNA from all four mutants.

These results are discussed below, together with the results obtained from the chemical reactivity data.

Reactivity of 5S rRNA to Chemical Probes

As mentioned before, both the direct and the indirect methods were used to identify nucleotides reacting with the different chemical structure probes. The direct method allowed mapping of the reactivity of G(N7) and C(N3) to DMS, of A(N7) to DEPC, and of phosphates to ENU, after appropriate cleavage on both 5'- and 3'-end-labeled 5S rRNAs from all four mutants. A typical example is given in Figure 27 for Xlo87-90, and the data from several such experiments are summarized in Figures 28 to 32 for the four mutants and the wild-type, respectively. Spontaneous cleavages at some positions, occurring mainly at pyrimidine-adenosine dinucleotide sequences were observed in the incubation control. These cleavages have been observed in other RNA molecules (Carbon *et al.*, 1978; Romby *et al.*, 1985; Moazed *et al.*, 1986; Romby *et al.*, 1988), and they are not believed to be induced by contaminating nucleases, but are thought to reflect an intrinsic chemical instability, partly

Figure 27: Chemical modification of 3'-end labeled Xlo 87-90 5S rRNA. Autoradiogram of a long migration gel, showing modifications at the following positions: (C-N3 and G-N7) by means of DMS; (A-N7) by means of DEPC; and (phosphates) by means of ENU. Legend: C, incubation control; 1, native conditions; 2, semi-denaturing conditions; L, base hydrolysis ladder; T_1, T_1 sequencing reaction; U_2, U_2 sequencing reaction.

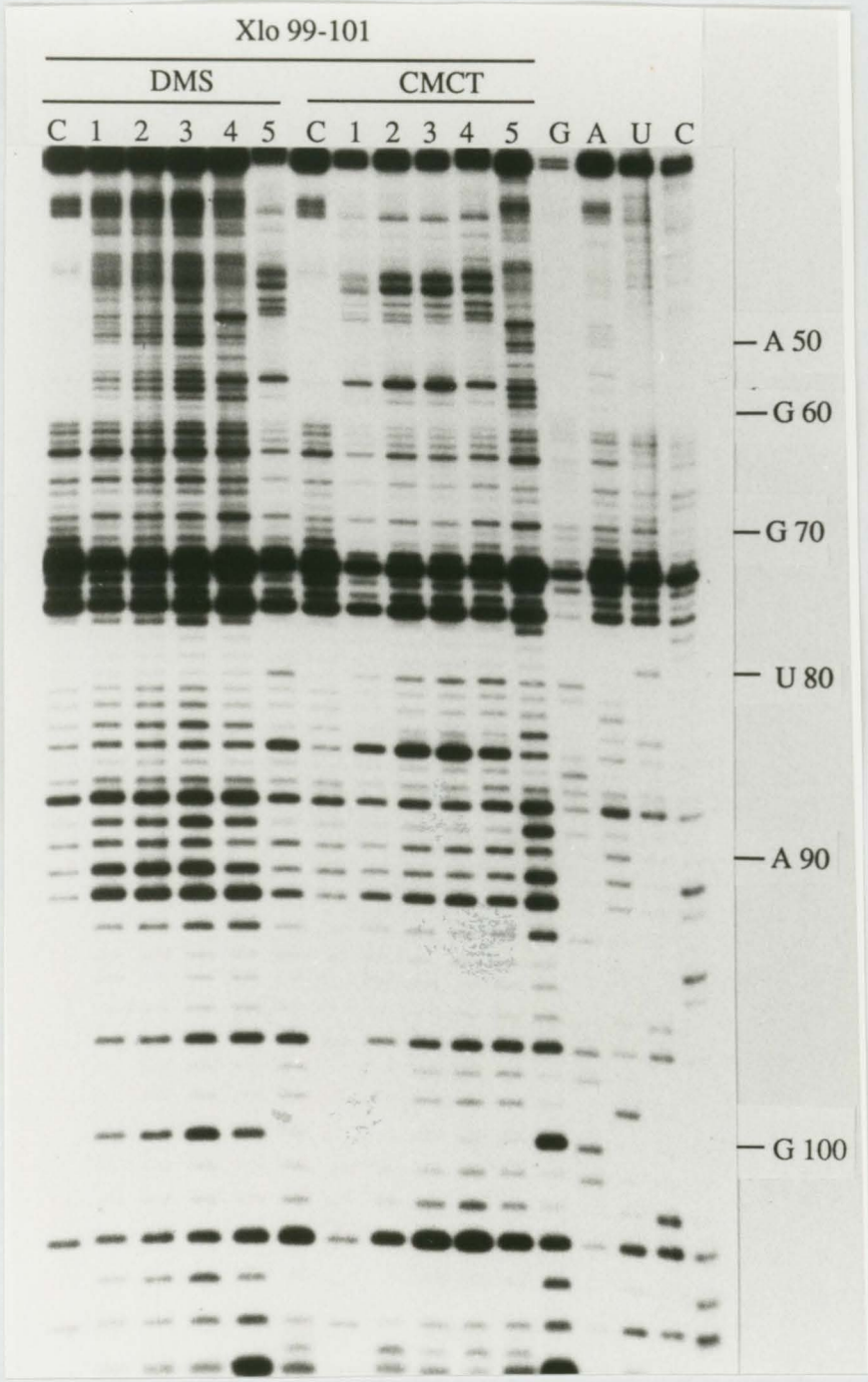

Figure 33: Chemical modification of Xlo 99-101 5S rRNA using the primer extension method. Autoradiogram of a short migration gel , showing modifications at the following positions: (A-N1 and C-N3) by means of DMS; and (G-N1 and U-N3) by means of CMCT. Native conditions: (C) incubation control; (1), DMS: 2 min., CMCT: 15 min.; (2), DMS: 5 min., CMCT: 30 min.; (3) DMS: 10 min., CMCT: 60 min. Semi-denaturing conditions: (4), DMS: 2min., CMCT: 15min.; (5), DMS: 5min., CMCT: 30 min. Lanes G, A, U and C are sequencing products generated in the presence of ddCTP, ddTTP, ddATP and ddGTP, respectively. Note: Lanes (5) are reversed.

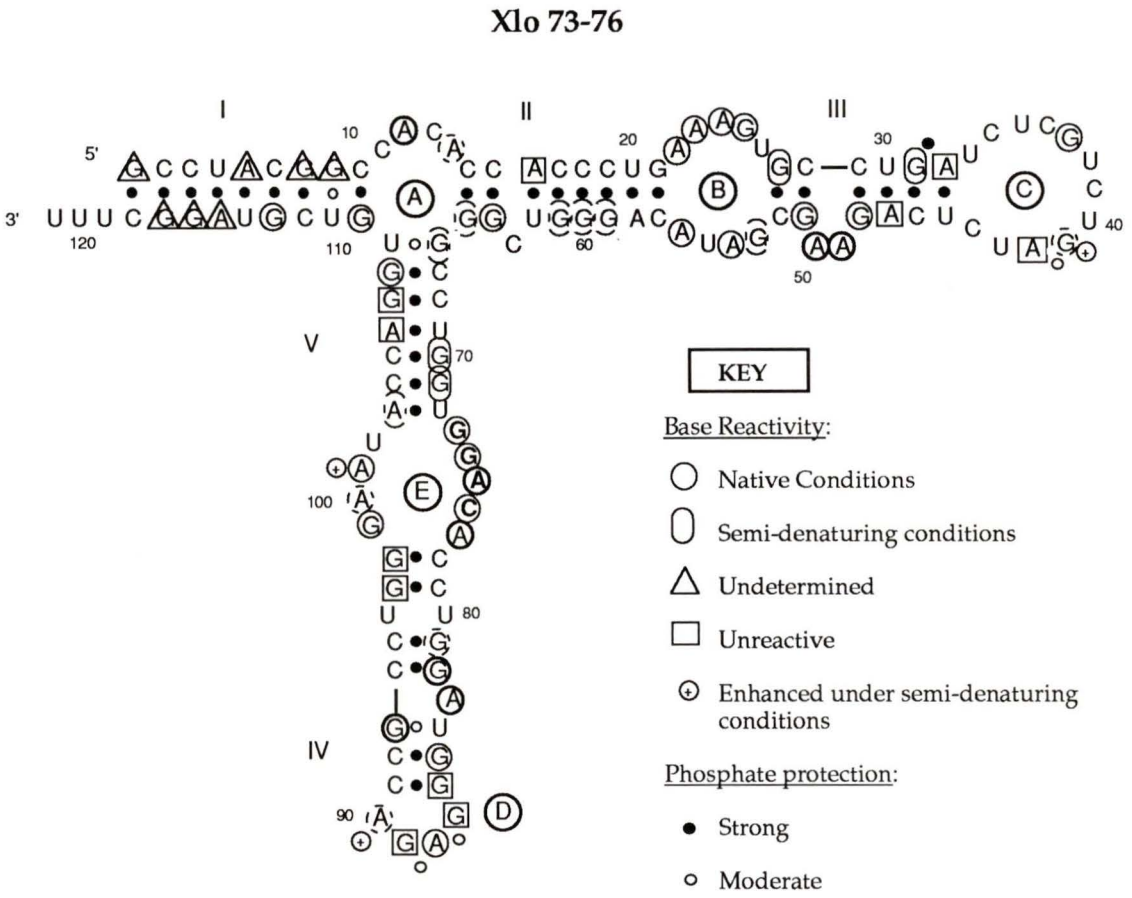

Figure 28: Summary of chemical modifications of purine N-7 positions and phosphates of mutant Xlo 73-76 5S rRNA. The extent of reactivity is indicated by: thick line, strong; thin line, moderate; broken line, weak.

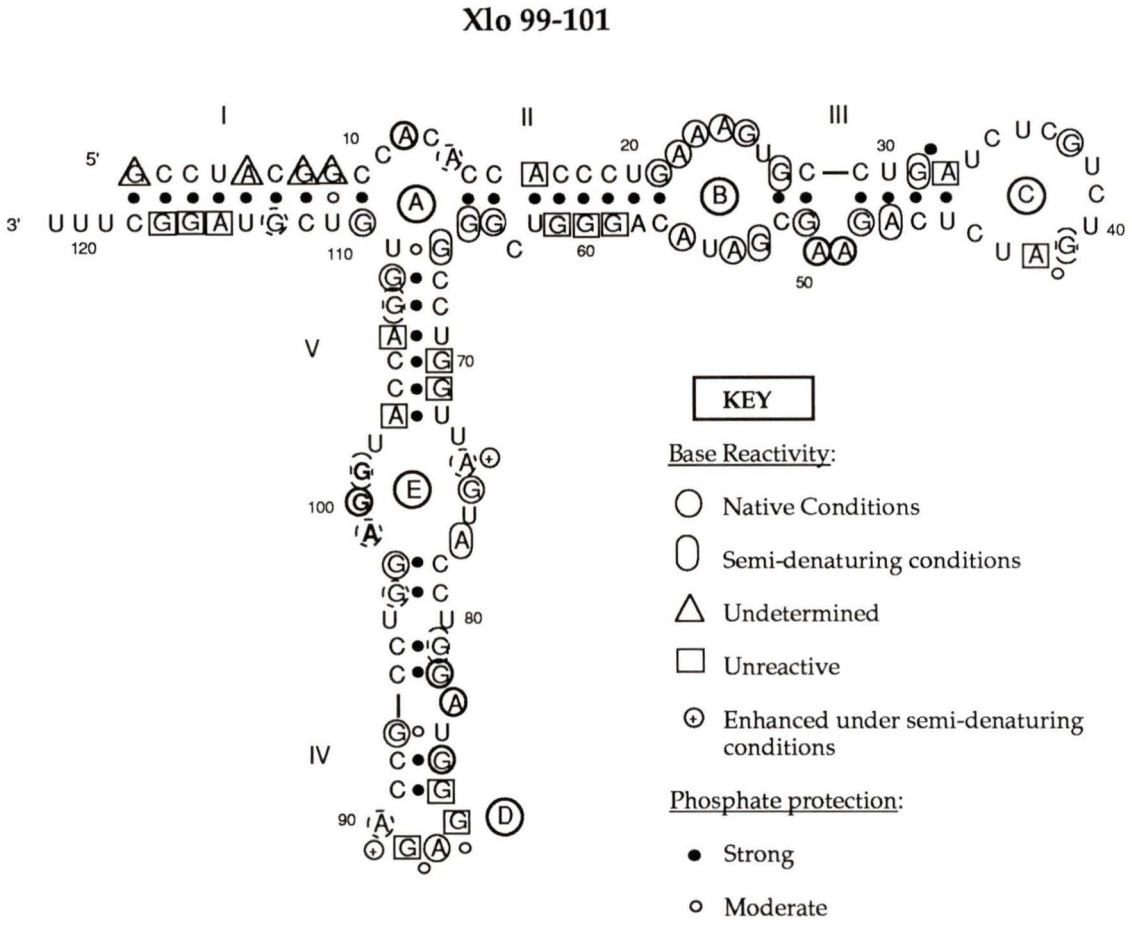

Figure 29: Summary of chemical modifications of purine N-7 positions and phosphates of mutant Xlo 99-101 5S rRNA. The extent of reactivity is indicated by: thick line, strong; thin line, moderate; broken line, weak.

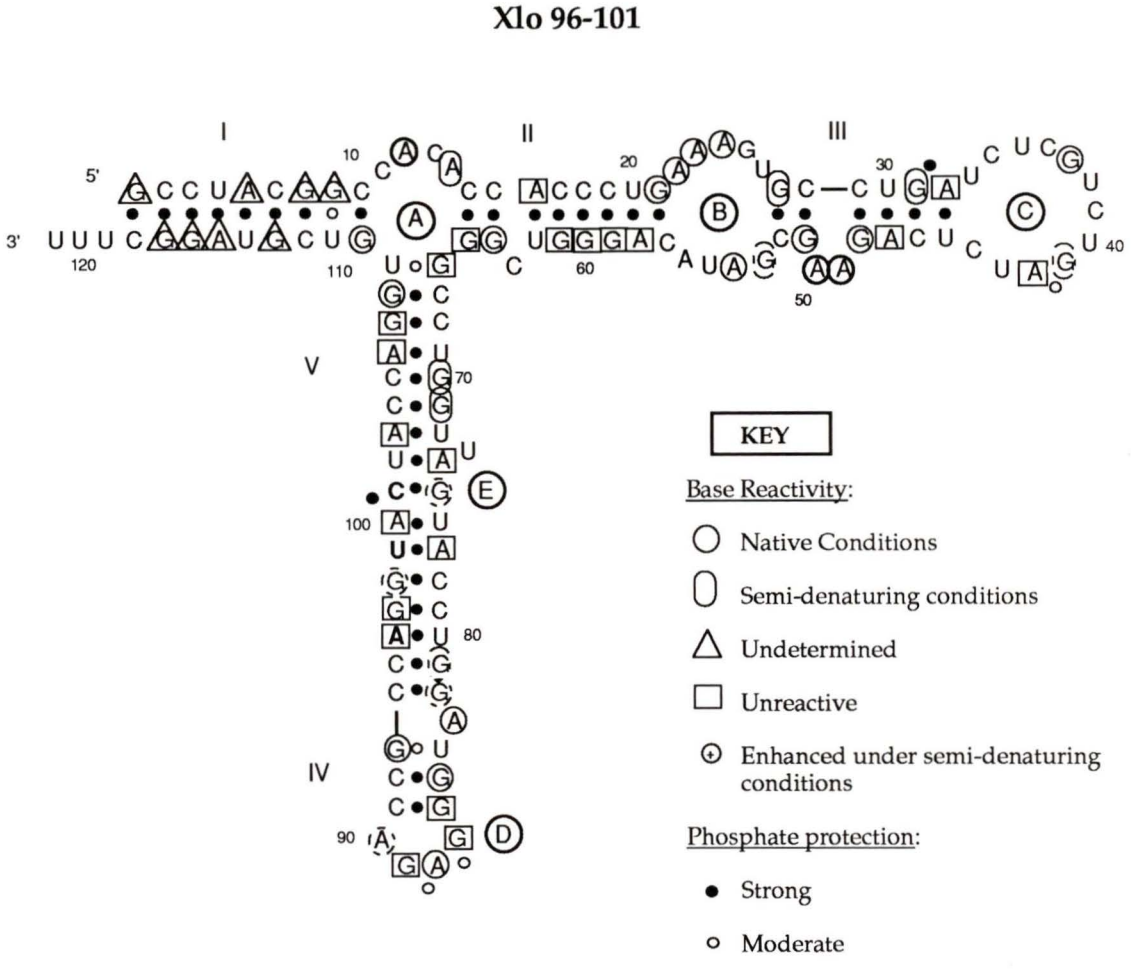

Figure 30: Summary of chemical modifications of purine N-7 positions and phosphates of mutant Xlo 96-101 5S rRNA. The extent of reactivity is indicated by: thick line, strong; thin line, moderate; broken line, weak.

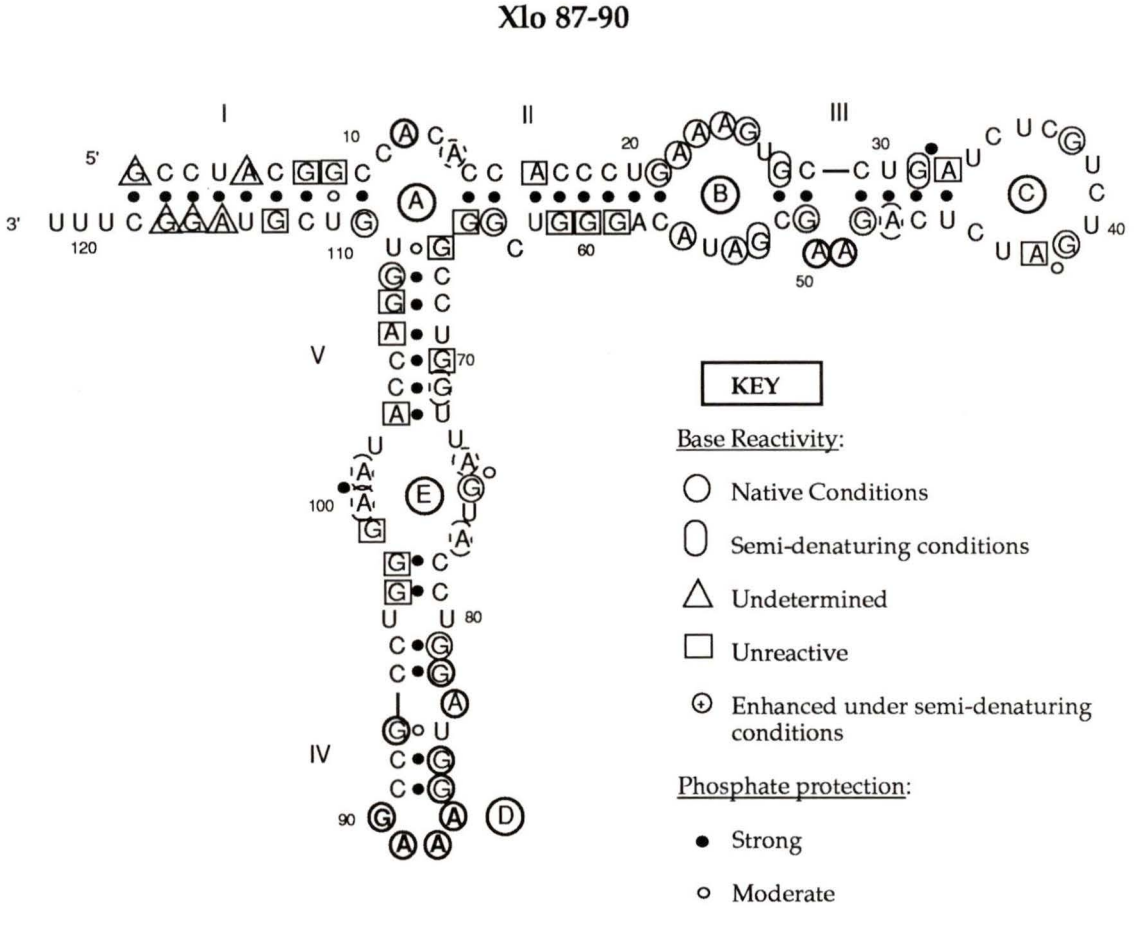

Figure 31: Summary of chemical modifications of purine N-7 positions and phosphates of mutant Xlo 87-90 5S rRNA. The extent of reactivity is indicated by: thick line, strong; thin line, moderate; broken line, weak.

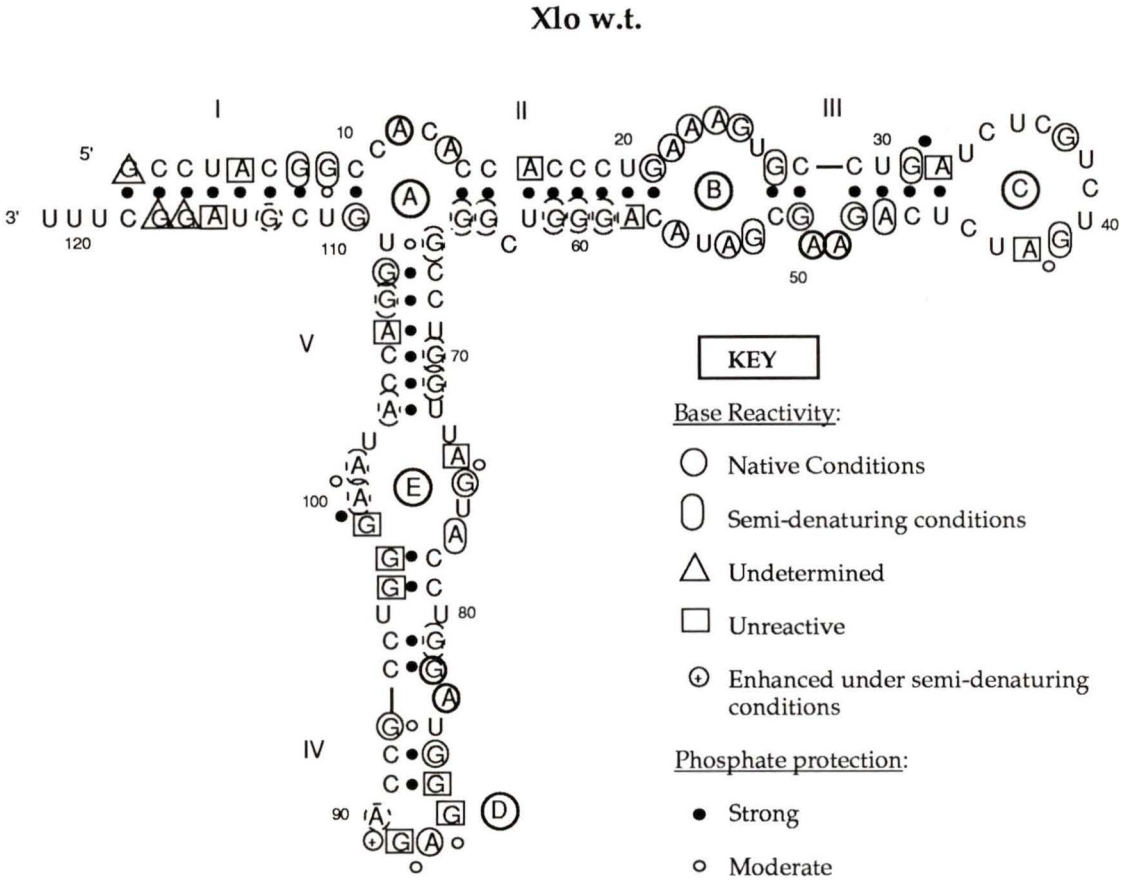

Figure 32: Summary of chemical modifications of purine N-7 positions and phosphates of Xlo w.t. 5S rRNA. The extent of reactivity is indicated by: thick line, strong; thin line, moderate; broken line, weak.

caused by a particular flexibility at those positions leading to alkaline-type hydrolysis (Moras *et al.*, 1983) In the indirect method, unlabeled 5S rRNAs from each of the four mutants were subjected to chemical modification. The modified 5S rRNAs were then used as a template for primer extension. Modification at Watson-Crick positions stopped the progress of reverse transcriptase and yielded prematurely terminated DNA fragments. Therefore, this technique allowed probing of each base at one of its Watson-Crick positions through the use of DMS for A(N1) and C(N3), and of CMCT for G(N1) and U(N3). A typical experiment is shown in Figure 33 for Xlo99-101. In the incubation controls there are some artifact bands in some areas, which made the interpretation of the autoradiogram difficult. The results from several experiments on each of the four mutants and the wild type 5S rRNAs have been analyzed and are summarized in the secondary structure models in Figures 34 to 38.

The reactivity towards DMS, CMCT, and DEPC was found to be dependent on the buffer conditions. Under native conditions (presence of magnesium, 20°C) a number of nucleotides involved in hydrogen bonding are unreactive. Under semi-denaturing conditions (absence of magnesium, 20°C), several nucleotides which were unreactive under native conditions become reactive. This latter observation confirms the crucial role played by magnesium in the folding of RNA and indicates the existence of rather weak interactions. With regards to Watson-Crick base pairing positions, the nucleotides that become reactive under semi-denaturing conditions are primarily located in helices. In general, nucleotides in loops are expected to be reactive at their Watson-Crick positions. However, it is interesting to note that some nucleotides located in loops are unreactive under native

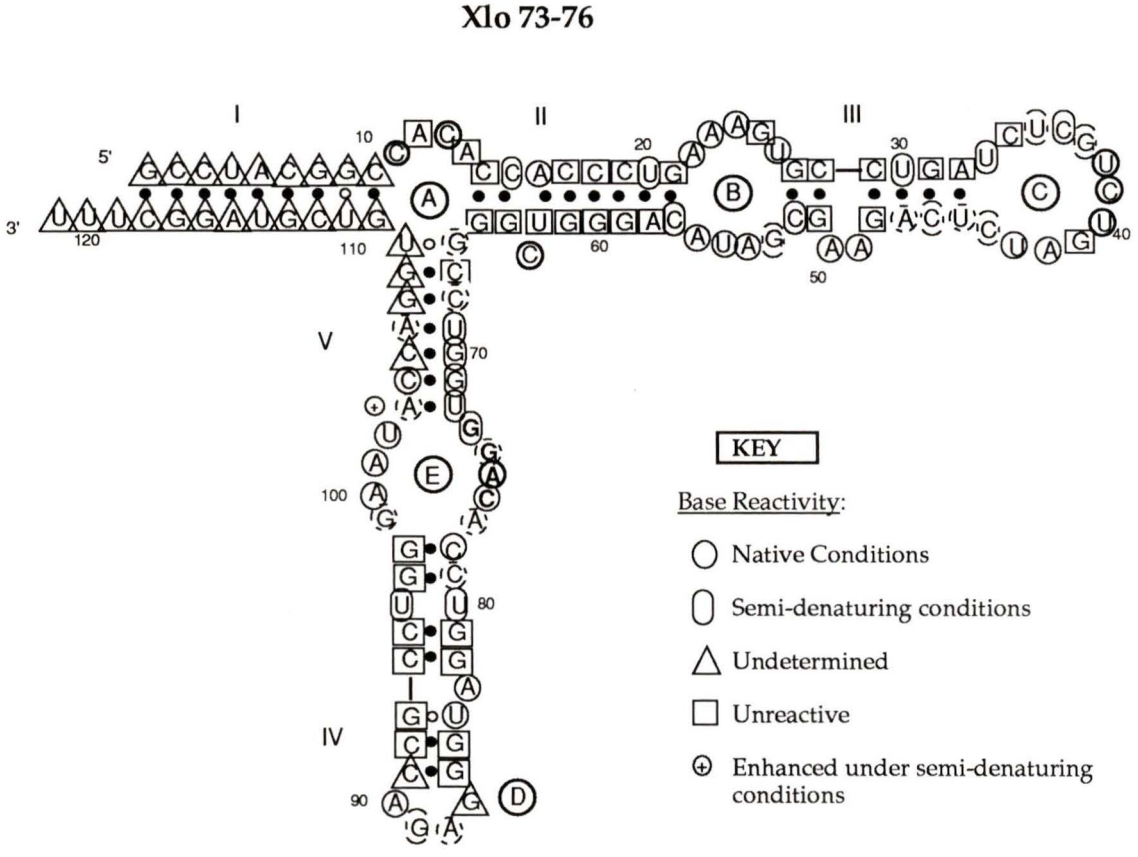

Figure 34: Summary of chemical modifications of A(N-1), G(N-1), C(N-3) and U(N-3) positions of Xlo 73-76 5S rRNA. The extent of reactivity is indicated by: thick line, strong; thin line, moderate; broken line, weak.

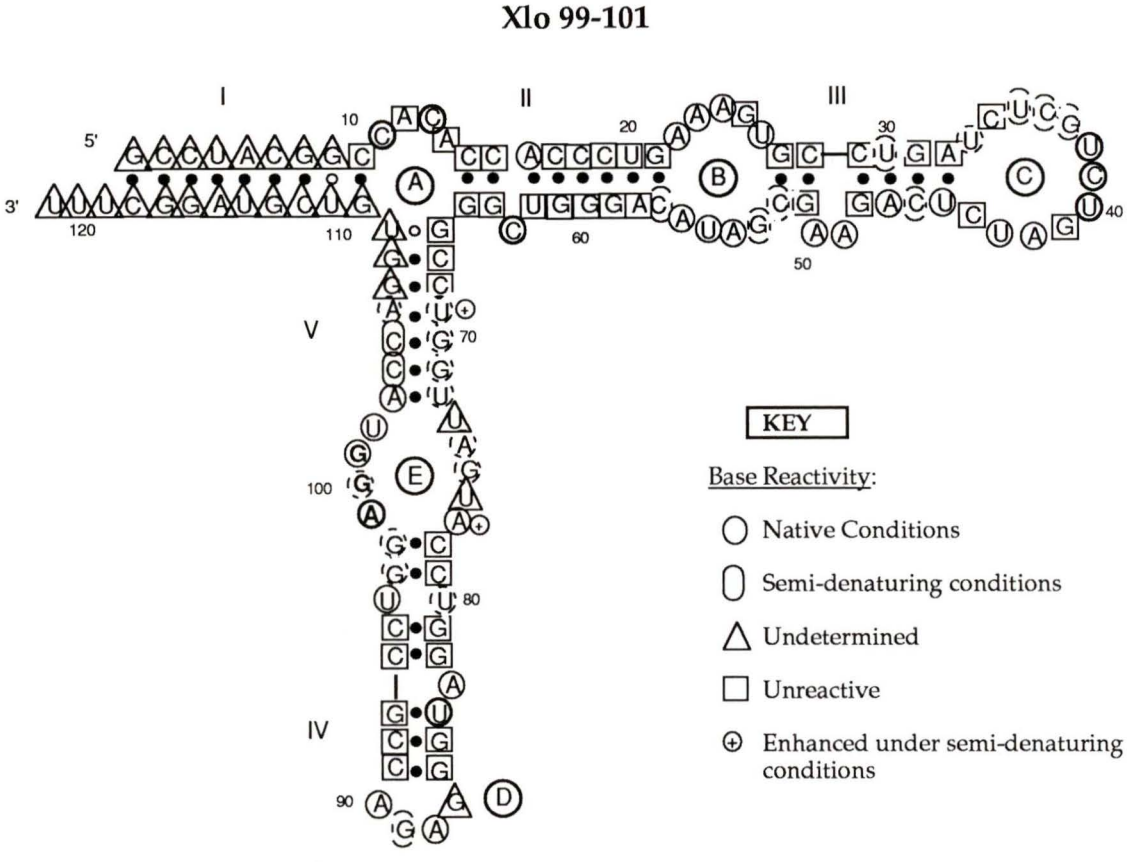

Figure 35: Summary of chemical modifications of A(N-1), G(N-1), C(N-3) and U(N-3) positions of Xlo 99-101 5S rRNA. The extent of reactivity is indicated by: thick line, strong; thin line, moderate; broken line, weak.

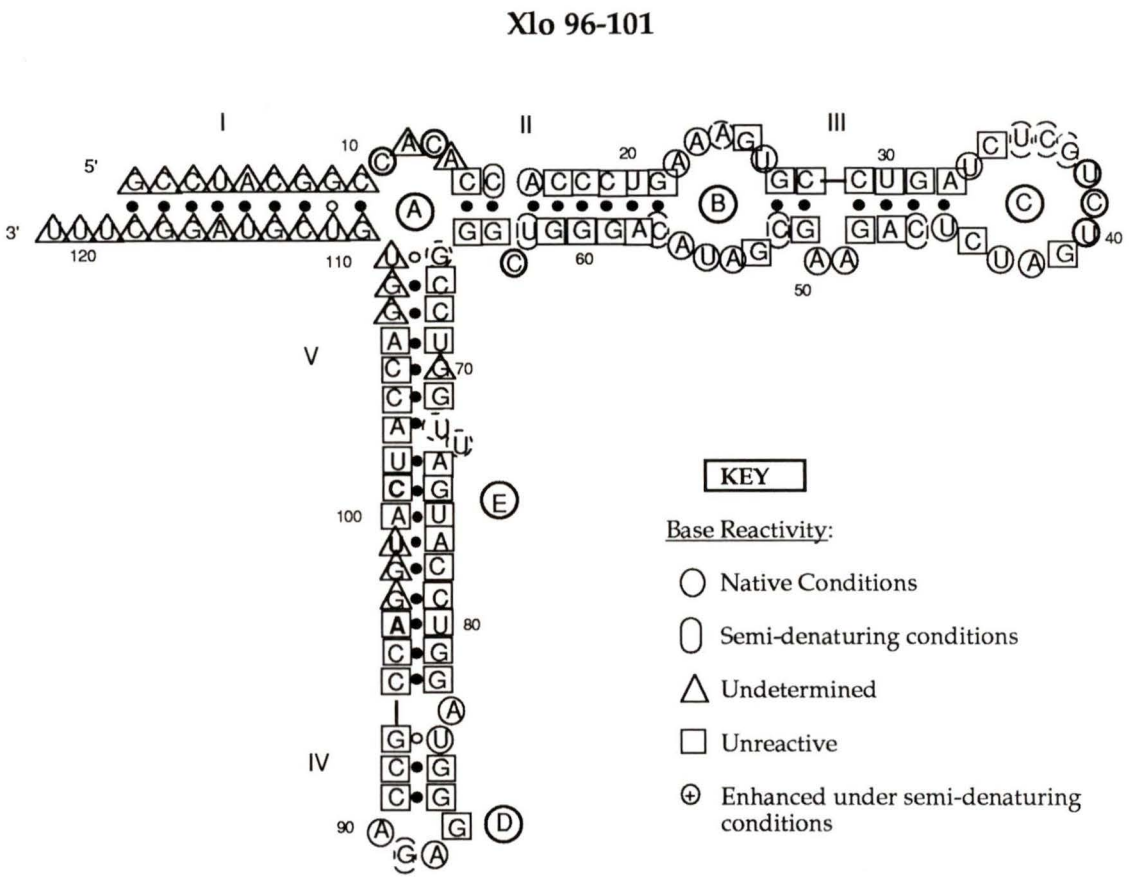

Figure 36: Summary of chemical modifications of A(N-1), G(N-1), C(N-3) and U(N-3) positions of Xlo 96-101 5S rRNA. The extent of reactivity is indicated by: thick line, strong; thin line, moderate; broken line, weak.

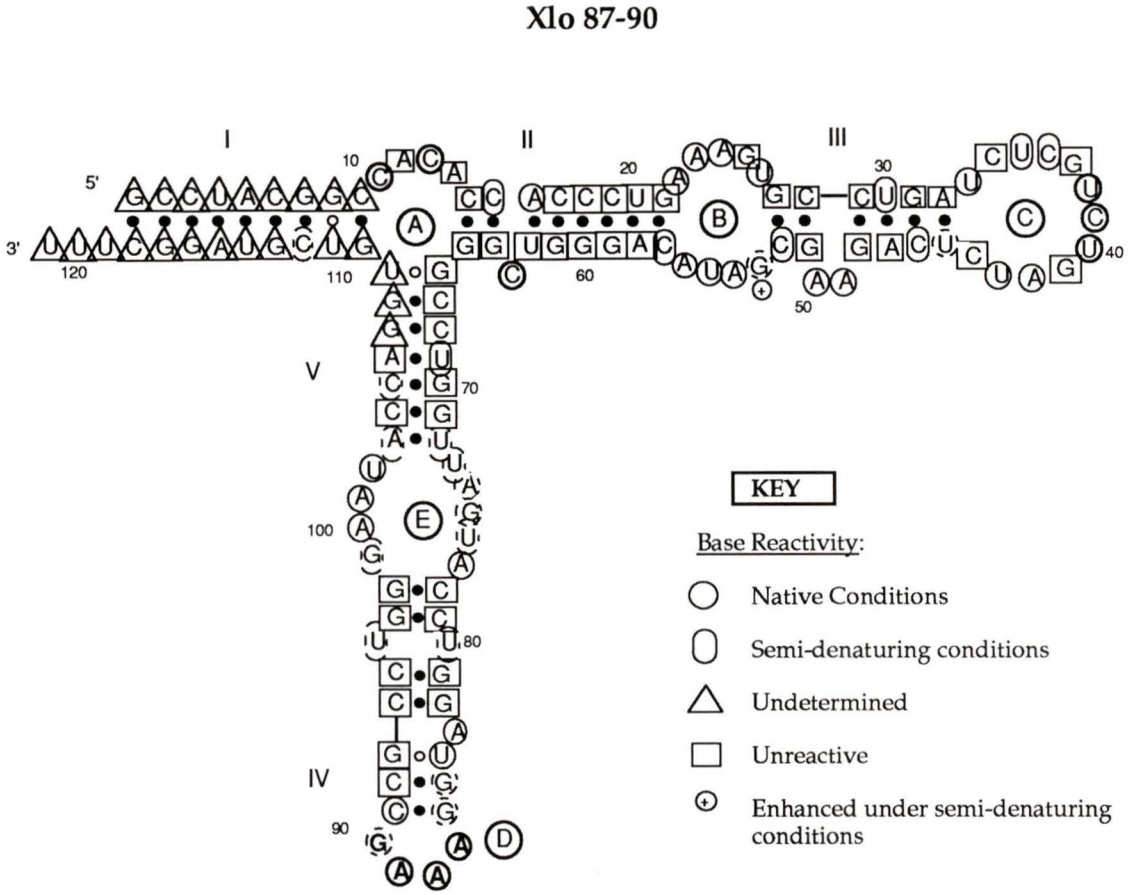

Figure 37: Summary of chemical modifications of A(N-1), G(N-1), C(N-3) and U(N-3) positions of Xlo 87-90 5S rRNA. The extent of reactivity is indicated by: thick line, strong; thin line, moderate; broken line, weak.

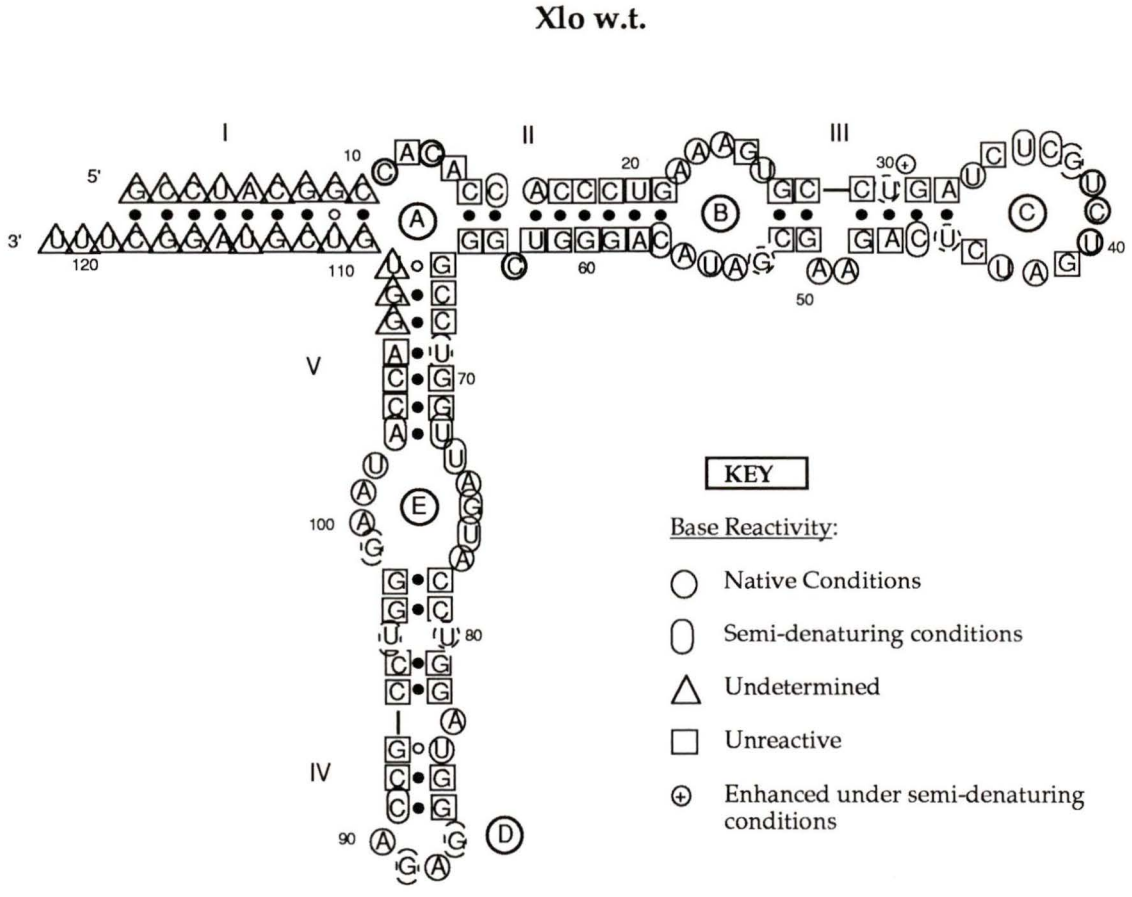

Figure 38: Summary of chemical modifications of A(N-1), G(N-1), C(N-3) and U(N-3) positions of Xlo w.t. 5S rRNA. The extent of reactivity is indicated by: thick line, strong; thin line, moderate; broken line, weak.

conditions but reactive under semi-denaturing conditions. These positions, which are not involved in the secondary folding of 5S rRNA, might participate in tertiary interactions.

The structure of 5S rRNA can be divided into three stems. The first stem is composed of helix **I** containing the 5'- and 3'- ends of 5S rRNA, and of the single-stranded internal loop **A** (nucleotides 10-13). The second stem contains helices **II** and **III**, separated by the internal loop **B**, and terminated by the hairpin loop **C** (nucleotides 33-44). The third stem comprises helices **IV** and **V** separated by the internal loop **E** and terminated by the hairpin loop **D** (nucleotides 87-90). In order to facilitate understanding of the results obtained from chemical and enzymatic probes, in the following section results from the three stems will be discussed separately. In addition, the results from the 5S rRNA of each of the four mutants will be compared to the results from the wild-type 5S rRNA.

First stem

Loop A

In loop **A**, the 5S rRNA from each of the mutants and the wild-type have the same chemical reactivity. The $CACA_{13}$ sequence is found to be reactive at both C-N3 and A-N7 positions under native conditions, with position $N7(A_{13})$ being only mildly reactive under these conditions (Figures 28-32 and 34-38). These results, together with the observation that loop **A** is fully accessible to single-strand specific nucleases in all these 5S rRNAs (Figures 21 to 25), indicate that the nucleotides in this loop appear to be essentially single-stranded and unaffected by the base changes introduced in the altered 5S rRNAs. It is expected that all nucleotides in a loop are reactive at their Watson-Crick positions. However, it should be pointed out that both A_{11}

and A_{13} are unreactive at their N1 position in all four mutants and wild-type 5S rRNA.

In the three-dimensional model for the complete *Xenopus* oocyte 5S rRNA proposed by Westhof (in press), which is based upon solution structure experimental data of *Xenopus laevis* oocyte 5S rRNA obtained by Romaniuk *et al.* (1988) and computer graphic modelling, loop **A** is proposed to have an open conformation without tight stacking, owing to the mild reactivity of position N7(A_{13}) (Figure 10). According to these authors, 5S rRNA has a distorted Y-shaped structure with a short stalk made of stem 1 and with the arms of the Y made of stems 2 and 3. The orientation of the stalk with respect to the arms is believed to be controlled by residues of the internal loop **A**, and by the coaxiality between helices **II** and **V**. It is proposed that this structure can be generated by pairing the highly conserved and unreactive residues A_{13} and G_{66} in loop **A** so that helices **II** and **V** form a continuous helix (Westhof *et al.*, in press).

Helix **I**

The chemical reactivity results in helix **I** were not possible to assess. Owing to the nature of the primer extension method, it was not possible to obtain any information on the reactivity of either nucleotides 103-121, where the priming site for reverse transcriptase is located, or the adjacent region to this priming site, where pausing of the enzyme is observed. A likely explanation for these stops or pauses is the fact that it is difficult for reverse transcriptase to melt certain regions where folding of RNA occurs, especially since reverse transcription is done in the presence of magnesium (Ehreshman *et al.*, 1987). The nucleotide sequence 1-9 was not well resolved in gels, and the chemical reactivity of these nucleotides could not be assessed.

Second Stem

Loop B

In the *Xenopus laevis* oocyte 5S rRNA secondary structure, the internal loop **B** is located between base pairs 21-57 and 27-52, with five residues between positions 21-27 and four residues between positions 52 and 57. From the chemical reactivity data of each of the four mutant 5S rRNAs, one can observe that in loop **B,** six of the nine nucleotides exhibit a strong reactivity at N7 positions under native conditions, indicating that these residues are fully exposed. The guanosine at position 53 becomes reactive under semi-denaturing conditions (Figures 28 to 31). Similarly, all residues exhibit a strong reactivity at Watson-Crick positions under native conditions in the 5S rRNA from all four mutants, with the exception of nucleotides at position 25 and 53 which are unreactive (Figures 34 to 37). However, the guanosine at position 53 becomes reactive under semi-denaturing conditions in mutants Xlo73-76 and Xlo99-101 (Figure 35 and 36). In mutant Xlo87-90, G_{53} is mildly reactive under native conditions, but it has an increased reactivity under semi-denaturing conditions, thus suggesting the existence of different conformational populations in this mutant (Figure 37). These chemical reactivity results are largely identical with those obtained from the oocyte wild-type 5S rRNA (Figures 32 and 38). This observation together with the presence of several single-strand specific RNase cleavages in loop **B** of all these 5S rRNAs (Figures 21-25), confirms that this loop is not affected by any of the mutations introduced in the third stem of 5S rRNA, since it remains single-stranded, as previously suggested (Romaniuk *et al.*, 1988). According to the *Xenopus* oocyte 5S rRNA structure model proposed by Westhof *et al.* (in press), loop **B** presents an unusually open structure because of the high

reactivity both of purines at N7 positions and of nucleotides at Watson-Crick positions under native conditions, and the absence of base stacking.

Helices II and III

In helices **II** and **III**, the reactivity to chemical probes in the 5S rRNA from each of the four mutants is largely identical to that obtained for the wild-type 5S rRNA (Figures 28-38). These results indicate that the mutations introduced in the third stem of *Xenopus* oocyte 5S rRNA did not affect the structure of these two helices, since the absence of reactivity at Watson-Crick positions under native conditions and the presence of some RNase V_1 cuts confirm their continuous presence. Helix **II** appears to be more stable than helix **III**, although there is reactivity at Watson-Crick positions in A_{16} under native conditions and in C_{15} under semi-denaturing conditions. This last observation could be due to a slight wedge between the base pairs 15-64 and 16-62, formed by residue C_{63} which appears to be bulging out of helix **II**, since its N3 position and N7 (G_{64}) are reactive under native conditions in all the 5S rRNAs. In helix **III** of each mutant 5S rRNA, some of the residues such as U_{30}, C_{46} and C_{52} become reactive at their Watson-Crick positions under semi-denaturing conditions. U_{45}, however, is only mildly reactive under native conditions (Figures 34-37). Possibly the reason for the moderate reactivity of U_{45} at N3 position is that this residue is part of a terminal base pair. Reactivity or marginal reactivity is often observed in terminal base pairs, especially in A-U base pairs located at the junction of internal loops. This reactivity is believed to result from an increased flexibility in these particular regions (Ehresmann *et al.*, 1987). For example, in *E. coli* 16S rRNA some reactivity in terminal A-U base pairs located at the junction of internal loops has been observed (Baudin *et al.*, 1987).

In helix **III** the chemical reactivity at N7(A_{49}), N1(A_{50}), as well as two strong RNase T_2 cleavages observed after A_{49} and A_{50} in each mutant 5S rRNA, confirm the presence of two bulged residues at positions A_{49} and A_{50}. These observations matched the chemical reactivity and enzymatic accessibility of the wild-type 5S rRNA in this region (Figures 21-38). It is believed that the configuration given by bulged nucleotides does not disturb the double helix since a similar structure is known to occur in yeast $tRNA^{Phe}$, where U_{59} and C_{60} loop out and are stacked upon each other (Hingerty *et al.*, 1978). In summary, the chemical reactivity observed in the mutant 5S rRNAs agrees with that found in the wild-type in helices **II** and **III**, and show that the base changes introduced in the four mutants do not affect the structure of these helices.

The reactivity of the phosphates in each of the four mutant 5S rRNAs towards alkylation with ENU was tested under native conditions at 20°C and the results are shown in Figure 39. The phosphate at position 32 in helix **III** was found to be protected from reaction with ENU in the 5S rRNA of each of the four mutants and the wild-type (Figures 28-32).

Loop **C**

Loop **C** contains twelve residues and all nucleotides in this loop are remarkably conserved throughout evolution (Delihas *et al.*, 1984; Erdmann and Wolters, 1986). In comparison to loop **B**, residues in loop **C** appear to be less accessible in all four mutant 5S rRNAs. The chemical reactivity data of loop **C** residues are basically the same in the four 5S rRNA mutants and in the wild-type 5S rRNA. Of the three purine residues only G_{37} is clearly reactive at the N7 position under native conditions, whereas the N7 position of A_{42} is unreactive even under semi-denaturing conditions in all four

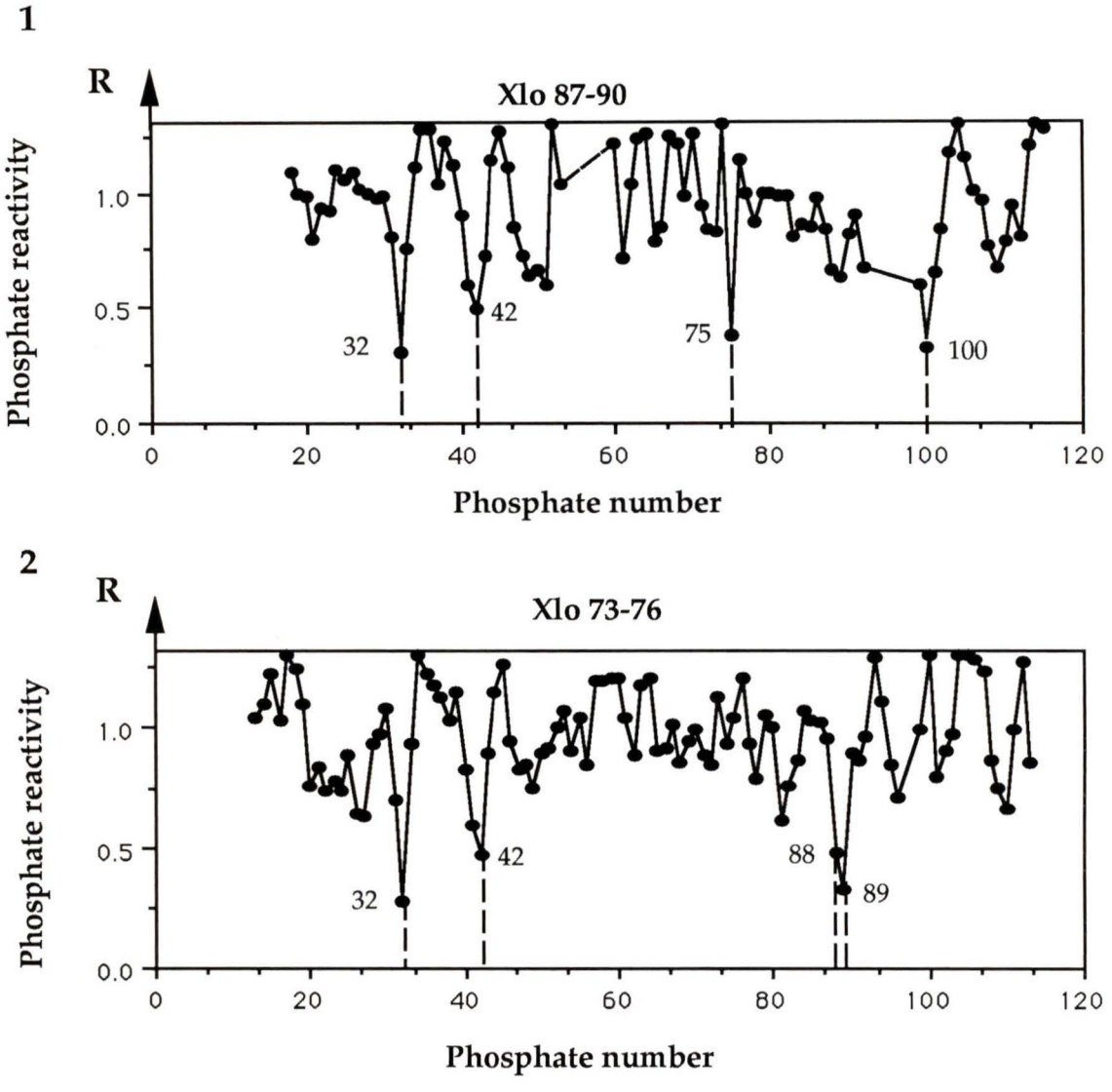

Figure 39: Pattern of phosphate reactivities to ENU under native conditions versus denatured conditions: (1), Xlo 87-90; (2), Xlo 73-76; (3), Xlo 96-101; and (4), Xlo 99-101. R values are the ratio between the intensities of the corresponding bands in both conditions. These intensities were measured as peak areas on the densitograms of the gels. A ratio R<1 means that alkylation of a given phosphate is lower in the native molecule than it is in the denatured one. R<0.5 indicates a strongly reduced reactivity (more than 50%). The reactivity of some phosphates could not be analyzed due to unspecific degradation, and are indicated by a dotted line connecting adjoining dots.

3

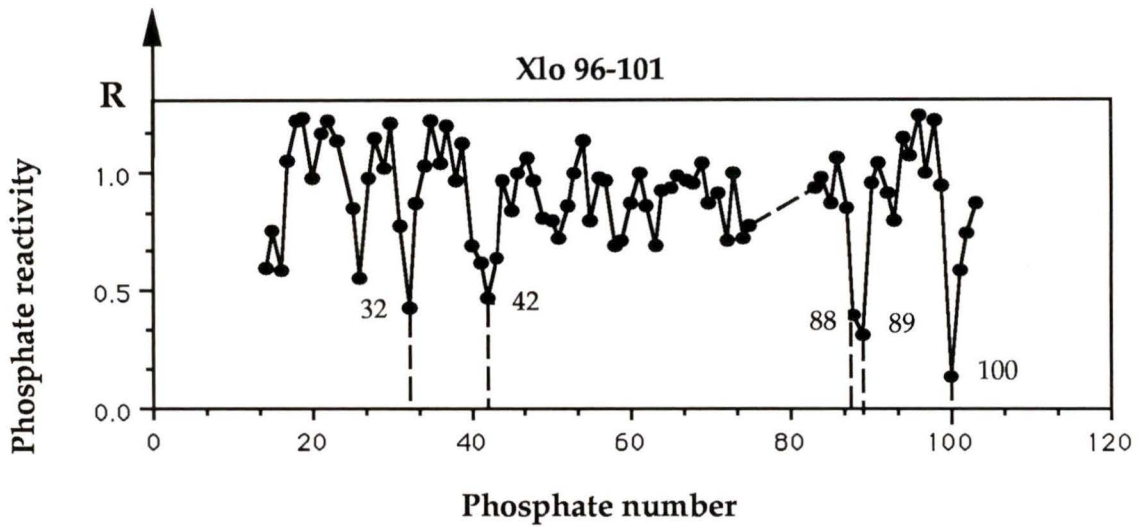

4

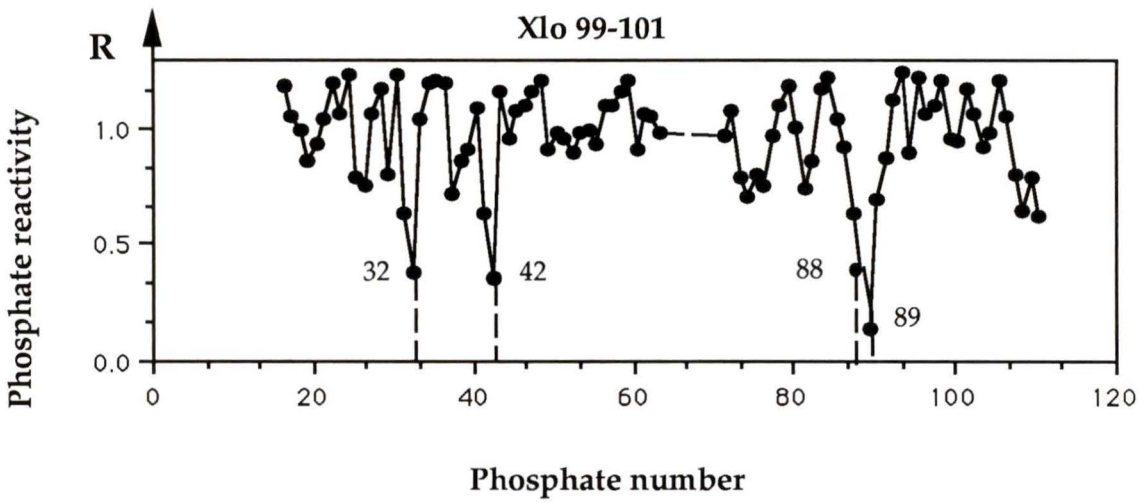

Figure 39 (continued).

mutants and as well as the wild type 5S rRNA(Figures 28 to 32). In mutants Xlo73-76, Xlo87-90 and wild-type 5S rRNA, the N7 position of G_{41} is mildly reactive under native conditions, but enhanced under semi-denaturing conditions (Figures 28 and 31). However, in Xlo96-101 and Xlo99-101 G_{41} is only reactive under semi-denaturing conditions (Figures 29 and 30). At the Watson-Crick positions the sequence UCU_{40} appears to be highly reactive under native conditions and very susceptible to cleavage by single-strand specific nucleases in all the mutants and the wild type (Figures 21-25 and 34-38). However, the sequence UCG_{37} of loop **C** is unreactive at the Watson-Crick positions under native conditions, and only partially reactive under semi-denaturing conditions, whereas C_{34}, G_{41} and C_{44} are totally unreactive in the 5S rRNAs from all mutants. The absence of reactivity of these residues in loop **C** can be explained by the presence of a structured conformation within this loop (see below).

This loop presents some notable features. The extension of helix **III** into loop **C** was proposed by Andersen *et al.* (1984) in studies conducted to probe the structure of *Xenopus laevis* oocyte 5S rRNA with ribonucleases. Based on their results, two U-C non-canonical base pairs and base pairing between U_{35}-A_{42} and C_{36}-G_{41} were postulated, leaving loop **C** with only four nucleotides. In addition, Christiansen *et al.* (1987) published a study comparing the accessibility of *Xenopus laevis* oocyte 5S rRNA to enzymatic and chemical probes in the presence and absence of TFIIIA. In this study V_1 RNase cuts after U_{33} and U_{35} together with moderate reactivity of U_{33}, C_{34}, U_{43} and C_{44} to chemical probes provided additional support for the extension of helix **III** into loop **C**. More recently, Westhof *et al.* (in press) in their computer graphic model of *Xenopus laevis* oocyte 5S rRNA, provided

support for the extension of helix **III** into loop **C**. According to this model, the two pyrimidine residues on each side of loop **C** (C_{34} and C_{44}) are inside the loop stacked on the end of helix **III**, thereby protecting their N3 positions. This model includes the same two base-pairs previously proposed by Andersen *et al.* (1984). The base pair U_{35}-A_{42} is postulated to be in reverse Hoogsteen, while C_{36}-G_{41} is a Watson-Crick base pair. It is interesting to note that these positions are phylogenetically conserved: C_{36} and G_{41} are invariant; position 35 is always a pyrimidine and position 42 is either A or C.

The results of moderate reactivity at N3 positions for U_{35} and C_{36}, together with the non-reactivity at Watson-Crick positions for N3(C_{34}), N1(G_{37}), N1(G_{41}) and N3(C_{44}) observed in the wild-type 5S rRNA support the base pairing of U_{35}-A_{42} and C_{36}-G_{41} (Figure 38). The fact that these results are very similar to the ones obtained in the 5S rRNAs from each of the four mutants indicates that this proposed base pairing is not affected by any of the mutations that have been introduced (Figures 34-37).

In a different study, the extension of helix **III** by the pairing of U_{33}-A_{42} and C_{34}-G_{41} in wheat germ 5S rRNA was proposed (Li *et al.*, 1987). However, this model is only partially supported by the chemical reactivity data obtained from *Xenopus* oocyte 5S rRNA. The formation of the base pair U_{33}-A_{42} is not supported by the reactivity of N3(U_{33}) and N1(A_{42}) under native conditions observed in each of the four mutants and in w. t. 5S rRNAs (Figures 34-38).

In loop **C**, the lower reactivity of phosphate 42 towards ENU alkylation in all four mutants and wild type 5S rRNA suggests that this phosphate may be involved in a hydrogen bond (Figures 28-32). It should be pointed out that this phosphate is between A_{42}, which is unreactive at its N7 position, and G_{41}, which is unreactive at its N1 position under native conditions. This

phosphate protection may indicate either that the phosphate is directly involved in the same interactions as its neighbouring bases, or that this loop may be stabilized by magnesium coordination. It is believed that the protection of phosphate at position 42 in *Xenopus laevis* 5S rRNA may reflect the presence of a specific magnesium ion binding site in loop **C** (Romaniuk *et al.*, 1988).

Several tentative tertiary interactions have been proposed, especially for *E. coli* 5S rRNA, which would bring loop **C** into close proximity with region **E** (Böhm *et al.*, 1981; Hancock and Wagner, 1982; Pieler and Erdmann, 1982), and in some eukaryotic 5S rRNAs, interactions between loop **C** and loop **D** have been postulated (McDougall and Nazar, 1983; Göringer and Wagner, 1986). However, these tertiary interactions are not supported by the results obtained during the course of this project (see below page #115).

Third Stem

Loop E

It is in the third stem that base changes were introduced to make all four mutants. Loop **E** is commonly represented as single-stranded and located between helices **IV** and **V**. However, it has been suggested that this loop contains unusual base pairing, especially A-G pairs, which would extend helix **V** (Stahl *et al.*, 1981; Andersen *et al.*, 1984; Christiansen *et al.*, 1987; Romaniuk *et al.*, 1988; Romby *et al.*, 1988). The reactivity results obtained with chemical probes have provided a more detailed picture of the conformation of loop **E**. There are several differences in the reactivity to chemical probes of loop **E** in the 5S rRNA from mutants: Xlo73-76, Xlo99-101 and Xlo96-101 compared to that observed in wild-type 5S rRNA.

The chemical reactivity of loop **E** in *Xenopus* oocyte 5S rRNA shows that only the N7 of G75 is reactive under native conditions, while A_{74}, A_{100} and A_{101} are partially reactive under semi-denaturing conditions and G_{99} remains unreactive (Figure 32). At the Watson-Crick positions the AAU_{102} sequence is reactive under native conditions. On the other side of the loop, A_{74} and A_{77} are reactive at the N1 position under native conditions, while the rest of the residues become partially reactive at their respective Watson-Crick positions only under semi-denaturing conditions (Figure 38). It is normal for all nucleotides in a loop to be reactive at their Watson-Crick positions. However, the chemical reactivity data observed in loop **E** of *X. laevis* oocyte 5S rRNA, together with the lack of single-strand specific nuclease cleavages in this region (Figures 25, 32 and 38) suggested that a complex conformation exists in this loop (Romaniuk *et al.*, 1988). This conformation is believed to reflect base pairing between the nucleotides of this loop forming an additional secondary structure. Romaniuk *et al.* (1988) proposed a model for the structure of loop **E** in *X. laevis* 5S rRNA, consisting of non-canonical base pairing between U_{73}-U_{102}, A_{74}-A_{101}, G_{75}-A_{100} and U_{76}-G_{99}, leaving A_{77} unpaired (Figure 4). However, in the 5S rRNA from mutants Xlo73-76 and Xlo99-101 the reactivities at the N7 positions are quite different. In Xlo73-76, G_{73}, G_{74}, A_{75}, A_{77}, G_{99} and A_{101} are fully reactive under native conditions, while A_{100} is only partially reactive under these conditions (Figure 28). In mutant Xlo99-101, G_{75} and G_{100} are fully reactive under native conditions, while A_{74} and A_{99} are partially reactive, and G_{101} is only partially reactive under semi-denaturing conditions (Figure 29).

Similarly, there are differences between the wild-type 5S rRNA and these two mutants in their reactivities at Watson-Crick positions. In mutant Xlo73-

76, nucleotides A_{100}, A_{101} and U_{102} are fully reactive at their respective Watson-Crick positions under native conditions, while N1(G_{99}) is only partially reactive under these conditions. On the other side of the loop, N1(A_{75}), N3(C_{76}) and N1(A_{77}) are fully reactive under native conditions. N1(G_{74}) is only partially reactive under native conditions, while N1(G_{75}) is only reactive under semi-denaturing conditions (Figure 34). In mutant Xlo99-101, the reactivities at Watson-Crick positions are as follows: N1(A_{99}) and N3(U_{102}) are fully reactive under native conditions, while GG_{101} is partially reactive at the N1 position under these conditions. On the other side of the loop, N1(A74) and N1(G75) are only partially reactive under native conditions, while N1(A_{77}) is fully reactive. Unfortunately, positions U_{73} and U_{76} are undetermined, since the autoradiogram shows two very strong pauses of reverse transcriptase at these positions (Figure 35).

After modifications were introduced in Xlo96-101 5S rRNA, the structure that corresponds to loop E consists of Watson-Crick base pairs. As one can see from the reactivity to chemical probes in this region, there is less reactivity at both N7 and Watson-Crick positions compared to the reactivity of wild-type 5S rRNA. At N7 positions, only G_{75} and G_{98} are mildly reactive under native conditions, while the rest of the nucleotides are totally unreactive (Figure 30). At the Watson-Crick positions, only the N3 position of both U_{72} and U_{73} is mildly reactive under native conditions, whereas the rest of the nucleotides are totally unreactive. However, the reactivity of residues G_{98}, U_{99} and C_{101} is undetermined due to strong pauses of reverse transcriptase at these positions (Figure 36).

It is interesting to note that in mutant Xlo87-90, which does not have a mutation in loop E, the reactivity to chemical probes at N7 and Watson-Crick

positions in this loop is similar to that in the wild-type 5S rRNA. There are only minor differences: in Xlo87-90, both N7(A_{74}) and N1(G_{75}) are only partially reactive under semi-denaturing conditions (Figures 31 and 37). In addition, the absence of cleavage by any single-strand specific nucleases in loop **E** of Xlo87-90, as observed in wild-type 5S rRNA, suggests that loop **E** in this mutant may adopt a conformation similar to that in wild-type 5S rRNA (Figure 24).

Given the increased chemical reactivity and susceptibility to cleavage by single-strand specific nucleases in loop **E** of mutants Xlo73-76 and Xlo99-101, compared to the observed reactivities in wild-type 5S rRNA, it appears that the proposed conformation of loop **E** has been disrupted in these two mutants. The results obtained from these mutants can be explained using the model structure of loop **E** proposed by Westhof *et al.* (in press). In this model, which is based upon the chemical reactivity data of *Xenopus* oocyte 5S rRNA obtained by Romaniuk *et al.* (1988) and computer graphic modelling, non-canonical base pairing with an unusual hydrogen bonding pattern was postulated for loop **E**. This pattern presents the following features: i) in the case of the base pair U-U, it was proposed that the hydrogen-bonds: U_{73}(N3-H, O4)-U_{102}(O2, N3-H) occurred; ii) the next base pair in the sequence is A-A, connected by means of the following N6...N7 hydrogen-bonds: A_{74}(N6-H, N7-H)-A_{101}(N7-H, N6-H), with A_{101} in the syn orientation with respect to the sugar. The formation of this base pair can be correlated with the non-reactivity of these adenines at their N7 position, and their reactivity at N1 position observed under native conditions. These hydrogen-bonds have already been observed between A_9 and A_{23} in the crystal structure of $tRNA^{Asp}$ (Westhof *et al.*, 1985); iii) this base pair is followed by a G-A base

pair with the following hydrogen-bonds: G_{75}(N1-H, O6)-A_{100}(N7-H, N6-H). In this case A_{100} also adopts the syn conformation around its glycosyl bond. This base pair can be correlated with the absence of reactivity of A_{100}(N7) and G_{75}(N1); as well as the reactivity of A_{100}(N1) and G_{75}(N7) under native conditions; iv) the last non-canonical base pair of loop **E** is U_{76}-G_{99}, with the following hydrogen bonds: U_{76}(N3-H, 02)-G_{99}(06, N1-H), which would explain the mild reactivity observed at their respective Watson-Crick positions under semi- denaturing conditions . This last base pair is followed by A_{77} which is not base paired, but stacked inside the helix forming a slight wedge; this explains both its reactivity at N1 position, and its non-reactivity at N7 position under native conditions (Figure 40). These proposed interactions are in agreement with the chemical reactivities observed for the nucleotides of loop **E** in *X. laevis* oocyte 5S rRNA, with the exception of the U_{73}-U_{102} pairing. This pairing is only partially supported by the data, since Romaniuk *et al* (1988) were unable to determine the reactivity of the U_{102} residue. However, in the present project it was found that U_{102} is indeed reactive at its N3 position under native conditions (Figure 38). This reactivity of U_{102} suggests that the base pairing U_{73}-U_{102} may have only one hydrogen bond: U_{73}(N3-H)-U_{102}(O2).

As it can be seen from the chemical reactivity results obtained from the mutants of loop **E**, the positions of nucleotides 73, 74, 75, 76, 99, 100 and 101, postulated to be involved in non-canonical base pairs in the wild-type 5S rRNA appear to be chemically reactive in mutants Xlo73-76 and Xlo99-101 (Figures 28, 29, 34 and 35). These results indicate that the proposed non-canonical base pairing of loop **E** is absent in these two mutants. Moreover, since chemical reactivity occurs at both N7 and Watson-Crick

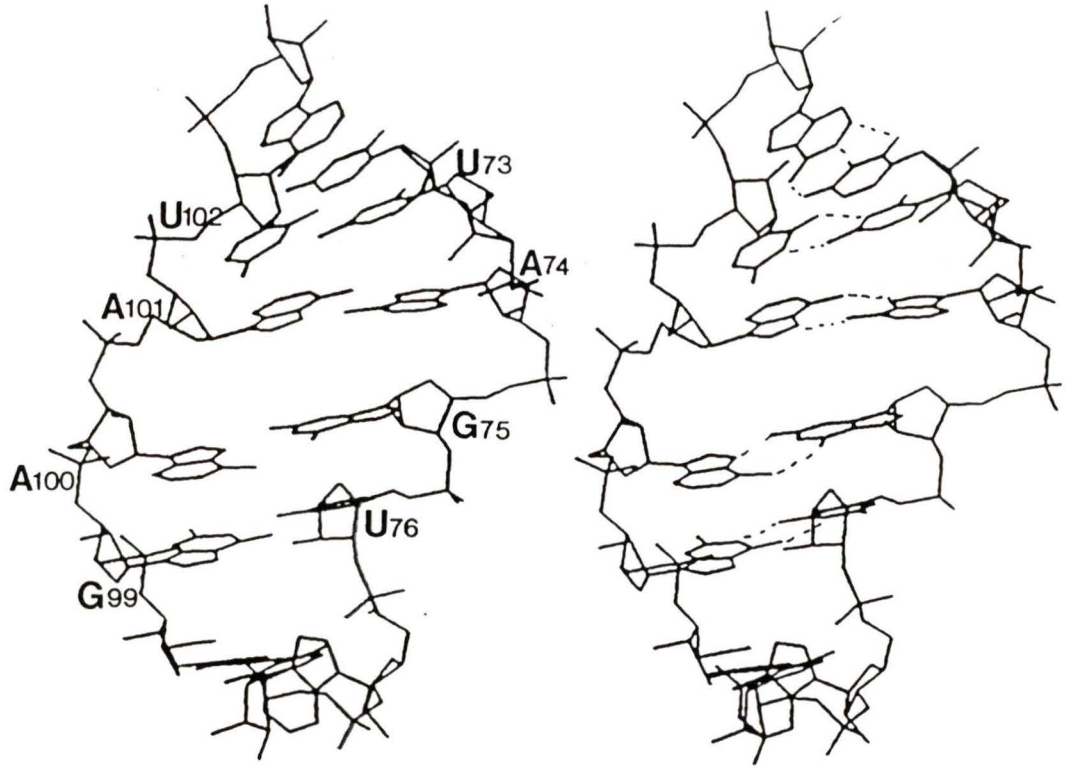

Figure 40: Stereoscopic view of the three dimensional model of the internal loop **E** in *Xenopus laevis* oocyte 5S rRNA. Base pair U72-A103 is at the top of the drawing. Phosphate backbone is shown by heavy lines and the hydrogen bonds by broken lines (courtesy of Pascale Romby).

positions in loop **E** of both mutants, the possibility of the formation of alternative secondary structures in these mutants, different from the one mentioned above, seems unlikely. These chemical reactivity results, together with the occurrence of accessibility to several single-strand specific nucleases in loop **E** of both mutants, indicate that the extended base pairing between helices **IV** and **V** no longer takes place in these mutants, and show that this region has now become a single-strand interior loop in both mutants. In mutant Xlo73-76, position A_{77}-N7 is strongly reactive under native conditions, suggesting that this nucleotide is not stacked inside the helix as it is in the wild-type 5S rRNA (Figure 28). The chemical reactivity results obtained from mutant Xlo96-101 indicate that the nucleotides in region **E** are unreactive, since they are now involved in Watson-Crick base pairing. It is interesting to note that all adenines in this newly formed helix are found unreactive at position N7 to DEPC, while guanines are only mildly reactive to DMS under native conditions (Figure 30). This observation is believed to be correlated with the fact that DEPC is more sensitive to base stacking than DMS, because of its higher molecular weight (Ehresmann *et al.*, 1987). At the Watson-Crick positions, only two nucleotides are mildly reactive under native conditions: U_{72} and U_{73}. However, their reactivity was expected since in order to create the Watson-Crick base pairing in this region, U_{73} was left unpaired (Figure 36).

In addition, as shown in Figure 32, phosphates at positions 75, 100 and 101 are protected from reaction with ENU in region **E** of wild-type 5S rRNA. The phosphate protection in this region may represent the presence of a magnesium binding site (Romaniuk *et al.*,1988). It is believed that the presence of magnesium is required to neutralize the negative charges of

phosphates in order to maintain and stabilize the particular conformation of loop **E** (Westhof *et al.*, in press). For example, in spinach chloroplast 5S rRNA, protected phosphates have also been found in irregular helices that contain non-canonical base pairs (Romby *et al.*, 1988). Magnesium is believed to be involved in this protection; it may also account for the stability of this region. The phosphate protection pattern in the mutants of loop **E** is quite different from the one in wild-type 5S rRNA. For example, in Xlo73-76 phosphates at positions 75, 100 and 101 are fully reactive to ENU and thus unprotected (Figures 28 and 39). In Xlo99-101 these three phosphate positions are also reactive to ENU (Figures 29 and 39), and in Xlo96-101 only the phosphate at position 100 is protected from reaction with ENU (Figures 30 and 39). However, the phosphate protection observed for Xlo87-90 is almost the same as the phosphate protection pattern in wild-type 5S rRNA. The phosphates at positions 75 and 100 are protected from ENU reactivity in this mutant (Figures 31 and 39).

In summary, the results of reactivity towards ENU indicate that the pattern of phosphate protection against this chemical probe in the 5S rRNA from mutants of loop **E** varies from that observed in wild-type 5S rRNA. In wild-type 5S rRNA three phosphates are protected from reaction with ENU in the unusual structure of loop **E**. Magnesium binding is believed to account for this protection, resulting in "ion shielding" as it was described to occur in tRNA (Romby et al., 1985). However, the protection of these phosphates appears to change when mutations are introduced in loop **E** of *Xenopus* oocyte 5S rRNA. From the ENU reactivity results in mutants Xlo73-76 and Xlo99-101 (where no protection in loop **E** is observed at all), and from the chemical reactivity results which suggest that the non-canonical base

pairing of loop **E** has been disrupted in these two mutants, one can conclude that the tight binding site for magnesium must be conformation dependent. The loss of loop **E** conformation leads to the loss of the tight binding site for magnesium in this loop of both mutants. In the 5S rRNA from mutant Xlo96-101, where phosphate protection is observed only at position 100, and which contains Watson-Crick base pairing along the third stem, magnesium does not appear to be required to maintain this stable conformation to the same extent as it is required in wild-type 5S rRNA. However, in mutant Xlo87-90 the ENU reactivity observed in loop **E** is almost the same as that in wild-type 5S rRNA, with the exception that the phosphate protection from reaction with ENU at position 101 is lost in this mutant. Perhaps this loss of protection is correlated with the mild reactivity of N7(A_{74}) observed in Xlo87-90 under native conditions.

The structure of *Xenopus* oocyte 5S rRNA has been previously examined for enzymatic accessibility. In this study, the lack of single-strand specific nucleases, coupled with the presence of some RNase V_1 cleavages in loop **E**, resulted in the proposal of a conformation for loop **E** that consists of base pairs between A_{74}-U_{102}, G_{75}-A_{101}, U_{76}-A_{100} and A_{77}-G_{99}, leaving U_{73} unpaired (Andersen *et al.*, 1984) (Figure 3). This same base paired conformation for loop **E** was later supported by Christiansen *et al.* (1987), in a study on the accessibility of *Xenopus* oocyte 5S rRNA to RNases and chemical probes. However, this proposed structure of loop **E** is not supported by the chemical reactivity results in loop **E** obtained in this study of *Xenopus* oocyte 5S rRNA. In the first place, the base pair A_{74}-U_{102} is not possible given the observed reactivity of both N1(A_{74}) and N3(U_{102}) under native conditions. Secondly, formation of U_{76}-A_{100} seems unlikely given the strong reactivity of

N1(A_{100}) in native conditions, and the reactivity of N3(U_{76}) under semi-denaturing conditions. Finally, the proposal of U_{73} being unpaired is not supported by the observed reactivity at its N3 position under semi-denaturing conditions (Figure 38). If this nucleotide were unpaired, one would expect its N3 position to be fully reactive under native conditions. It should be pointed out that in mutant Xlo96-101, which has the same base paired conformation as that proposed by Andersen *et al.* (1984), but with the difference that all the base pairs are Watson-Crick in this mutant, residue U_{73}, which is unpaired, is fully reactive at its N3 position under native conditions (Figure 36).

The fact that Andersen *et al.* (1984) observed RNase V_1 cleavages at positions U_{73}, U_{76} and U_{102} in loop **E** of *Xenopus* oocyte 5S rRNA, whereas none of these cleavages were observed by Romaniuk *et al.* (1988) reflects differences in salt, buffer and temperature conditions used during nuclease digestion. It has been shown that variations in pH, Mg^{2+} concentration and incubation temperature change the cleavage pattern of the same 5S rRNA (Toots *et al.*, 1982; Rabin *et al.*, 1983; Romaniuk *et al.*, 1988).

Helix **V**

Only positions N3(U_{69}), N3(U_{72}) and N1(A_{102}) in helix **V** of wild-type 5S rRNA are reactive under semi-denaturing conditions. The absence of reactivity at Watson-Crick positions in helix **V**, together with the presence of some RNase V_1 cleavages, confirm the existence of this helix (Figures 25 and 38). However, the chemical and enzymatic reactivity in the 5S rRNA from mutants Xlo73-76, Xlo99-101 and Xlo96-101 is different from that of w. t. 5S rRNA. In helix **V** of mutant Xlo73-76, N3(C_{104}) is reactive under native conditions , while N1(A_{103}), N1(A_{106}), N1 (G_{66}) and N3(C_{68}) are only partially reactive under these conditions, with N1(A_{103}) enhanced under semi-

denaturing conditions. N3(U_{69}), N1(G_{70}) and N1(G_{71}) were also observed to be reactive under semi-denaturing conditions (Figure 34). Helix **V** in mutant Xlo99-101 displays the following reactivities at Watson-Crick positions: N1(A_{103}) is reactive under native conditions, while the N1 position of A_{106}, G_{70}, G_{72}, and the N3 position of U_{69} and U_{72} are only mildly reactive under the same conditions, with U_{69} enhanced under semi-denaturing conditions. However, the N3 positions of C_{104} and C_{105} are found to be reactive under semi-denaturing conditions (Figure 35). As one can see from these results, the increased reactivity at Watson-Crick positions in helix **V** of both mutants indicates that the stability of this helix has decreased. This observation suggests that the base changes introduced in loop **E** of mutants Xlo73-76 and Xlo99-101 have disrupted the stability of helix **V** to a certain extent. For example, the nucleotides in the base pair A_{103}-U_{72} are only reactive at their respective Watson-Crick positions under semi-denaturing conditions in the wild-type 5S rRNA (Figure 38). However, in mutant Xlo99-101 this A-U base pair is reactive under native conditions. It is interesting to note that the chemical reactivity results at Watson-Crick positions in helix **V** of mutant Xlo87-90 (where loop **E** has the same sequence as the wild-type 5S rRNA) are basically the same as those obtained in the wild-type 5S rRNA (Figures 37 and 38). Since helix **V** remains unchanged in Xlo 87-90; it becomes apparent that the base substitutions introduced in this mutant did not affect the stability of this helix. In mutant Xlo96-101, N3(U_{69}) and N1(A_{103}) are totally unreactive, while the N3 position of U_{72} and U_{73} are reactive under native conditions, since U_{73} was left unpaired in order to create Watson-Crick base pairing in loop **E** (Figure 36). It is possible that U_{72} and U_{73} may alternate in the formation of this bulge. The absence of reactivity at Watson-Crick positions

indicates that the additional base pairing has made helix **V** more stable in this mutant.

Helix **IV**

In helix **IV**, the reactivity of A_{83} at both N1 and N7 positions under native conditions in wild-type 5S rRNA confirms the presence of this residue as a bulged nucleotide closed by the base pairs C_{94}-G_{82} and G_{93}-U_{84} (Figures 32 and 38). The fact that this reactivity is also observed in A_{83} of helix **IV** from all four mutants indicate that this bulged nucleotide is not affected by any of the base substitutions introduced in any of the mutants studied here (Figures 28-31 and 34-37). The observation that the U_{84}-N3 position is reactive to CMCT under native conditions indicates that the base pair G_{93}-U_{84} is not very stable. However, it is not unusual for a base pair that is closing a bulged or internal loop to have a reduced stability, resulting in local flexibility (Romaniuk *et al.*, 1988). Andersen *et al.* (1984), based upon phylogenetic sequence comparison, proposed that in *Xenopus* oocyte 5S rRNA the bulged nucleotide is actually U_{84}, and that it is closed by the base pairs G_{93}-A_{83} and C_{92}-G_{85} (Figure 3). However, the high reactivities observed at the A_{83}-N7 position to DEPC and at the A_{83}-N1 position to DMS in all four mutants and wild-type 5S rRNA do not support this proposed interaction. The possibility of a dynamic equilibrium between the two forms, with either A_{83} or U_{84} bulging out, has previously been proposed (De Wachter *et al.*, 1984). In fact it has been observed that most of the residues within helices which are reactive to chemical probes under native conditions are those immediately adjacent to bulged nucleotides (Romaniuk *et al.*, 1988). The reactivity of these sites is believed to result from the dynamic properties of the base pairs closing the bulge, which would then explain the observed reactivities at U_{84}-N3, G_{82}-N7,

G_{85}-N7 and G_{92}-N7 positions. Therefore, the possibility of an equilibrium in helix **IV** between the bulged A and bulged U conformation is believed to exist, since the conformation around bulged residues is flexible, allowing articulation in the 5S rRNA molecule (De Wachter *et al.*, 1984). In helix **IV** of *Xenopus* oocyte 5S rRNA, U_{80} and U_{96} (which appear to be in a non-pairing opposition in the secondary structure model), are unreactive at their N3 positions under native conditions (Figure 38). Based on this observation, a non-canonical base pair between these uridines, involving two hydrogen bonds between U_{80}(N3-H, O4) and U_{96}(O2, N3-H), was proposed by Romaniuk *et al.* (1988). This U-U pair appears to have the same reactivity at the N3 position in mutants Xlo73-76 and Xlo87-90. However, this U-U pair is fully reactive at the N3 position under native conditions in mutant Xlo99-101 (Figure 35). Moreover, there is also a mild reactivity at the N1 position of both G_{97} and G_{98} under native conditions in this mutant, indicating that helix **IV** is not as stable as it is in the wild-type 5S rRNA. This result is presumably due to the base changes introduced in the 3' side of loop **E** in this mutant. Interestingly enough helix **IV** seems to have almost the same reactivity and to be as stable in mutant Xlo73-76 as it is in the wild-type 5S rRNA (Figure 34). In this mutant, however, the N1 position of C_{78} is reactive under native conditions, whereas the N1 position of C_{79} is only mildly reactive under native conditions. The Watson-Crick positions of nucleotides in helix **IV** are unreactive in mutant Xlo96-101, except for residues A_{83} and U_{84} as mentioned before. The absence of reactivity at Watson-Crick positions in helix **IV** of this mutant suggests that the Watson-Crick base pairing of loop **E** has made this helix more stable in this mutant (Figure 36).

Loop D

The reactivity to chemical probes in loop **D** is basically the same in the 5S rRNA from wild-type and the 5S rRNA from mutants: Xlo73-76, Xlo99-101 and Xlo96-101 (Figures 28-30 and 34-36). In all these 5S rRNAs, A_{88} is fully reactive at both its N7 and N1 positions, while A_{90} is partially reactive at its N7 position under native conditions, but enhanced under semi-denaturing conditions, and fully reactive at its N1 position under native conditions. Residues G_{87} and G_{89} are unreactive at their N7 positions but partially reactive at their N1 position under semi-denaturing conditions. Note that N1(G_{87}) is undetermined in Xlo73-76 and Xlo99-101, and totally unreactive in Xlo96-101 (Figures 34-36). However, in the 5S rRNA from Xlo87-90 the base changes in loop **D** have made this loop fully reactive at both N7 and N1 positions in all four nucleotides under native conditions (Figure 31 and 37). Phosphates at positions 88 and 89 are protected from reaction with ENU under native conditions in the wild-type, Xlo73-76, Xlo99-101 and Xlo96-101 5S rRNAs (Figures 28-30, 32 and 39). It is interesting to note that a similar result has been reported for the analogous phosphates in three other eukaryotic 5S rRNA molecules (McDougall and Nazar, 1983). However, in the 5S rRNA from mutant Xlo87-90 the protection of these phosphates in loop **D** is completely lost (Figures 31 and 39).

The chemical reactivity data of loop **D** in *Xenopus* oocyte 5S rRNA together with the accessibility of this region to single-strand specific nucleases, suggests that this loop adopts an unusual conformation (Romaniuk *et al.*, 1988) (Figures 25, 32 and 38). The same pattern of reactivity at Watson-Crick and N7 positions as that in loop **D** of *Xenopus* 5S rRNA has been observed in other four-membered loops in 16S rRNA (Baudin *et al.*, 1987). Given this

similarity of reactivities, it has been suggested that loop **D** adopts a characteristic conformation that might be stabilized by magnesium coordination (Romaniuk *et al.*, 1988). McDougall and Nazar (1983) found phosphate protection from reaction with ENU at residues A_{88} and G_{89} in eukaryotic 5S rRNAs, and proposed that this phosphate protection was an indication of tertiary structure formation. In *X. laevis* wild-type 5S rRNA, phosphates at residues A_{88} and G_{89} are also found protected from reaction with ENU. But in this case the phosphates are believed to participate in a magnesium binding site, required to stabilize the conformation of loop **D** (Romaniuk *et al.*, 1988). The presence of a magnesium binding site in a loop has already been observed in the crystallographic structure of yeast $tRNA^{Phe}$ (Rich *et al.*, 1977). Based on the chemical reactivity data of loop D in *X. laevis* 5S rRNA obtained by Romaniuk *et al.* (1988), Westhof *et al.* (in press) have postulated in their computer graphic model of *X. laevis* oocyte 5S rRNA that G_{87} and A_{90} interact via hydrogen bonds $N2(G_{87})...N7(A_{90})$ and $N3(G_{87})...N6(A_{90})$, with the turn made at the phosphate of A_{88}. The turn of the loop in this region may explain the low reactivity of this phosphate towards ENU, and the proposed conformation of this loop may explain the low reactivity of the two guanines at their N1 position, and the absence of reactivity at their N7 position. However, the hydrogen-bond interaction between nucleotides 87 and 90 proposed to occur in the wild-type, seems unlikely in Xlo87-90, given the reactivity of these two nucleotides at their N1 and N7 positions under native conditions, as well as the reactivity of phosphates at positions 88 and 89 (Figures 31 and 37).

In summary, the chemical reactivity results obtained in loop **D** of Xlo87-90 indicate that the conformation of this loop is very different from that in

the wild-type and the other three mutants. One can see that the characteristic conformation of loop **D** believed to be stabilized by Mg^{2+} coordination in the wild-type 5S rRNA is non-existent in Xlo87-90, since loop **D** in this mutant becomes strongly reactive to chemical probes and more accessible to single-strand specific nucleases at every position (Figures 24, 31 and 37). The reactivity to ENU of phosphates at positions 88 and 89 in Xlo87-90 suggests that the magnesium binding site, postulated to occur in the wild type, is absent in this mutant. The reason for this absence may be the fact that the loss of loop **D** conformation in Xlo87-90 leads to the loss of the magnesium tight binding site. Moreover, it is important to note that in Xlo87-90 5S rRNA, not only are the four nucleotides of loop **D** more fully reactive to chemical probes at both N7 and N1 positions under native conditions, but also some nucleotides in helix **IV** adjacent to the loop become more susceptible to chemical probes. For example, G_{86} is reactive at its N7 position under native conditions in Xlo87-90, while it is unreactive in wild-type 5S rRNA (Figures 31 and 32). Similarly, G_{85}, G_{86} and C_{91} are fully reactive at their respective Watson-Crick positions under native conditions in Xlo87-90 5S rRNA, while they are unreactive in wild-type 5S rRNA (Figures 37 and 38). These observations suggest that the base changes introduced in loop **D** of mutant Xlo87-90 have destabilized helix **IV** to a certain extent, since this helix appears less stable in Xlo87-90 than in wild-type 5S rRNA. Furthermore, it has been observed in thermal denaturation studies of model hairpins that the loop sequence GNGA (which is the sequence of loop **D** in eukaryotic 5S rRNA, and certain loops in eubacterial 16S rRNA) stabilizes the double strand helix adjacent to the loop. When mutations are introduced in this tetranucleotide sequence, the melting point of the helix decreases by 3-4°C (Olke Uhlenbeck,

personal communication). This observation may explain the increased chemical reactivity observed in helix **IV** of mutant Xlo87-90 and suggests that both the sequence and the conformation of loop **D** may be important in maintaining the stability of this helix. It may also explain why residues G_{87}, G_{89} and A_{90} of loop **D** are highly conserved in eukaryotic 5S rRNA.

Several authors have proposed tentative tertiary interactions, especially for *E. coli* 5S rRNA, which would bring loop **C** and the 5' side of region **E** in close proximity (eg. Böhm *et al.*, 1981; Hancock and Wagner, 1982; Pieler and Erdmann, 1982; Göringer and Wagner, 1986) (Figures 5-8). However, the positions involved in these interactions do not appear to be phylogenetically conserved in eukaryotic 5S rRNA. In the case of *X. laevis* oocyte 5S rRNA, this tertiary interaction does not appear to take place, since it is not supported by the data obtained from mutants of region **E** (Xlo73-76, Xlo99-101 and Xlo96-101). If there was such an interaction between nucleotides of region **E** and nucleotides in loop **C**, one would expect that the base substitutions introduced in region **E** would disrupt this interaction. If this were the case, then the enzymatic and chemical reactivity data of loop **C** of these mutants would be drastically different compared to the reactivity in wild-type 5S rRNA. However, as shown in Figures 21-23, 25, 28-30, 32 34-36 and 38 the reactivity of loop **C** is fundamentally the same in all these 5S rRNAs.

On the other hand, the data obtained from these three mutants support the hypothesis concerning the structure of region **E** in the three-dimensional model for *Xenopus laevis* oocyte 5S rRNA, postulated by Westhof *et al.* (in press) on the basis of experimental data and graphic modelling (Figures 10 and 40). In this model 5S rRNA has a Y-shaped structure. Their results confirm the existence of the five helices and the two external loops (**C** and **D**)

predicted by the consensus secondary structure model of 5S rRNA. However, loop **E** is represented as a complex and organized structure that displays unusual features such as non-canonical base pairing, and is not involved in tertiary interactions with loop **C.** According to these authors non-canonical base pairs are widely distributed in RNA molecules, where they are believed to introduce kinks or irregularities, which as a result may influence the geometry of the RNA molecules and in turn may provide specific signals for protein recognition. This particular conformation of loop **E** is believed to require the presence of magnesium in order to be stabilized, and several phosphates, probably involved in magnesium coordination have been localized in this region (Westhof *et al.*, in press).

There are several observations that confirm the structure of region **E** as proposed in these authors' model

1) The results obtained from mutants Xlo73-76 and Xlo99-101 indicate that the base substitutions we introduced in loop **E** have caused a drastic change in both the chemical reactivity and the enzymatic accessibility of this region, as compared to that in wild-type 5S rRNA. In these mutants, the nucleotides in region **E** become reactive at the positions postulated to be involved in non-canonical base pairing in wild-type 5S rRNA. In fact, some of these residues are reactive at both the N7 and the Watson-Crick positions. Indeed, the reactivity of region **E** in these mutants indicates that the new conformation of this region is more like an unpaired internal loop. In these mutants, moreover, there is an increased reactivity at Watson-Crick positions in residues located adjacent to loop **E** in helices **IV** and **V**, suggesting that the disruption of non-canonical base pairing in region **E** has weakened the stability of these helices.

2) Unlike wild-type 5S rRNA, in these mutants region **E** becomes very accessible to single-strand specific nucleases.

3) In these mutants, phosphates in region **E** have an increased reactivity to ENU in residues proposed to be involved in magnesium coordination in wild-type 5S rRNA.

4) The fact that in these mutants the chemical reactivity and enzymatic accessibility of residues in the rest of the molecule (corresponding to stems 1 and 2) is the same as those in wild-type 5S rRNA, does not support a tertiary interaction of region **E** with loop **C** or any other part of the molecule.

5) The particular conformation of loop **E** seems to be an intrinsic feature of loop **E**, since a truncated *X. laevis* 5S rRNA (which contains helices **IV**, **V** and loops **E** and **D**) appears to adopt the same structure as the corresponding region of the entire 5S rRNA molecule (unpublished results).

Various researchers have proposed other tentative tertiary interactions between loop **C** and loop **D**. In eukaryotes, McDougall and Nazar (1983) have postulated a model of 5S rRNA structure in which the two arms that constitute regions **C** and **D** of the secondary structure model overlap to form a "lollipop"-like structure tertiary structure (Figure 9). Meanwhile, a Watson-Crick base pair tertiary interaction between the sequence $UCUC_{36}$ of loop **C** and the $GAGA_{90}$ sequence of loop **D** was postulated on the basis of enzymatic accessibility by Toots *et al.* (1982) in rat liver 5S rRNA.

However, several of our results tend to contradict these proposed interactions between loop **C** and loop **D**.

1) The results obtained in *Xenopus* 5S rRNA wild-type do not support a Watson-Crick base pair tertiary interaction between $UCUC_{36}$ and $GAGA_{90}$, given the chemical reactivity in loop **D** both of the A residues (A_{88} and A_{90})

at their N1 position under native conditions, and of the G residues (G_{87} and G_{89}) at their N1 positions under semi-denaturing conditions. Even though the tetranucleotide $CUCG_{37}$ of loop **C** is only partially reactive at Watson-Crick positions under semi-denaturing conditions, the formation of the base pair U_{33}-A_{90} proposed in this tertiary interaction, is also contradicted by the reactivity of both of these residues at Watson-Crick positions under native conditions (Figure 38).

2) If a tertiary base pair interaction between loops **C** and **D** was taking place, one would expect to see changes in the chemical reactivity and enzymatic accessibility of loop **C** in mutant Xlo87-90, since the base substitutions in loop **D** would have disrupted this interaction. However, both the chemical reactivity and the enzymatic accessibility of loop C is the same in Xlo87-90 as it is in wild-type 5S rRNA (Figures 24, 25, 31. 32, 37 and 38).

3) Toots *et al.* (1982) showed that the resistance of regions 33-36 and 87-90 of rat liver 5S rRNA to S_1 nuclease cleavage was consistent with their proposed interaction between loops **C** and **D**. However, according to the enzymatic cleavage data obtained from the wild-type 5S rRNA, loop **D** is not resistant but reactive to single-strand specific nucleases (Figure 25).

4) We saw above that the results obtained in this project support the *X. laevis* 5S rRNA tertiary structure model postulated by Westhof *et al.* (in press) with regard to loop **E**. The chemical reactivity and enzymatic accessibility results obtained from mutant Xlo87-90 also support the structure they proposed for loop **D**. According to their model, loop **D** is an external loop in which residues G_{87} and A_{90} interact via hydrogen-bonds. The protection of phosphates from reaction with ENU at positions 88 and 89, was

explained by the assumption of a magnesium binding site in this region. The base substitutions introduced into this loop in mutant Xlo87-90 have disrupted these proposed hydrogen-bond interactions, as is apparent from the fact that loop **D** becomes very reactive in all four residues at both N7 and N1 positions, and very accessible to single-strand specific nucleases (Figures 24, 31 and 37). In addition, the reactivity of phosphates towards ENU at positions 88 and 89 in Xlo87-90, may be explained by the fact that the conformation of loop **D**, which appears to be more open and accessible in this mutant, seems to cause the loss of the magnesium binding site in this loop.

It should be pointed out that the diversity of results that gives rise to such different 5S rRNA structure models, could in fact reflect actual tertiary conformational differences between these 5S rRNAs. For example, although they have a common ancestry, prokaryotic and eukaryotic 5S rRNAs appear to be structurally different. On the other hand, the diversity of results could be due to differences in salt, buffer and temperature conditions used during enzymatic and chemical modification. For example, Pieler and Erdmann (1982) in their experiments based on enzymatic accessibility that led to the proposal of a three-dimensional structural model of eubacterial 5S rRNA, carried out nuclease S_1 digestion in the absence of magnesium, unlike the procedure followed during the present project. We can see that a perfect coordination of results of attempts to determine the structural conformation of 5S rRNA is difficult given the numerous possible variables affecting the assays from different labs. It is for this reason that we have studied the structure of *Xenopus* 5SrRNA under carefully controlled conditions using all available chemical and enzymatic structure probes.

CONCLUSION

This work represents a contribution towards trying to determine the exact three-dimensional structure of *Xenopus laevis* oocyte 5S rRNA. By carrying out base substitutions in loops **E** and **D** of this 5S rRNA, and studying the resulting structure by means of chemical and enzymatic probes, some new light has been shed on the currently proposed conformation of loops **E** and **D** in this molecule.

The results obtained during this project support the conclusion that the computer graphic model proposed by Westhof (in press) for the structure of *X. laevis* oocyte 5S rRNA provides the most accurate picture yet suggested of the conformation of region **E** and loop **D**. The value of this model lies in its combination of data from several different sources, such as enzymatic and chemical probing, protein binding, phylogenetic comparison, and tRNA crystallographic data, into a structure that makes sense in terms of design and stability. This model is basically Y-shaped, with helices **II** and **V** almost coaxial. As can be seen in Figure 10, this model displays an extended structure that closely follows the secondary structure of 5S rRNA, and does not accommodate any long-range tertiary interactions between loop **C** and region **E** or loop **D**. The high accessibility of *X. laevis* oocyte 5S rRNA to structure-specific probes supports this Y-shaped model, and suggests that little tertiary folding occurs in this molecule (Westhof, in press). The validity of this model of the structure of region **E** and loop **D** is now further supported by the structure probing of the four mutants studied here. The results obtained concerning the effect of such mutations on the conformation of 5S rRNA support the unusual base pairing interactions which, according to

these authors, occur in region **E** and loop **D**. Furthermore, these results do not support the existence of a tertiary long-range interaction between region **E** or loop **D** and some other distal part of the molecule.

The currently proposed model of *X. laevis* 5S rRNA by Westhof (in press) could be further tested and refined by introducing mutations at various positions on the molecule, other than the ones studied in this project. For example, on residues of loop **A** which are considered critical in the tertiary folding of 5S rRNA (Christiansen *et al.*, 1987; Romaniuk *et al.*, 1989; Westhof et al., in press). Chemical and enzymatic mapping could be used to study the effect of these mutations. In this manner, by combining experimental structural analysis with site-directed mutagenesis, crystallography and graphic modelling, it may be possible to further clarify the relationship between the structure and function of 5S rRNA.

BIBLIOGRAPHY

Abdel-Meguid, S. S., Moore, P. B. and Steitz, T. A. (1983) *J. Mol. Biol. 171*, 207-215.

Andersen, J. and Delihas, N. (1986) *J. Biol. Chem. 261*, 2912-2917.

Andersen, J., Delihas, N., Hanas, J. S., and Wu C.-W. (1984) *Biochemistry. 23*, 5752-5759.

Aubert, M., Scott, J. F., Reynier, M. and Monier, R. (1968) *Proc. Natl. Acad. Sci. U.S.A. 61*. 292-299.

Azad, A. A. (1979) *Nucleic Acids Res. 7*, 1913-1929.

Azad, A. A., and Lane, B. G. (1973) *Can. J. Biochem. 51*, 1669-1672.

Baudin, F., Ehresmann, C., Romby, P., Nougel, M., Lempereur, L., Bachellerie, J. P., Ebel, J. P. and Ehresmann, B. (1987) *Biochimie 69*, 1081-1096.

Bellemare, G., Jordan, B. R., Rocca-Serra, J. and Monier, R. (1972) *Biochimie 54*, 1453-1466.

Birkenmeier, E. H., Brown, D. D. and Jordon, E. (1978) *Cell 15*, 1077.

Brookes, P. and Lawley, P. D. (1961) *Biochem. J. 80*, 496-503.

Brown, R. S., Ferguson, C., Kingswell, A., Winkler, F. K. and Leonard, K. R. (1988) *Proc. Natl. Acad. Sci. U.S.A. 85*, 3802-3804.

Brown, R. S. (1985) *European Molecular Biology Laboratory Research Reports (EMBL, Heidelberg)*. 74-75.

Brownlee, G. G., Sanger, F., and Barrel, B. G. (1968) *J. Mol. Biol. 34*, 374-386.

Cantor, C. R., and Schimmer, P. R. (1980) *Biophysical Chemistry Part III* (Freeman, W. F. and Company eds.), San Francisco. 1146-1160.

Carbon, P., Ehresmann, C., Ehresmann, B., and Ebel, J. P. (1978) *FEBS Lett. 94*, 152-156.

Cech, T. R. and Bass B.L. (1986) *Annual Review of Biochemistry 55*, 599-629.

Christensen, A., Mathiesen, M., Peattie, D. and Garret, R. A. (1985) *Biochemistry 24* , 2284-2291.

Christiansen, J., Douthwaite, S. R., Christensen, A. and Garret, R. A. (1985) *EMBO J. 4* 1019-1024.

Christiansen, J., Brown, R. S., Sprout, B. S., and Garrett R. A. (1987) *EMBO J. 6,* 453-460.

Clark, W.,and Lake, J. A. (1983) *J. Bact. 157,* 971-974.

Delihas, N. and Andersen, J. (1982) *Nucleic Acids Res. 10,* 7323-7343.

Delihas, N., Andersen, J. and Singhal, R. P. (1984) *Prog. Nucleic Acids Res. 31,* 161-190.

De Wachter, R., Chen, M. and Vandenberghe, A. (1982) *Biochimie 64,* 311-329.

De Wachter, R., Chen, M. and Vandenberghe, A. (1984) *Eur. J. Biochem. 143,* 175-182.

Digweed, M., Pieler, T., Kluwe, D., Schuster, L., Walker, R. and Erdmann, V. A. (1986) *Eur. J. Biochem. 154,* 31-39.

Douthwaite, S. and Garret, R. A. (1981) *Biochemistry 20,* 7301-7307.

Dumas, P. Mores, D., Florentz, C., Giege, R., Verlaan, A., Van Belkum, A., and Pleij, C.W.A. (1987) *J. Biomol. Str. Dyn. 4,* 707-728.

Ehresmann, C., Baudin, F., Mougel, M., Romby, P., Ebel, J. P., and Ehresmann, B. (1987) *Nucl. Acids Res. 15,* 9109-9128.

Erdmann, V. A. (1981) *Nucl. Acids Res. 9,* r25-r42.

Erdmann, V. A. (1982) *Nucl. Acids Res. 10,* r93-r116.

Erdmann, V. A., Fahnestock, S., Higo, K., and Nomura, M. (1971) *Proc. Natl. Acad. Sci. U.S.A. 68,* 2932.

Erdmann, V. A., and Wolters, J. (1986) *Nucl. Acids Res. 14,* r1-r59.

Egami, F. and Nakamura, K. (1969) in *Microbial RNase,* Springer Verlag, Berlin, Heidelberg, N.Y. 18-23.

Ehrenberg, L., Fedorcsak, I. and Solymosy, F. (1976) *Prog. Nucl. Acid Res. Mol. Biol. 16*, 189-262.

Fox J. W. and Wong K. P. (1979) *J. Biol. Chem. 254*, 10139-10144.

Garrett, R. A., Douthwaite, S. and Noller, H. F. (1981) *Trends Biochem. Sci. 6*, 137-139.

Garret, R. A. and Olesen, S. O. (1982) *Biochemistry 21*, 4823-4830.

Gaunt-Klopfer, M., and Erdmann, V. A. (1975) *Biochim. Biophys. Acta 390*, 226-230.

Gihlam, P. T. (1962) *J. Amer. Chem. Soc. 84*, 687-689.

Göringer, H. U., and Wagner, R. (1984) *J. of Biol. Chem. 259*, 491-100.

Göringer, H. U., Bertram S. and Wagner, R. (1986) *Nucl. Acids Res. 14*, 7473-7485

Guerrier-Takada, C., Gardiner, K., Marsh, T., Pace, N., and Altman, S. (1983) *Cell 35*, 849-857.

Grundstrom, T., Zenke, W. M., Wintzerith, M., Matthes, H. W. D., Staub, A., and Chambon, P. (1985) *Nucl. Acids Res. 13*, 3305-3316.

Hancock, J., and Wagner, R. (1982) *Nucl. Acids Res. 10*, 1257-1269.

Hingerty, B., Brown, R. S. and Jack, A. (1978) *J. Mol. Biol. 124*, 523-534.

Huber, P. W. and Wool, I. G. (1986) *Proc. Natl. Acad. Sci. U.S.A. 83*, 1593-1597.

Inoue, T. and Cech, T. R. (1985) *Proc. Natl. Acad. Sci. U.S.A. 82*, 648-652.

Jack, A., Ladner, J. E. and Klug, A. (1976) *J. Mol. Biol. 108*, 619-649.

Jensen, D. E. and Reed, D. J. (1978) *Biochemistry 17*, 5098-5107.

Kao, T. M. and Crothers, D. M. (1974) *Proc. Natl. Acad. Sci. U.S.A. 77*, 3360-3364.

Kime, M. J. and Moore, P. B. (1982) *Nucl.Acids Res. 10*, 4973-4983.

Kime, M. J. and Moore, P. B. (1983) *Biochemistry 22*, 2622-2629.

Kjems, J., Olesen, S. E. and Garrett, R. A. (1985) *Biochemistry 24*, 241-250.

Kochetov, N. K. and Budowski, E. I. (1972) in *Organic chemistry of nucleic Acids*, Plenum Press, New York.

Kusmierek, J. T. and Singer B. (1976) *Biochim. Biophys. Acta 442*, 420-431.

Lorenz, S., Hartmann, R., Piel, N., Ulbrich, N. and Erdmann V. A. (1987) *Eur. J. Biochem. 163*, 239-246.

Lavery, R. and Pullman, A. (1984) *Biophys. Chem. 19*, 171-181.

Lawley, P. D. and Brookes, P. (1963) *Biochem. J. 89*, 117-138.

Lecanidou, R. and Richards, E. G. (1975) *Eur. J. Biochem. 56*, 127-133.

Leonard, N. J., McDonald, J. J., Henderson, R. E. L., and Reichmann, D. E. (1971) *Biochemistry 10*, 3335-3342.

Lempereur, L., Nicoloso, M., Riehl, N., Ehresmann, C., Ehresmann, B., and Bachellerie, J. P. (1985) *Nucl. Acids Res. 13*, 8339-8357.

Li, S. J., Wu, J. and Marschall, A. G. (1987) *Biochemistry 26*, 1578-1585.

Lo, A. C., and Nazar, R. N. (1982) *J. Biol. Chem. 257*, 3516-3524.

Mac Donell, M. T. and Colwell, R. R. (1985) *J. Mol. Evol. 22*, 237-242.

Moazed, D., Stern, S., and Noller, H. F. (1986) *J. Mol. Biol. 187*, 339-416.

Moras, D., Dock, A.,Dumas,P., Westhof, E., Romby, P., and Giege, R. (1983) in *Nucleic Acids: The Vector of Life* (Pullman, B.& Jortner, J. Eds.) Vol. 16, pp403-411, Reidel, Dordrecht, The Netherlands.

Morikawa, K., Fujiyoshi, Y., Ishizuka, K., Sugimaya, J., Kawakami, M. and Takemura, S. (1986) *J. Microsc. 142*, 247-258.

Morikawa, K., Kawakami, M. and Takemura, S. (1982) *FEBS Lett. 145*, 194-196.

Mougel, M., Eyermann, F., Westhof, E., Romby, P., Expert-Bezançon, A., Ebel, J. P., Ehresmann, B., and Ehresmann, C. (1987) *J. Mol. Biol. 198*, 91-107.

Naylor, R., Ho, N. W. Y. and Gihlam, P. T. (1966) *J. Amer. Chem. Soc. 87*, 4209-4210.

Nazar, R. N., Willick, G. E. and Matheson, A. T. (1979) *J. Biol. Chem. 254*, 1506-1512.

Neimark, H., Andersen, J., and Delihas, N. (1983) *Nucl. Acids Res. 11*, 7569-7574.

Noller, H. F., and Garrett, R. A. (1979) *J. Mol. Biol. 132*, 621-636.

Nomura, M. (1973) *Science 179*, 864-872.

Nussinov, R., Tinoco, I., Jr. and Jacobson, A. B. (1982) *Nucl. Acids Res. 10*, 351-363.

Ofengand, J., and Henes, C. (1969) *J. Biol. Chem. 244*, 6241-6253.

Osterberg, R., Sjoberg, B. and Garret, R. A. (1979) *Eur. J. Biochem. 68*, 481-487.

Pieler, T. Guddat, U. Oei, S. L. and Erdmann, V. A. (1986) *Nucl. Acids Res. 14*, 6313-6326.

Peattie, D. A. (1979) *Proc. Natl. Acad. Sci. U.S.A. 76*, 1760-1764.

Peattie, D. A., and Gilbert, W. (1980) *Proc. Natl. Acad. Sci. U.S.A. 77*, 4679-4682.

Pelham, H. R. B. and Brown, D. D. (1980) *Proc. Natl. Acad. Sci. U.S.A. 77*, 4170-4174.

Phillips, G. P. and Timko, J. L. (1972) *Analyt. Biochem. 45*, 319-325.

Picard, B. and Wegnez, M. (1979) *Proc. Natl. Acad. Sci. U.S.A. 76*, 241-245.

Pieler, T., and Erdmann, V. A. (1982) *Proc. Natl. Acad. Sci. U.S.A. 79*, 4599-4603.

Pieler, T. and Erdmann, V. A. (1983) *FEBS Lett. 157*, 283-287.

Pieler, T., Erdmann, V. A. and Apell, B. (1984) *Nucl. Acids Res. 12*, 8393-8406.

Quigley, G. J., Wang, A., Seeman, N. C., Suddath, F. L., Rich, A., Sussman, J. L., and Kim, S. H. (1975) *Proc. Natl. Acad. Sci. U.S.A. 72*, 4866-4870.

Raacke, I. D. (1971) *Proc. Natl. Acad. Sci. U.S.A. 68*, 2357-2360.

Rabin, D., Kao, T. M. and Crothers, D. M. (1983) *J. Biol. Chem. 258*, 10813-10816.

Romaniuk, P. J. (1985) *Nucl. Acids Res. 13*, 5369-5387.

Romaniuk, P. J., Leal de Stevenson, I., Ehresmann, C., Romby, P., and Ehresmann, B. (1988) *Nucl. Acids Res. 16*, 2295-2312.

Romaniuk, P. J., Leal de Stevenson, I. and You, Q. (1989) "Molecular Biology of RNA" in *UCLA Symposia on Molecular and Cellular Biology, 94*, Cech, T. ed., Alan R. Liss Inc., New York, N.Y.

Romby, P., Moras, D., Bergdoll, H., Dumas, P., Vlassov, V. V., Westhof, E., Ebel, J. P., and Giegé, R. (1985) *J. Mol. Biol. 184*, 455-471.

Romby, P., Moras, D., Dumas, P., Ebel, J. P. and Giegé, R. (1987) *J. Mol. Biol. 195*, 193-204.

Romby, P., Westhof, E., Moras, D., Giegé, R., Houssier, C., and Grosjean, H. (1986) *J. Biomol. Str. Dyn. 4*, 193-203.

Romby, P., Westhof, E., Toukifimpa, R., Mache, R., Ebel, J. P., Ehresmann, C. and Ehresmann, B. (1988) *Biochemistry 27*, 4721-4730.

Rosset, R. and Monier, R. (1963) *Biochim. Biophys. Acta 68*, 653-658.

Sanger, F., Nicklen, S., and Coulson, A. R. (1977) *Proc. Natl. Acad. Sci. U.S.A. 74*, 5463-5467.

Segall, J., Matsui, T. and Roeder, R. G. (1980) *J. Biol. Chem. 255*, 11986-11991.

Shastry, B. S., Ng, S.-Y. and Roeder, R. G. (1982) *J. Biol. Chem. 257*, 12979-12986.

Shatsky, I. N., Evstafievea, A. G., Bystrova, A. A., Bogdanov, A. A. and Vassiliev, V. D. (1980) *FEBS Lett. 121*, 97-100.

Silberklang, M., Gillam, A. M. and Raj Bhandary, V. L. (1977) *Nucl. Acids Res. 4*, 4091-4108.

Silberklang, M., Raj Bhandary, V. L., Lück, A., and Erdmann, V. A. (1983) *Nucl. Acids Res. 11*, 605-617.

Singer, B. (1976) *Nature 264*, 333-339.

Singer, B. and Fraenkel-Conrat, H. (1976) *Biochemistry 14*, 772-782.

Sneath, B., Vary, C., Pavlakis, G., and Vournakis, J. (1986) *Nucl. Acids Res. 14*, 1365-1378.

Stahl, D. A., Pace, B., Marsh, T. and Pace, N. R. (1984) *J. Biol. Chem. 259*, 11448-11453.

Sussman, J. L. and Podjarny, A. D. (1985) *Acta Crystallogr. 39*, 495-505.

Toots, I., Metspalu, A., and Saarma, M. (1981) *Nucl. Acids Res. 9*, 5331-5343.

Toukifimpa, R., Razier, C., Romby, P., Ehresmann, C., Ehresmann, B. and Mache, R. (1988) submitted for publication.

Troutt, A., Savin, T., Curtis, W. C., Celentano, J. and Vournakis, J. (1982) *Nucl. Acids Res. 10*, 653-663.

Uchida, T., Anma, T. and Egami, F. (1970) *J. Biochem. 67*, 91-102.

Van Stolk, B. J. and Noller, H. F. (1984) *J. Mol. Biol. 180*, 151-177.

Vincze, A., Henderson, R. E. L., McDonald, J. J. and Leonard, N. J. (1973) *J. Amer. Soc. 95*, 2677-2682.

Westhof, E., Dumas, P. and Moras, D. (1985) *J. Mol. Biol. 184*, 119-145.

Westhof, E., Romby, P., Romaniuk, P. J., Ebel, J. P., Ehresmann, C. and Ehresmann, B. (1989) *J. Mol. Biol.*, in press.

Wing, R., Drew, H., Takano, T., Broca, C., Tanaka, S., Itakura, K., and Dickerson, R. E. (1980) *Nature 287*, 755-758.

Wintermeyer, N. and Zachau, H. G. (1975) *FEBS Lett. 58*, 306-309.

Woese, C. R. and Fox, G. E. (1977) *Proc. Natl. Acad. Sci. U.S.A. 74*, 5088-5092.

Wolters, J., and Erdmann, V. A. (1988) *Nucl. Acids Res. 16* Supl., r1-r70.

VITA

Surname: Leal Carretero Given Names: María Luisa Isabel

Place of Birth: Guadalajara, México. Date of Birth: June 21, 1958

Educational Institutions Attended:

UNIVERSITY OF VICTORIA, B.C. 1980 to 1984

UNIVERSITY OF VICTORIA, B.C. 1987 to 1989

Degrees and Diplomas:

B. Sc. (First Class) 1984 University of Victoria, B.C.

Honours and Awards:

Dean's Scholarship, 1987/88 and 1988/89

Post-Graduate Scholarship, Natural Sciences and Engineering Research Council of Canada, 1989/90

Publications:

Romaniuk, P.J, Leal de Stevenson, I., and Wong, H.-H.A. (1987), "Defining the Binding Site of *Xenopus* Transcription Factor IIIA on 5S rRNA using Truncated and Chimeric 5S rRNA Molecules", Nucleic Acids Research 15, 2737ff.

Romaniuk, P.J., Leal de Stevenson, I., Ehresmann,C., Romby, P., and Ehresmann, B. (1988), "A Comparison of the Solution Structures and Conformational Properties of the Somatic and Oocyte 5S rRNAs of *Xenopus laevis* ", Nucleic Acids Research 16, 2295ff.

Romaniuk,P.J., Leal de Stevenson, I., and You, Q., "The Specificity of the RNA Binding Activity of *Xenopus* Transcription Factor IIIA", in The Molecular Binding of RNA: UCLA Symposia on Molecular and Cellular Biology, Volume 94 (New York:Alan R. Liss, 1988).

I hereby grant the rigtht to lend my thesis (the title of which is shown below) to users of the University of Victoria Library, and to make single copies only for such users or in response to a request from the Library of any other university, or similar institution, on its behalf or for one of its users. I further agree that permission for extensive copying of this thesis for scholarly purposes may be granted by me or a member of the University designated by me. It is understood that copying or publication of this thesis for financial gain shall not be allowed without my permission.

Title of Thesis

A STRUCTURAL ANALYSIS OF *Xenopus laevis* 5 S rRNA.

Author 

M. L. ISABEL LEAL CARRETERO

June 17, 1989.

National Library
of Canada

Bibliothèque nationale
du Canada

Canadian Theses Service

Service des thèses canadiennes

Ottawa, Canada
K1A 0N4

The author has granted an irrevocable non-exclusive licence allowing the National Library of Canada to reproduce, loan, distribute or sell copies of his/her thesis by any means and in any form or format, making this thesis available to interested persons.

L'auteur a accordé une licence irrévocable et non exclusive permettant à la Bibliothèque nationale du Canada de reproduire, prêter, distribuer ou vendre des copies de sa thèse de quelque manière et sous quelque forme que ce soit pour mettre des exemplaires de cette thèse à la disposition des personnes intéressées.

The author retains ownership of the copyright in his/her thesis. Neither the thesis nor substantial extracts from it may be printed or otherwise reproduced without his/her permission.

L'auteur conserve la propriété du droit d'auteur qui protège sa thèse. Ni la thèse ni des extraits substantiels de celle-ci ne doivent être imprimés ou autrement reproduits sans son autorisation.

ISBN 0-315-53758-2

Canada